

Performance Level 2 Tests on a 29-in. Open Concrete Bridge Rail

Midwest Roadside Safety Facility (MwRSF) Center for Infrastructure Research

Department of Civil Engineering
University of Nebraska-Lincoln
1901 Y Street, Building C
Lincoln, Nebraska 68588-0601
Telephone (402) 472-6864

Sponsored by the
Midwest States Regional Pooled Fund - Fiscal Year 1994
Project Number: SPR-3(017)
Nebraska Department of Roads (NDOR)
1500 Nebraska Hwy 2
P.O. Box 94759
Lincoln, Nebraska 68509-4759

Transportation Research Report TRP-03-51-95

June 1996

TECHNICAL REPORT STANDARD TITLE PAGE

1. Performing Organization Report No. TRP-03-51-95	2. Report Date June 1996	3. Type of Report Final Report
4. Title and Subtitle Performance Level 2 Tests on a 29-in. Open Concrete Bridge Rail		
5. Author(s) Holloway, J.C., Faller, R.K., Wolford, D.F., Dye, D.L., Sicking, D.L.		
6. Performing Organization Name and Address Midwest Roadside Safety Facility (MwRSF) Civil Engineering Department University of Nebraska - Lincoln 1901 Y St., Bldg C Lincoln, Nebraska 68588-0601 (402) 472-6864		
7. Sponsoring Agency Name and Address Nebraska Department of Roads 1500 Nebraska Highway 2 Lincoln, NE 68502		
8. Contract or Grant No. SPR-3(017), FY-94 Midwest States Regional Pooled Fund Program		
9. Abstract <p>A safety performance evaluation of a 737-mm (29-in.) high open concrete bridge rail was conducted for the Nebraska Department of Roads (NDOR). The evaluation included four full-scale crash tests at two critical impact locations. Concerns regarding structural adequacy, snagging at the gap, single-unit truck rollover, and occupant compartment deformation of pickups were to be addressed at each critical impact location. Each impact location was evaluated with a single-unit truck and a ballasted pickup truck. The safety performance of the 737-mm (29-in.) high open concrete bridge rail was shown to meet the Performance Level 2 (PL-2) requirements specified in the American Association of State Highway and Transportation Officials (AASHTO) <i>Guide Specifications for Bridge Railings</i>, 1989.</p>		
10. Keywords Highway Safety, Crash Tests, Bridge Railings, Open Concrete Rail, Expansion Gap		11. Distribution Statement No restrictions. This document is available to the public from the sponsoring agency.
12. Security Classification (of this report) Unclassified	13. Security Classification (of this page) Unclassified	14. No. of Pages 87

DISCLAIMER STATEMENT

The contents of this report reflect the views of the authors who are responsible for the facts and the accuracy of the data presented herein. The contents do not necessarily reflect the official views or policies of the Nebraska Department of Roads nor the Federal Highway Administration. This report does not constitute a standard, specification, or regulation.

ACKNOWLEDGMENTS

The authors wish to acknowledge several sources that made this project possible: the Midwest States Regional Pooled Fund Program consisting of the Nebraska Department of Roads, Iowa Department of Transportation, Kansas Department of Transportation, Missouri Highway and Transportation Department, and the Minnesota Department of Transportation for sponsoring this project; and the Center for Infrastructure Research, University of Nebraska-Lincoln for matching support.

A special thanks is also given to the following individuals who made a contribution to the completion of this research project.

Midwest Roadside Safety Facility

B. T. Rosson, Ph.D., P.E., Assistant Professor
J. D. Reid, Ph.D., Assistant Professor
B. G. Pfeifer, P.E., Research Associate Engineer
K. L. Krenk, Field Operations Manager
Undergraduate and Graduate Research Assistants

Nebraska Department of Roads

Gale Barnhill, P.E., Bridge Division
Leona Kolbet, Research Coordinator

Missouri Department of Transportation

Pat McDaniel, P.E., Design Special Assignments Engineer

Kansas Department of Transportation

Ron Seitz, P.E., Road Design Squad Leader

Iowa Department of Transportation

David Little, P.E., Design Methods Engineer

Minnesota Department of Transportation

Khani Sahebjam, P.E., State Aid Bridge Engineer

Federal Highway Administration

Milo Cress, P.E., Nebraska Division Office

Dunlap Photography

James Dunlap, President and Owner

TABLE OF CONTENTS

	Page
DISCLAIMER STATEMENT	i
ACKNOWLEDGMENTS	ii
TABLE OF CONTENTS	iv
1 INTRODUCTION	1
1.1 Background	1
1.2 Problem Statement	3
1.3 Objective	4
1.4 Scope	5
2 TEST CONDITIONS	6
2.1 Test Facility	6
2.1.1 <u>Test Site</u>	6
2.1.2 <u>Vehicle Tow System</u>	6
2.1.3 <u>Vehicle Guidance System</u>	6
2.2 Nebraska Open Concrete Bridge Rail Design Details	7
2.3 Test Vehicles	17
2.4 Data Acquisition Systems	26
2.4.1 <u>High-Speed Photography</u>	26
2.4.2 <u>Accelerometers and Rate Gyro</u>	27
2.4.3 <u>Speed Trap Switches</u>	28
3 PERFORMANCE EVALUATION CRITERIA	29
4 TEST RESULTS	32
4.1 Test NEOCR-3	32
4.2 Test NEOCR-4	42
4.3 Test NEOCR-5	49
4.4 Test NEOCR-6	60
5 DISCUSSION	69
6 CONCLUSIONS	71
7 REFERENCES	73
8 APPENDIX	74
8.1 Appendix A. Accelerometer and Rate Gyro Analysis Plots	75

LIST OF FIGURES

	Page
1. Bridge Rail Design Details	10
2. Photographs of Nebraska Open Concrete Rail	11
3. Layout and Design Details of Nebraska Open Concrete Bridge Rail	12
4. Concrete Deck Attachment Detail	13
5. Reinforcement Layout for Bridge Deck	14
6. Reinforcement Layout for 2-ft. Posts	15
7. Reinforcement Layout for Bridge Rail	16
8. Test Vehicle, Test NEOCR-3	18
9. Test Vehicle Dimensions and Weights, Test NEOCR-3	19
10. Test Vehicle, Test NEOCR-4	20
11. Test Vehicle Dimensions and Weights, Test NEOCR-4	21
12. Test Vehicle, Test NEOCR-5	22
13. Test Vehicle Dimensions and Weights, Test NEOCR-5	23
14. Test Vehicle, Test NEOCR-6	24
15. Test Vehicle Dimensions and Weights, Test NEOCR-6	25
16. Impact Location, Test NEOCR-3	34
17. Summary and Sequential Photographs, Test NEOCR-3	35
18. Additional Sequential Photographs, Test NEOCR-3	36
19. Full-Scale Crash Test, Test NEOCR-3	37
20. Full-Scale Crash Test, Test NEOCR-3	38
21. Bridge Rail Damage, Test NEOCR-3	39
22. Bridge Rail Damage at Expansion Gap, Test NEOCR-3	40
23. Test Vehicle Damage, Test NEOCR-3	41
24. Impact Location, Test NEOCR-4	44
25. Summary and Sequential Photographs, Test NEOCR-4	45
26. Additional Sequential Photographs, Test NEOCR-4	46
27. Bridge Rail Damage, Test NEOCR-4	47
28. Test Vehicle Damage, Test NEOCR-4	48
29. Impact Location, Test NEOCR-5	51
30. Summary and Sequential Photographs, Test NEOCR-5	52
31. Additional Sequential Photographs, Test NEOCR-5	53
32. Full-Scale Crash Test, Test NEOCR-5	54
33. Full-Scale Crash Test, Test NEOCR-5	55
34. Bridge Rail Damage, Test NEOCR-5	56
35. Test Vehicle Damage, Test NEOCR-5	57
36. Undercarriage Damage, Test NEOCR-5	58
37. Occupant Compartment Damage, Test NEOCR-5	59

LIST OF FIGURES (continued)

	Page
38. Impact Location, Test NEOCR-6	62
39. Summary and Sequential Photographs, Test NEOCR-6	63
40. Additional Sequential Photographs, Test NEOCR-6	64
41. Full-Scale Crash Test, Test NEOCR-6	65
42. Full-Scale Crash Test, Test NEOCR-6	66
43. Bridge Rail Damage, Test NEOCR-6	67
44. Test Vehicle Damage, Test NEOCR-6	68

LIST OF TABLES

	Page
1. Crash Test Conditions and Evaluation Criteria	30
2. AASHTO Evaluation Criteria	31
3. Summary of Safety Performance Results	72

1 INTRODUCTION

1.1 Background

In 1986, a safety performance evaluation on an open concrete bridge rail was conducted for the Nebraska Department of Roads (NDOR) by ENSCO, Inc. of Springfield, Virginia (1). This open concrete bridge rail was constructed with a 356-mm (14-in.) wide x 406-mm (16-in.) deep rail, containing six No.6 longitudinal reinforcement bars. The rail was supported by concrete posts measuring 279-mm (11-in.) wide x 279-mm (11-in.) deep x 330-mm (13-in.) high, which contained six No. 7 vertical reinforcement bars. The posts were spaced 2.3-m (7-ft 6-in.) on centers. Although the open concrete bridge rail design incorporated a 76-mm (3-in.) expansion gap, the simulated bridge rail used in testing did not contain an expansion gap.

ENSCO, Inc. conducted two full-scale vehicle crash tests during this investigation according to the criteria specified in the *Recommended Procedures for the Safety Performance Evaluation of Highway Appurtenances*, National Cooperative Highway Research Program (NCHRP) Report No. 230 (2). The first test was conducted with a 2,043-kg (4,504-lb) sedan at impact conditions of 96.6 kph (60 mph) and 25 degrees. The second test was conducted with an 817-kg (1,800-lb) mini-compact sedan with impact conditions of 96.6 kph (60 mph) and 20 degrees. The safety performance of the bridge rail was determined to be satisfactory according to the NCHRP Report No. 230 safety evaluation criteria. This study demonstrated that the geometry of the 737-mm (29-in.) open concrete bridge rail could safely accommodate full-size and mini-size automobiles. Additional information and test results for this study can be found in the referenced test report (1).

In 1991, a safety performance evaluation of a similar open concrete bridge rail design was conducted for NDOR by the Midwest Roadside Safety Facility (MwRSF) (3). Computer simulation modeling using BARRIER VII (4) was first used to assist in the verification of the structural adequacy of the bridge rail design prior to construction and testing. The simulation effort was also conducted to provide information for analysis and redesign of the bridge rail to satisfy the Performance Level 1 (PL-1) requirements specified in the American Association of State Highway and Transportation Officials (AASHTO) 1989 *Guide Specifications for Bridge Railings* (5).

There were a number of redesign phases based on the results of the computer simulation modeling (3). The final design was constructed with a 356-mm (14-in.) wide x 406-mm (16-in.) deep rail, including a 76-mm (3-in.) expansion gap, and supported by two different post sizes. The two posts located adjacent to the expansion gap measured 279-mm (11-in.) wide x 914-mm (36-in.) long x 330-mm (13-in.) high, and the remaining concrete posts measured 279-mm (11-in.) wide x 610-mm (24-in.) long x 330-mm (13-in.) high.

The longitudinal reinforcement in the rail was reduced from the No. 6 bars used in the previously tested design by ENSCO (1), and consisted of six No. 5 Grade 60 epoxy-coated bars. The 279-mm (11-in.) wide x 914-mm (24-in.) long posts were reinforced with three No. 4 bars and four No. 6 bars in the back side and traffic side locations, respectively. The 279-mm (11-in.) wide x 610-mm (36-in.) long posts were reinforced with five No. 6 bars in the back side and traffic sides.

Two full-scale vehicle crash tests were conducted according to the AASHTO PL-1 evaluation criteria (3). Tests NEOCR-1,2 were conducted with ballasted pickup trucks at the target impact conditions of 72.4 kph (45 mph) and 20 degrees. Test NEOCR-1 was conducted upstream of the gap location, to investigate both the structural adequacy of the posts and the potential for snagging on the downstream face of the expansion gap. Test NEOCR-2 was conducted at a midspan between two posts on the continuous section of the rail, to investigate the structural adequacy of the rail in which the longitudinal steel reinforcement had been reduced for economic considerations. The safety performance of the bridge rail was determined to be satisfactory. This study demonstrated that the open concrete bridge rail system could safely accommodate pickup truck impacts. Specific design details on the system and test results can be found in the referenced test report (3).

1.2 Problem Statement

Open concrete bridge railings are widely used by state highway departments across the nation. These barriers offer many advantages over parapet railing systems, which include efficient snow removal and improved drainage. Additionally, these systems provide less visual obstruction to the driver, and can be installed at a height of 813-mm (32 in.) while still accommodating a pavement overlay.

NDOR has traditionally used a 737-mm (29-in.) high open concrete bridge railing for Performance Level 1 applications and parapet barriers when higher performance bridge rails were required. In view of the operational and aesthetic advantages of a 737-mm (29-in.) open concrete bridge railing, NDOR and the Midwest States Regional Pooled Fund Program requested that MwRSF examine the potential for this barrier to meet the Performance Level 2 standards as outlined in the AASHTO *Guide Specifications for Bridge Railings*, 1989 (5).

Since the Nebraska Open Concrete Bridge Rail, which is designed to meet Performance Level 2 standards, has a 114-mm (4 ½-in.) expansion-gap which does not provide structural continuity, the NDOR Bridge Division was again concerned with the structural adequacy of the two concrete posts adjacent to the gap. To address this concern a second series of full-scale vehicle crash tests were performed by the Midwest Roadside Safety Facility (MwRSF). Engineers were specifically concerned with the potential of large trucks to rollover and the potential for large lateral deflections in the posts and the attached rail adjacent to the gap. It was thought that the lateral deflections on the upstream side of the gap could be of sufficient magnitude to cause vehicle snagging.

1.3 Objective

The objective of this research project was to evaluate the Nebraska Open Concrete Bridge Rail according to Performance Level 2 (PL-2) as presented in the AASHTO *Guide Specifications for Bridge Railings* (5). The bridge rail was to be evaluated at two locations. The primary concern at the region around the gap was that deflections in the bridge rail during an impact may lead to vehicle snagging at the gap. The second series of tests were performed on the continuous rail section where the main concerns are the structural adequacy and the redirection capacity of the rail.

1.4 Scope

The scope of this project consisted of evaluating both regions of the Nebraska Open Concrete Rail according to the criteria for PL-2 bridge rails specified by AASHTO (5). The Guide Specifications for Bridge Railings (5) requires that Performance Level 2 (PL-2) bridge rails be tested with an 816-kg (1,800-lb) mini-compact sedan impacting at 96.6 kph (60 mph) and 20 deg, a 2449-kg (5400-lb) pickup impacting at 96.6 kph (60 mph) and 20 deg, and an 8,165-kg (18,000-lb) single-unit truck at an impact speed of 80.5 kph (50 mph) and 15 deg. As mentioned previously, a very similar open concrete bridge rail system with the same effective railing height and shape of railing face had been successfully tested by ENSCO, Inc. (1) in accordance with the guidelines set forth in NCHRP Report No. 230 (2). Since these test conditions are similar to the PL-2 small car test, it was determined that the PL-2 test with an 816-kg (1,800-lb) vehicle was not necessary. Therefore, only pickup and single-unit truck tests were to be conducted.

2 TEST CONDITIONS

2.1 Test Facility

2.1.1 Test Site

The test site facility is located at the Lincoln Air-Park on the NW end of the Lincoln Municipal Airport. The test facility is approximately 8-km (5 mi.) NW of the University of Nebraska-Lincoln. The site is surrounded and protected by a 2.4-m (8-ft) high chain-link security fence.

2.1.2 Vehicle Tow System

A reverse cable tow with a 1:2 mechanical advantage was used to propel the test vehicle. The distance traveled and the speed of the tow vehicle are one-half that of the test vehicle. The test vehicle is released from the tow cable before impact with the bridge rail. The fifth wheel, built by the Nucleus Corporation, was used in conjunction with a digital speedometer to increase the accuracy of the test vehicle impact speed.

2.1.3 Vehicle Guidance System

A vehicle guidance system developed by Hinch (6) was used to steer the test vehicle. A guide flag attached to the front left wheel and the guide cable was sheared off before impact. The 0.95-cm (3/8-in.) diameter guide cable was tensioned to 13.3 kN (3,000 lbs), and supported laterally and vertically every 30.5 m (100 ft) by hinged stanchions. The hinged stanchions stood upright while holding up the guide cable, but as the vehicle was towed down the line, the guide-flag struck and knocked each stanchion to the ground. The vehicle guidance system was approximately 610-m (2000-ft) long for the single unit truck tests and 460-m (1500-ft) long for the pickup truck tests.

2.2 Nebraska Open Concrete Bridge Rail Design Details

A detailed drawing of the Nebraska Open Concrete Bridge Rail is shown in Figure 1. Photographs of the actual installation are shown in Figure 2. The total length of the installation was 47.1 m (154 ft 4 5/8 in.), as shown in Figure 3. The installation consisted of three major structural components: (1) simulated concrete bridge deck, (2) concrete posts, and (3) concrete bridge rail. The design details for each of these components are shown in Figure 1.

The installation was constructed with a simulated bridge deck in order to test the post-to-deck connection as well as the rail itself. The length of the bridge deck was 37.0 m (121 ft 6 in.). The 20.3-cm (8-in.) thick deck had a total width of 1.75 m (5 ft 9 in.), producing a 0.94-m (3-ft 1-in.) cantilever. The deck was reinforced with two No. 5 transverse bars spaced at 11.4 cm (4½ in.) and 17.8 cm (7 in.) on the top and bottom rows, respectively. There was 6.4 cm (2.5 in.) of clear cover available on the top bar, and 2.5 cm (1 in.) on the bottom bar. Two No. 4 longitudinal bars were placed between the transverse bars and spaced at 30.5 cm (12 in.) centers. The transverse bars were attached to the existing concrete apron, as shown in Figure 4. Grade 60, epoxy-coated reinforcement was used in the deck. The reinforcement layout for the bridge deck is shown in Figure 5, details are shown in Figure 1.

The second major component of the installation was the concrete posts. Twenty reinforced concrete posts were constructed to support the reinforced concrete rail, as shown in Figure 1. There were three different post sizes incorporated in this installation. Seventeen 27.9-cm (11-in.) wide x 61.0-cm (24-in.) long x 33.0-cm (13-in.) high posts

(Post Nos. 2 through 4 and 6 through 20) were used to support the continuous rail. Two 27.9-cm (11-in.) wide x 91.4-cm (3-ft) long x 33.0-cm (13-in.) high posts (Post Nos. 4 and 5) were placed adjacent to the gap location in the rail. Finally, one buttress post was constructed measuring 30.5-cm (12-in.) wide x 1.9-m (6-ft. 1 ½-in.) long x 25.4-cm (10-in.) high (Post No. 1). The post spacing between the first and second posts was 3.2 m (10 ft 4 1/4 in.), between the second through fourth posts was 2.0 m (6 ft 8 in.), between the fifth and sixth post was 2.3 m (7 ft. 6 1/8 in.), between the sixth through the nineteenth posts was 2.4 m (8 ft 0 in.), and between the nineteenth and twentieth post, was 3.0 m (10 ft 0 in.). All distances stated above are from center to center of post and are shown in Figure 3. Reinforcement details for the posts are shown in Figure 1. The 27.9-cm (11-in.) x 61.0-cm (24-in.) posts were reinforced with three R401 or R406 vertical bars and four R601 or R602 vertical bars in the back side and traffic side locations of the post, respectively, as shown in Figure 6. In addition, three rows of R302 stirrups were placed at 12.7-cm (5-in.) centers with 5.1-cm (2-in.) of clear cover on all sides. The 27.9-cm (11-in.) x 91.4-cm (36-in.) posts were reinforced with five 601 or 602 vertical bars in both the back side and traffic side locations of the post. In addition, three rows of R303 stirrups were placed at 12.7-cm (5-in.) centers with 5.1-cm (2-in.) of clear cover on all sides. The buttress post was reinforced with three R603, four R406, and three R602 vertical bars in both the back side and traffic side locations of the post and 2 rows of R403 stirrups. Grade 60 epoxy-coated reinforcement was used in the posts.

The third major component of the installation was the concrete bridge rail. The bridge rail was 35.6-cm (14-in.) wide x 40.6-cm (16-in.) deep x 47.1-m (154-ft 4 5/8-in.) long, including an 11.4-cm (4 ½-in.) expansion gap between the fourth and fifth posts, and

had an effective railing height of 73.7 cm (29-in.). The reinforcement in the rail consisted of six longitudinal R502 or R503 bars and R301 vertical stirrups spaced at 60.9-cm (24-in) centers, as shown in Figure 7.

The concrete used for all of the above components was a Nebraska 47-BD Mix, with a minimum 24.1-Mpa (3500 psi) compressive strength and a 28-day compressive strength of 41.4 Mpa (6000 psi). The concrete compressive strengths at the time of the first test for both the simulated bridge deck and the monolithic concrete posts and attached rail were approximately 49.7 MPa (7,202 psi) and 46.8 Mpa (6,765 psi), respectively.

As previously stated, all of the reinforcement in the simulated bridge deck, posts, and rail was Grade 60 epoxy-coated rebar.

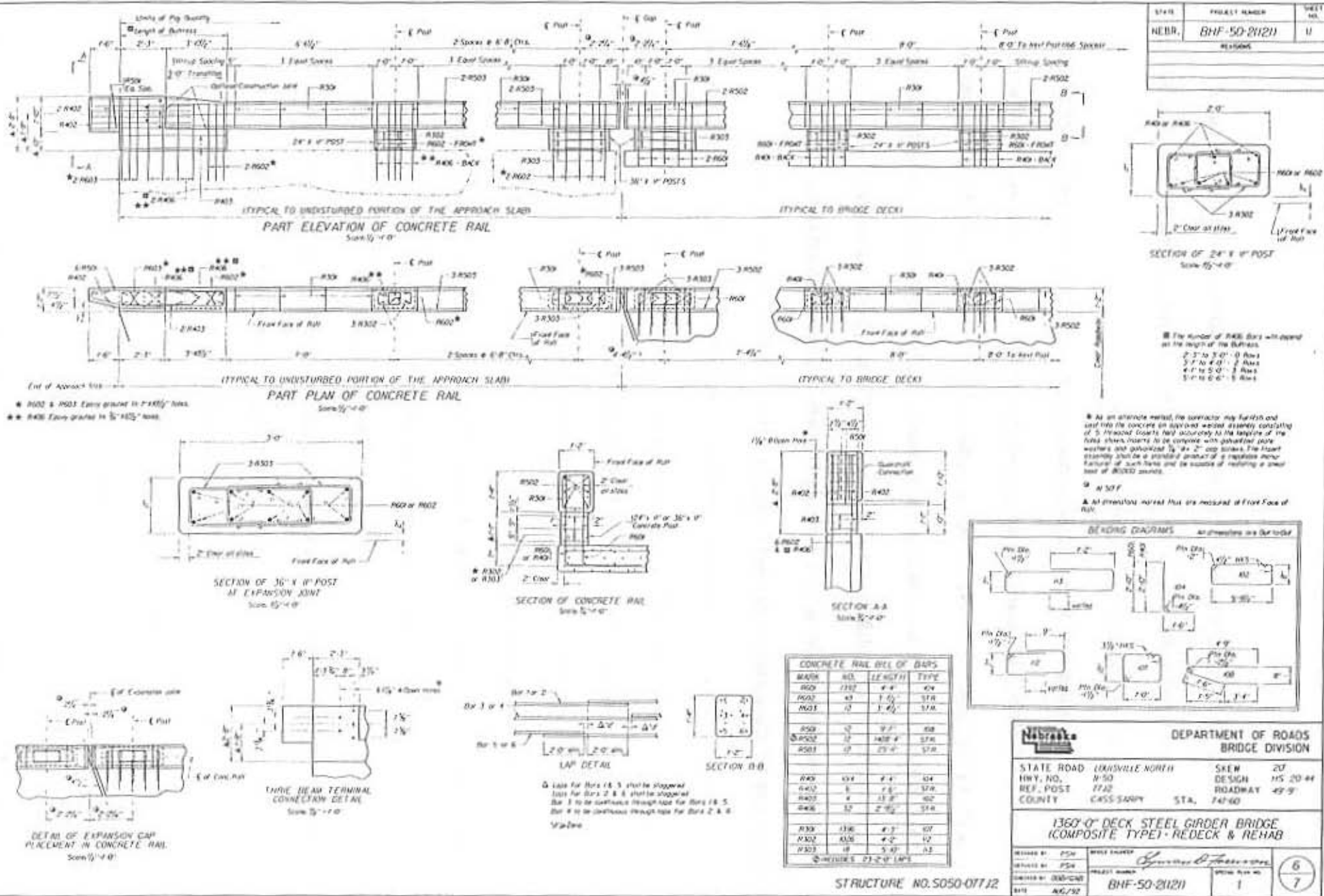


FIGURE 1. Bridge Rail Design Details

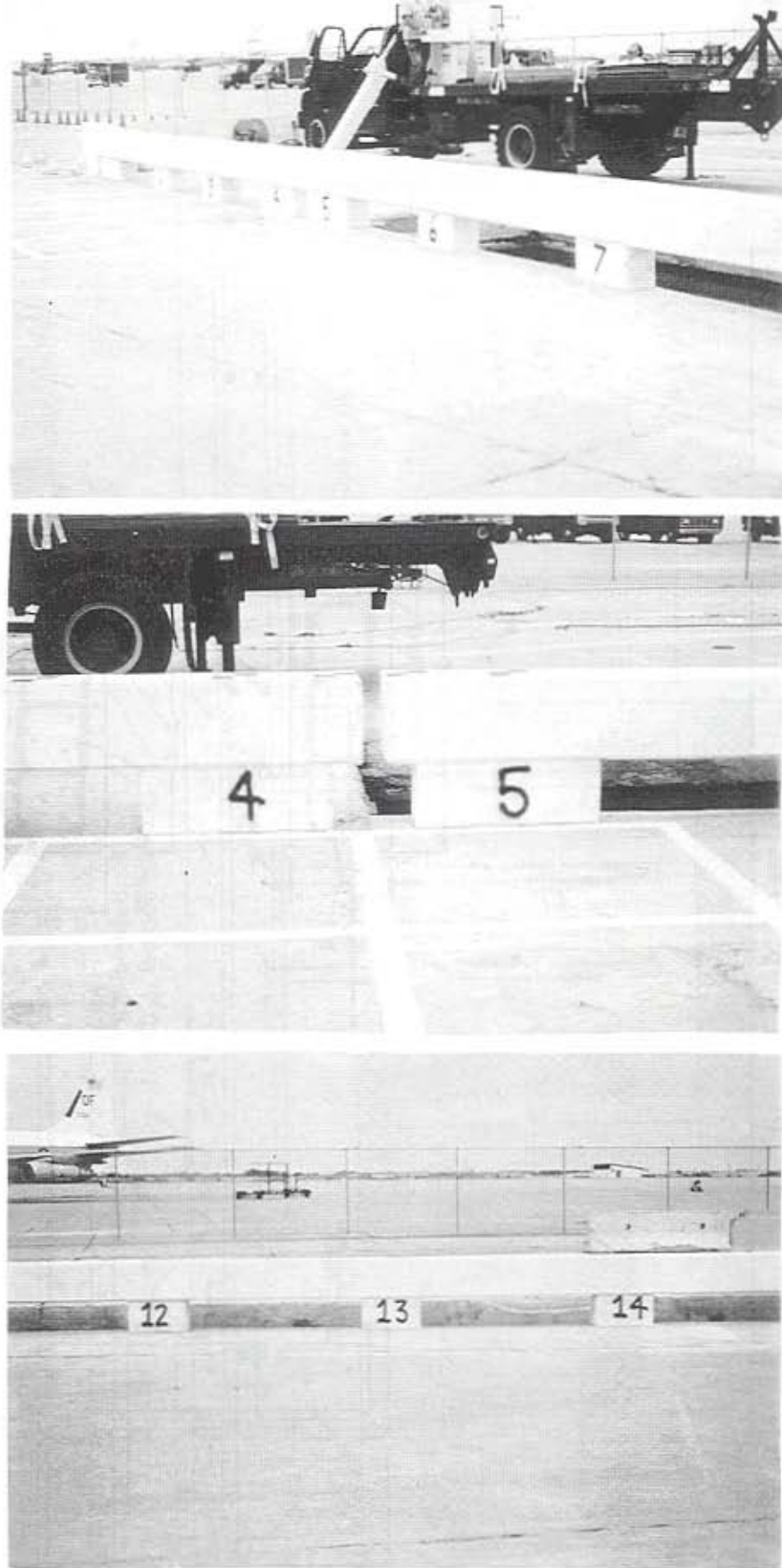


Figure 2. Photographs of Nebraska Open Concrete Bridge Rail.



12

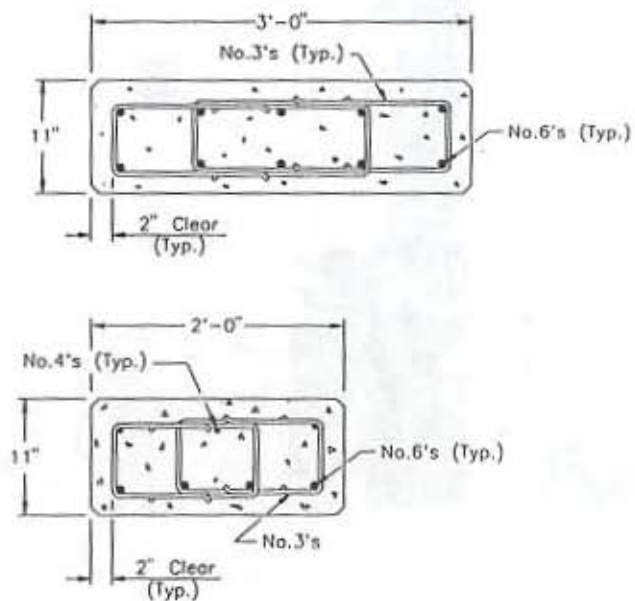
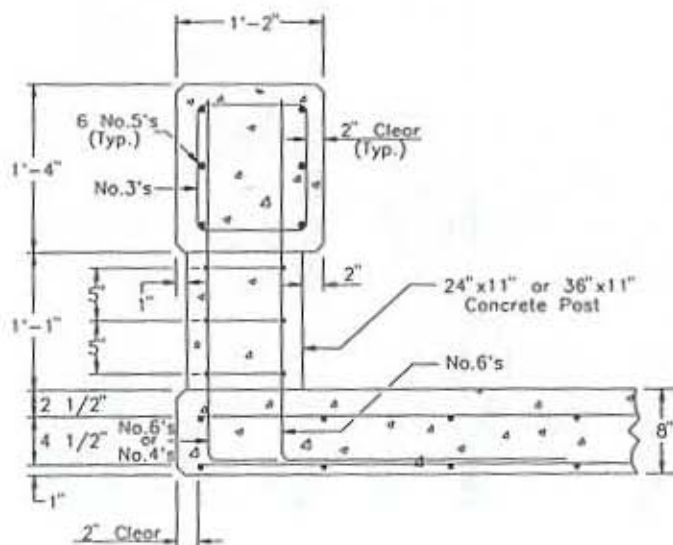


FIGURE 3. Layout and Design of the Nebraska Open Concrete Bridge Rail

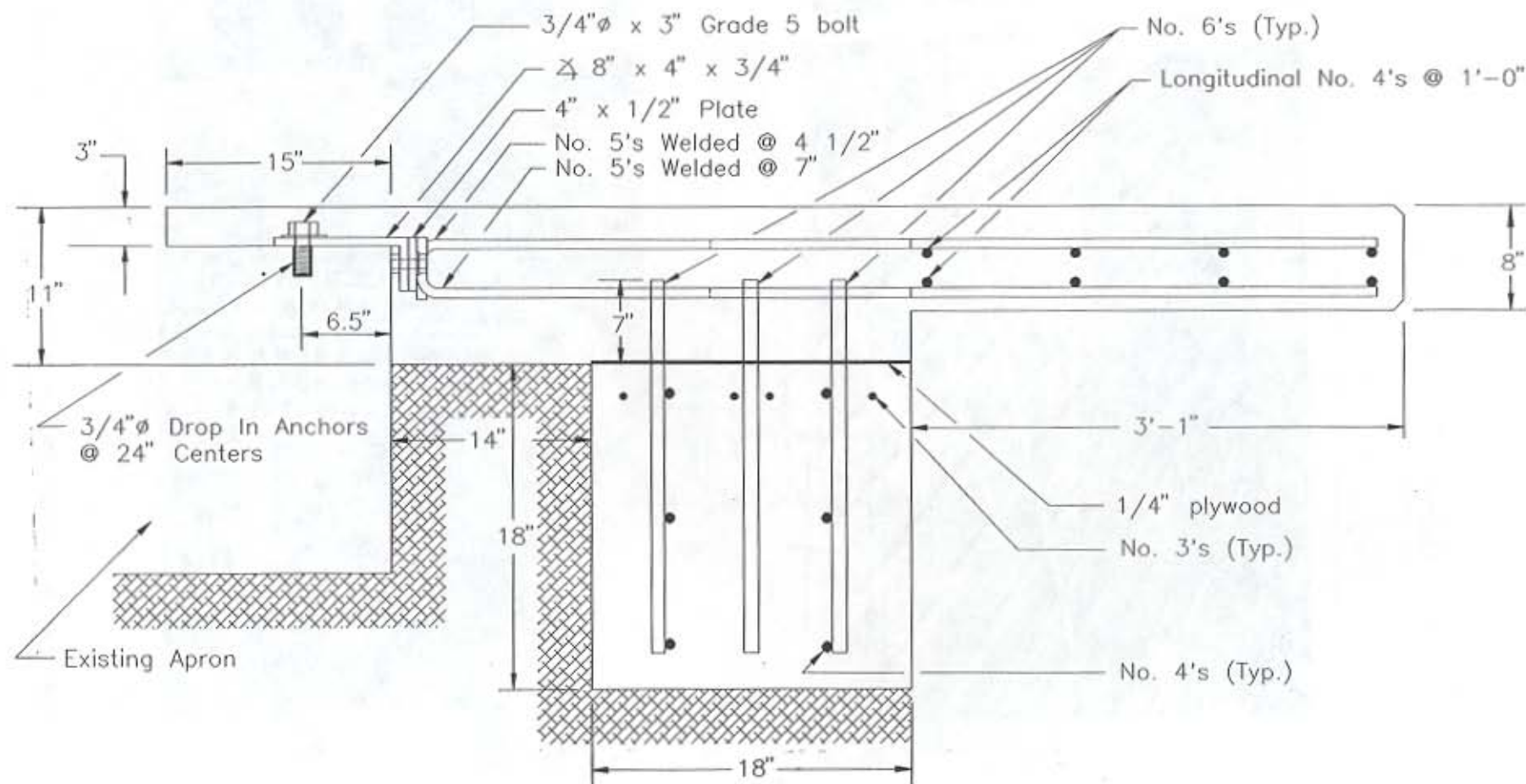


FIGURE 4. Concrete Deck Attachment Detail

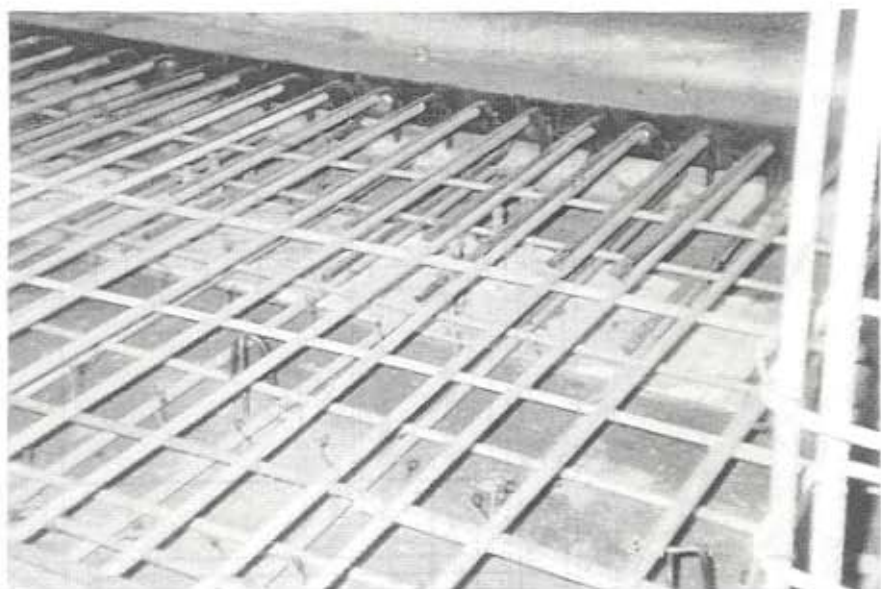


FIGURE 5. Reinforcement Layout for Bridge Deck

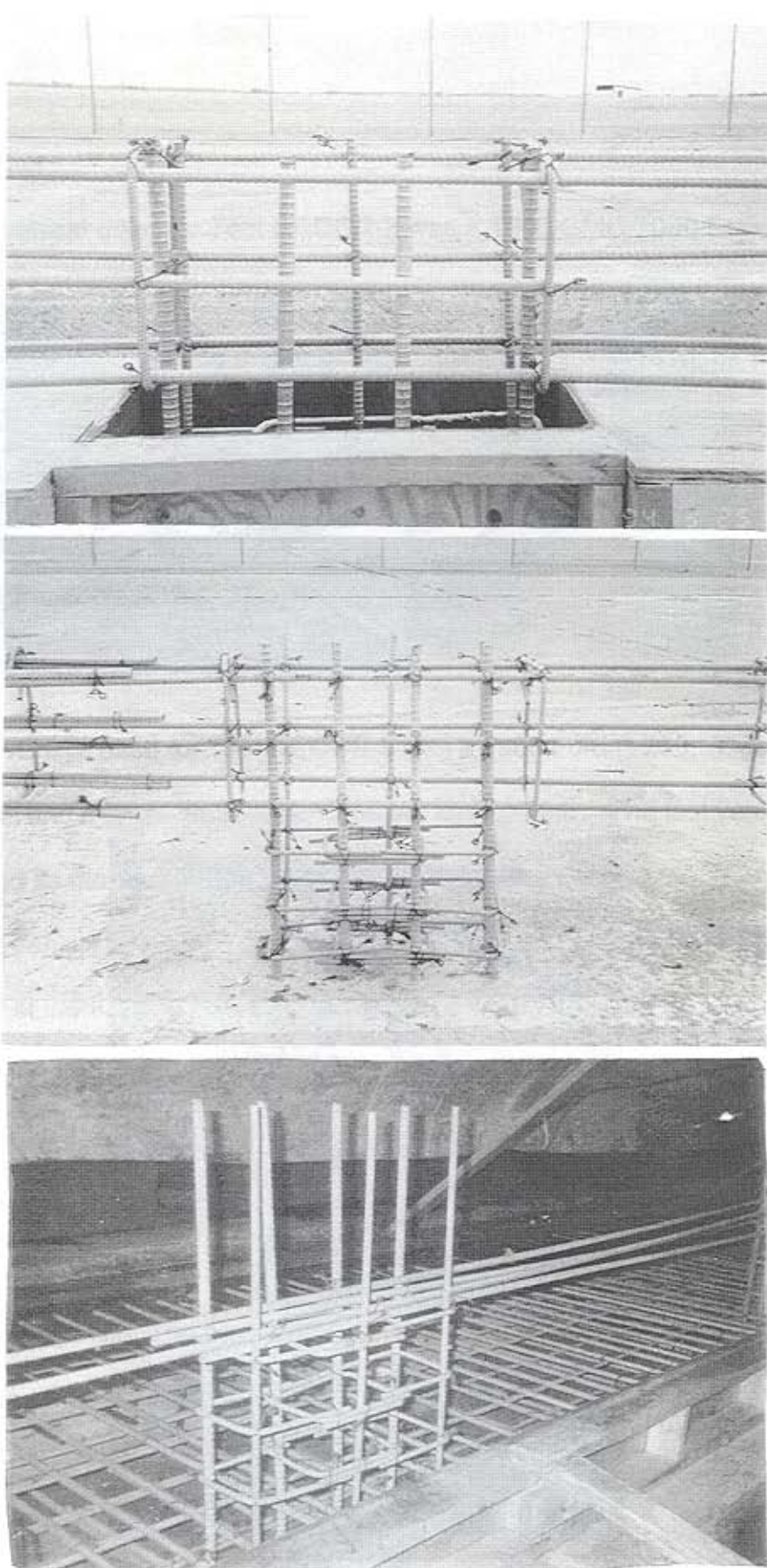


FIGURE 6. Reinforcement Layout for 2-ft Posts.

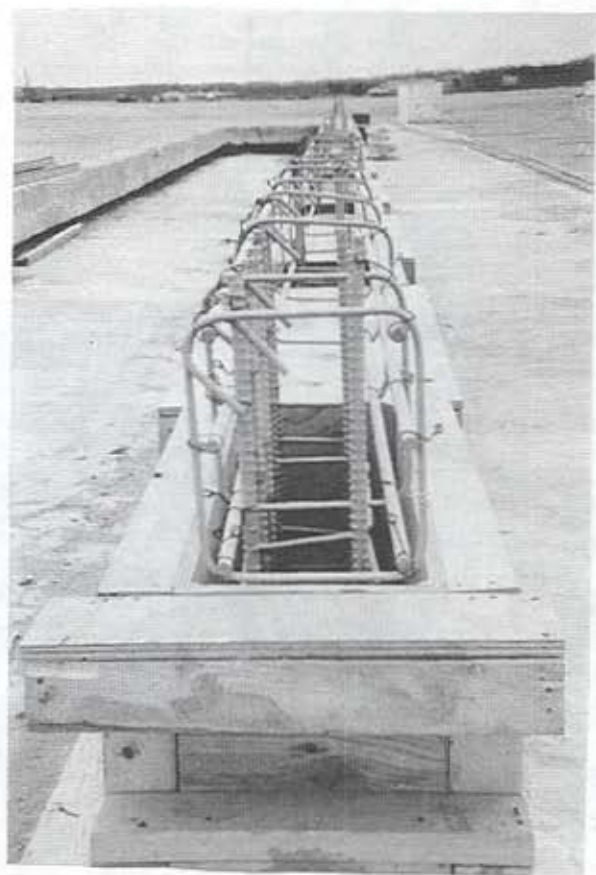
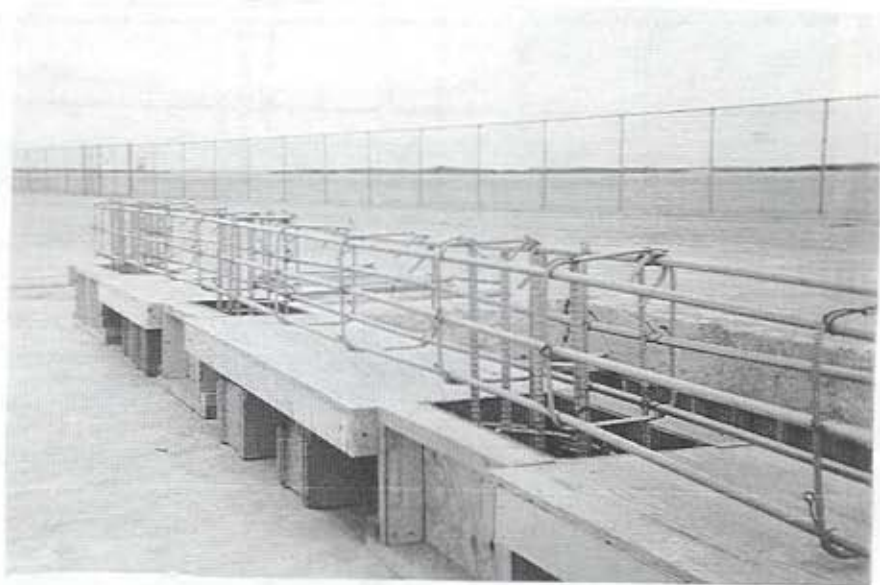


FIGURE 7. Reinforcement Layout for Bridge Rail

2.3 Test Vehicles

The test vehicle used for Test NEOCR-3 was a 1986 GMC 7000 Series truck with a 6.7-m (22 ft.) box. The test vehicle had a test inertial and a gross static weight of 8165 kg (18,000 lb.) The vehicle is shown in Figure 8 and its dimensions are shown in Figure 9.

The test vehicle used for Test NEOCR-4 was a 1987 GMC 7000 Series truck with a 6.7-m (22 ft.) box. This test vehicle had a test inertial and a gross static weight of 8165 kg (18,000 lb). The vehicle is shown in Figure 10, and its dimensions are shown in Figure 11.

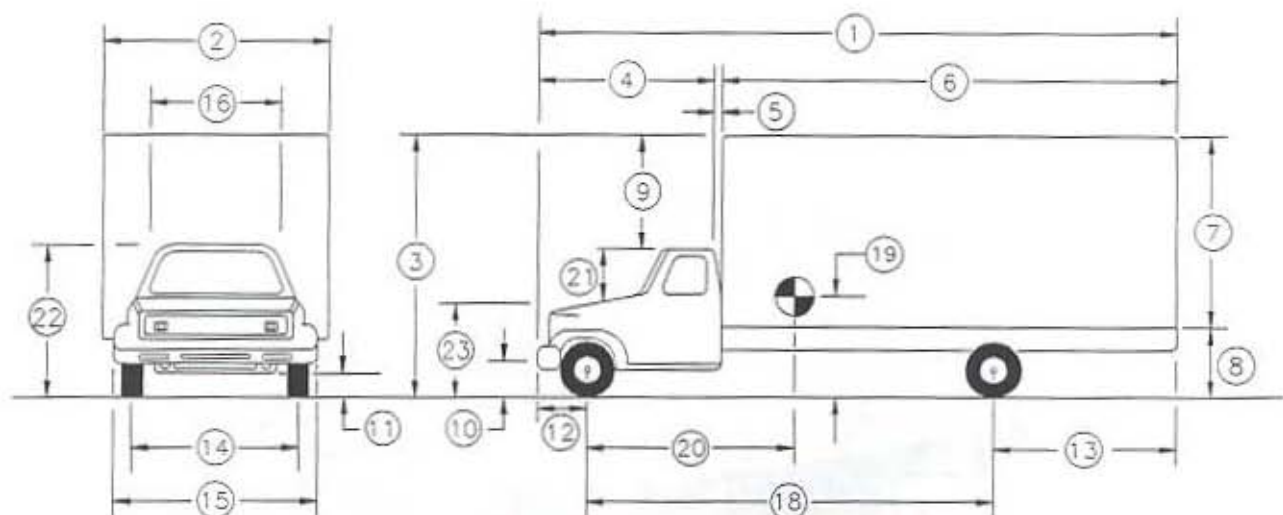
The test vehicle used for Test NEOCR-5 was a 1986 Ford F-250. This test vehicle had a test inertial and a gross static weight of 2447 kg (5,394 lb). The test vehicle is shown in Figure 12, and its dimensions are shown in Figure 13.

The test vehicle used for Test NEOCR-6 was a 1985 Dodge Ram 250. This test vehicle had a test inertial and gross static weight of 2449 kg (5,399 lb). The test vehicle is shown in Figure 14, and its dimensions are shown in Figure 15.

The front wheels of the test vehicle were aligned for camber, caster, and toe-in values of zero so that the vehicle would track properly along the guide cable. Two 5B flash bulbs were mounted on the roof of the vehicle to pinpoint the time of impact with the bridge rail on the high-speed film. The flash bulbs were fired by a pressure tape switch mounted on the front face of the bumper.



FIGURE 8. Test Vehicle, Test NEOCR-3



Model 1986 GMC 7000 Series

Test Inertial Weight: (kg/lbs)

Total Weight	<u>8165/(18000)</u>
Front Weight	<u>3906/(8612)</u>
Rear Axle Weight	<u>4258/(9388)</u>
Ballast	<u>3107/(6850)</u>

① Overall Length	<u>1011/(398)</u>	⑬ Rear Overhang	<u>323/(127)</u>
② Overall Width	<u>229/(90)</u>	⑭ Front Track Width	<u>196/(77)</u>
③ Overall Front Height	<u>328/(129)</u>	⑮ Front Bumper Width	<u>229/(90)</u>
④ Cab Length	<u>244/(96)</u>	⑯ Roof Width	<u>147/(58)</u>
⑤ Gap Length	<u>5.1/(2)</u>	⑰ Typical Tire Size and Diameter	<u>102/(40)</u>
⑥ Trailer/Box Length	<u>744/(293)</u>	⑱ Wheel Base	<u>610/(240)</u>
⑦ Rear Body Height	<u>216/(85)</u>	⑲ C.G. Height	<u>122/(48)</u>
⑧ Rear Ground Clearance	<u>112/(44)</u>	⑳ C.G. Longitudinal Distance	<u>318/(125)</u>
⑨ Roof Height Differential	<u>284/(45)</u>	㉑ Roof-Hood Distance	<u>51/(20)</u>
⑩ Front Ground Clearance	<u>45.8/(18)</u>	㉒ Roof Height	<u>216/(85)</u>
⑪ Minimum Ground Clearance	<u>27.9/(11)</u>	㉓ Hood Height	<u>160/(63)</u>
⑫ Front Overhang	<u>83.8/(33)</u>		

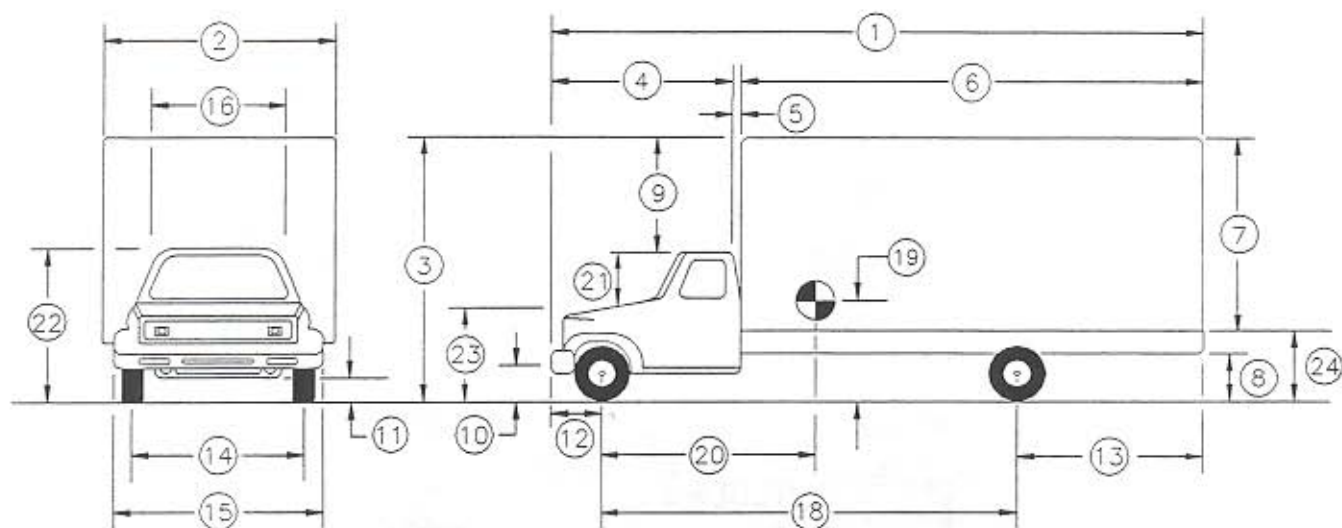
NOTE: NO SCALE

All measurements are in cm/(in.)

FIGURE 9. Test Vehicle Dimensions and Weights, Test NEOCR-3



FIGURE 10. Test Vehicle, Test NEOCR-4



Model 1987 GMC 7000 Series

Test Inertial Weight: (kg/lbs)

Total Weight 8165/(18000)

Front Weight 3890/(8576)

Rear Axle Weight 4275/(9424)

Ballast 2654/(5850)

① Overall Length	<u>996/(392)</u>	⑬ Rear Overhang	<u>311/(122.5)</u>
② Overall Width	<u>241/(95)</u>	⑭ Front Track Width	<u>196/(77)</u>
③ Overall Front Height	<u>337/(132.5)</u>	⑮ Front Bumper Width	<u>227/(89.5)</u>
④ Cab Length	<u>245/(96.5)</u>	⑯ Roof Width	<u>147/(58)</u>
⑤ Gap Length	<u>10.2/(4)</u>	⑰ Typical Tire Size and Diameter	<u>105.4/(41.5)</u>
⑥ Trailer/Box Length	<u>744/(293)</u>	⑱ Wheel Base	<u>605/(238)</u>
⑦ Rear Body Height	<u>216/(85)</u>	⑲ C.G. Height	<u>124/(49)</u>
⑧ Rear Ground Clearance	<u>82.6/(32.5)</u>	⑳ C.G. Longitudinal Distance	<u>316/(124.5)</u>
⑨ Roof Height Differential	<u>118/(46.5)</u>	㉑ Roof-Hood Distance	<u>61/(24)</u>
⑩ Front Ground Clearance	<u>44.5/(17.5)</u>	㉒ Roof Height	<u>215/(84.5)</u>
⑪ Minimum Ground Clearance	<u>29.2/(11.5)</u>	㉓ Hood Height	<u>152/(60)</u>
⑫ Front Overhang	<u>76.2/(30)</u>	㉔ Floor Height	<u>123/(48.5)</u>

NOTE: NO SCALE

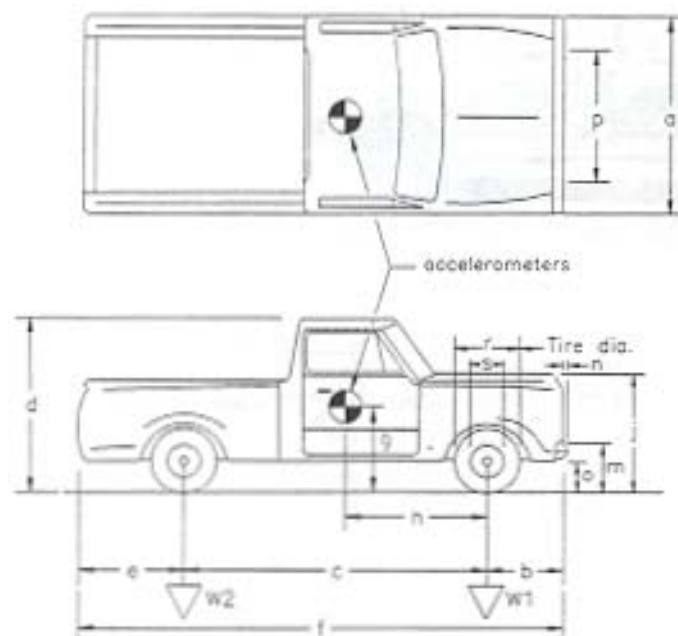
All measurements are in cm/(in.)

FIGURE 11. Test Vehicle Dimensions and Weights, Test NEOCR-4



FIGURE 12. Test Vehicle, Test NEOCR-5

Date: 9/1/94 Test No.: NEOCR-5 Model: F-250
 Make: Ford Vehicle I.D.#: 1FTHF25H7GPA58944
 Tire Size: LT235/85R16 Year: 1986 Odometer: 32505



Vehicle Geometry - cm (in.)

a 189/(74.5) b 71.1/(28)
 c 337/(132.5) d 189.2/(74.5)
 e 123/(48.5) f 533/(210)
 g 58.6/(27) h 183/(72)
 i - j 123/(48.5)
 k - l -
 m 58.6/(27) n 7.6/(3)
 o 47.6/(18.75) p 168/(66)
 r 77.5/(30.5) s 43.2/(17)

Engine Type: V8

Engine Size: 351 (5.8L)

Transmission Type:

Automatic or Manual

FWD or RWD or 4WD

Weight - (kg/lbs)	Curb	Test Inertial	Gross Static
W1	1070/(2360)	1119/(2467)	1119/(2467)
W2	807/(1780)	1328/(2927)	1328/(2927)
Wtotal	1878/(4140)	2447/(5394)	2447/(5394)

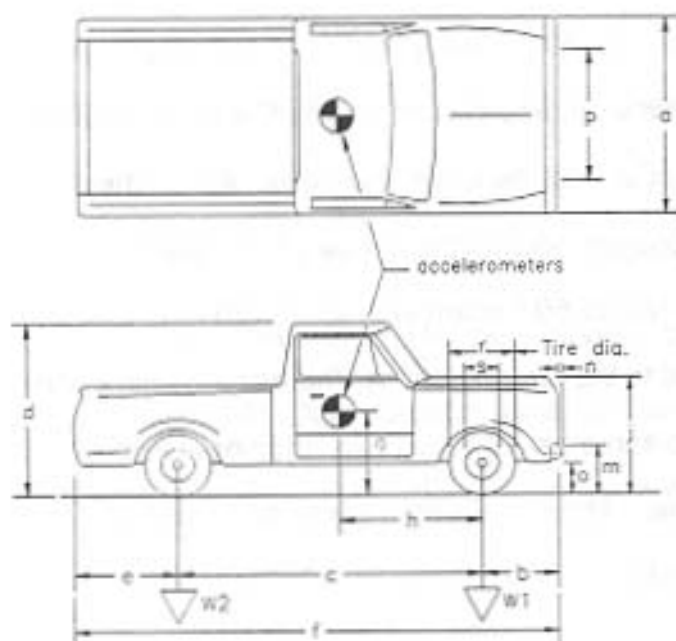
Note any damage prior to test: Driver-side door creased at front joint.

FIGURE 13. Test Vehicle Dimensions and Weights, Test NEOCR-5



FIGURE 14. Test Vehicle, Test NEOCR-6

Date: 10/20/94 Test No.: NEOCR-6 Model: Ram 250
 Make: Dodge Vehicle I.D.#: 1B7JD24T1FS5122
 Tire Size: 9.50-16.5LT Year: 1985 Odometer: 43718



Vehicle Geometry - cm (in.)

a	<u>196/(77)</u>	b	<u>81.3/(32)</u>
c	<u>333/(131)</u>	d	<u>178/(70)</u>
e	<u>117/(46)</u>	f	<u>544/(214)</u>
g	<u>58.6/(27)</u>	h	<u>178/(70)</u>
i	<u>-</u>	j	<u>119/(47)</u>
k	<u>-</u>	l	<u>-</u>
m	<u>63.5/(25)</u>	n	<u>10.2/(4)</u>
o	<u>45.7/(18)</u>	p	<u>165/(65)</u>
r	<u>73.7/(29)</u>	s	<u>43.2/(17)</u>

Engine Type: V8

Engine Size: 5.2 Liter

Transmission Type:

Automatic or Manual

FWD or RWD or 4WD

Weight - (kg/lbs)	Curb	Test Inertial	Gross Static
W1	1107/(2440)	1145/(2524)	1145/(2524)
W2	776/(1710)	1304/(2875)	1304/(2875)
Wtotal	1882/(4150)	2449/(5399)	2449/(5399)

Note any damage prior to test: Extensive rust to box floor and cab floor.

FIGURE 15. Test Vehicle Dimensions and Weights, Test NEOCR-6

2.4 Data Acquisition Systems

Vehicle reactions during the full-scale testing program were monitored with SVHS video, high-speed photography, accelerometers, rate gyro, and tape pressure switches. Each of these data acquisition systems are described in the following subsections.

2.4.1 High-Speed Photography

Five high-speed 16-mm cameras, with operating speeds of approximately 500 frames/sec, were used to film the crash tests. One Red Lake Model 51 LoCam high-speed camera, equipped with a wide-angle 12.5-mm lens, was placed behind the rail to capture the vehicle/rail interaction. A second LoCam camera was located above the test installation on a highrise truck in order to provide an overhead view of the impact. The third high-speed camera was a Red Lake Model 50 Locam with a 76-mm lens located downstream of the system on a line parallel to the installation. A Photec IV camera was placed in this same downstream location to serve as a backup. An additional Photec IV camera was placed perpendicular to the rail. Three additional cameras were used for documentary footage. These were a 16-mm Bolex (64 fr/sec), a SVHS video camera, and a 35-mm camera with a motor-drive shutter.

A grid was painted on the concrete surface parallel and perpendicular to the barrier at the location of each impact. The white-colored grid was incremented with 1.5-m (5-ft) divisions in both directions to give a visible reference system which could be used in the analysis of the overhead high-speed film. Targets, measuring 20.3-cm (8-in.) square, were also painted on the rail in order to monitor lateral displacement of the rail using the high-speed film. The film was analyzed using a Vanguard Motion Analyzer. Actual camera speeds and camera divergence factors were considered in the analysis of the high-speed film.

2.4.2. Accelerometers and Rate Gyro

Two triaxial piezoresistive accelerometer systems with a range of ± 200 G's (Endevco Model 7264) were used to measure vehicle accelerations. A Humphrey 3-axis rate transducer with a range of 250 deg/sec in each of the three directions (roll, pitch, and yaw) was used to measure the rotational rates. Since vehicle rotations become coupled in the presence of high rotation rates, an uncoupling procedure of the measured angular velocities was conducted. The accelerometers and rate gyro were rigidly attached to a metal block mounted near the vehicle's center of gravity.

Signals were transmitted and received via telemetry and stored on a Honeywell 101 Analog Tape Recorder. The signals were then conditioned by an onboard Series 300 Multiplexed FM Data System built by Metraplex Corporation. "Enhanced Graphics Acquisition and Analysis" (EGAA) software was used to digitize the data and store it for analysis with "Data Analysis and Display Software" (DaDiSP).

An Environmental Data Recorder (EDR-3), developed by Instrumented Sensor Technology (IST) of Okemos, Michigan was also used to record the accelerations during the full-scale tests at a sample rate of 3200 Hz. This self-contained unit consists of a triaxial accelerometer system, triggering upon impact and storing the data on board. The EDR-3 was configured with 256 kB of RAM memory and a 1,120 Hz filter. Computer software, "DynaMax 1 (DM-1)", was then used to download the EDR-3 unit and filter the data with a 180 Hz low-pass filter.

2.4.3 Speed Trap Switches

Six tape pressure switches spaced at 1.5-m (5-ft) intervals were used to determine the speed of the vehicle before and after impact. Each tape switch fired a strobe light and sent an electronic timing mark to the data acquisition system as the right front tire of the test vehicle passed over it. Test vehicle speeds were determined from recorded electronic timing mark data. Strobe lights and high speed film analysis were used only as a backup in the event that the electronic data was not available to determine the vehicle speeds.

3 PERFORMANCE EVALUATION CRITERIA

The safety performance objective of a bridge rail is to reduce death and injury to the occupants of errant vehicles and to protect lives and property on, adjacent to, or below a bridge (5). In order to prevent or reduce the severity of such accidents, special attention should be given to four major design factors. These factors are: (1) strength of the railing to resist impact forces; (2) effective railing height; (3) shape of the face of the railing; and (4) deflection characteristics of the railing (7).

The performance evaluation criteria used to evaluate the four crash tests were taken from the AASHTO *Guide Specifications for Bridge Railings* (5). Performance Level 2 (PL-2) criteria requires testing with an 816-kg (1,800-lb) mini-compact sedan at 96.6 kph (60 mph) and 20 deg, a 2449-kg (5400-lb) pickup at 96.6 kph (60 mph) and 20 deg, and an 8,165-kg (18,000-lb) single-unit truck at 80.5 (50 mph) and 15 deg. A similar bridge rail system with the same effective railing height and shape of railing face had been successfully tested in accordance with the guidelines set forth in NCHRP Report No. 230 (2) by ENSCO, Inc. (1). Therefore, on the basis of those test results, the 816-kg (1,800-lb) crash test was determined to be unnecessary and was not conducted. The test conditions for the required test matrix are shown in Table 1, and the specific evaluation criteria are shown in Table 2.

The safety performance of the bridge rail was evaluated according to three major factors: (1) structural adequacy, (2) occupant risk, and (3) vehicle trajectory after collision. These three evaluation criteria are defined and explained in NCHRP 230 (2). After each test, vehicle damage was assessed by the traffic accident scale (TAD) (8) and the vehicle damage index (VDI) (9). The impact locations were determined using criteria in NCHRP Report 350 (10) *Recommended Procedures for the Safety Performance Evaluation of Highway Features*.

TABLE 1. Crash Test Conditions and Evaluation Criteria

Guidelines	Performance Level	Appurtenance	Test Vehicle	Impact Conditions		Evaluation Criteria ¹	
				Speed	Angle	Required	Desirable
AASHTO	PL-2	Bridge Rail	Pickup Truck	96.6 km/h (60 mph)	20 deg	3. a,b,c,d	3. e,f,g,h
AASHTO	PL-2	Bridge Rail	Medium Single-Unit Truck	80.5 km/h (50 mph)	15 deg	3. a,b,c	3. d,e,f,h

¹ Evaluation criteria explained in Table 2.

TABLE 2. AASHTO Evaluation Criteria

3.a. The test article shall contain the vehicle; neither the vehicle nor its cargo shall penetrate or go over the installation. Controlled lateral deflection of the test article is acceptable.												
3.b. Detached elements, fragments, or other debris from the test article shall not penetrate or show potential for penetrating the passenger compartment or present undue hazard to other traffic.												
3.c. Integrity of the passenger compartment must be maintained with no intrusion and essentially no deformation.												
3.d. The vehicle shall remain upright during and after collision.												
3.e. The test article shall smoothly redirect the vehicle. A redirection is deemed smooth if the rear of the vehicle does not yaw more than 5 degrees away from the railing from time of impact until the vehicle separates from the railing.												
3.f. The smoothness of the vehicle-railing interaction is further assessed by the effective coefficient of friction μ , where $\mu = (\cos\theta - V_p/V)/\sin\theta$. <table><tr><td>μ</td><td>Assessment</td></tr><tr><td>0.0 - 0.25</td><td>Good</td></tr><tr><td>0.26 - 0.35</td><td>Fair</td></tr><tr><td>> 0.35</td><td>Marginal</td></tr></table>	μ	Assessment	0.0 - 0.25	Good	0.26 - 0.35	Fair	> 0.35	Marginal				
μ	Assessment											
0.0 - 0.25	Good											
0.26 - 0.35	Fair											
> 0.35	Marginal											
3.g. The impact velocity of a hypothetical front-seat passenger against the vehicle interior, calculated from vehicle accelerations and 0.61-m (2.0-ft) longitudinal and 0.31-m (1.0-ft) lateral displacements, shall be less than: <table><tr><td colspan="2">Occupant Impact Velocity</td></tr><tr><td>Longitudinal</td><td>Lateral</td></tr><tr><td>9.1 m/s (30 fps)</td><td>7.6 m/s (25 fps)</td></tr></table> and for the vehicle highest 10-ms average accelerations subsequent to the instant of hypothetical passenger impact should be less than: <table><tr><td colspan="2">Occupant ridedown Accelerations - g's</td></tr><tr><td>Longitudinal</td><td>Lateral</td></tr><tr><td>15</td><td>15</td></tr></table>	Occupant Impact Velocity		Longitudinal	Lateral	9.1 m/s (30 fps)	7.6 m/s (25 fps)	Occupant ridedown Accelerations - g's		Longitudinal	Lateral	15	15
Occupant Impact Velocity												
Longitudinal	Lateral											
9.1 m/s (30 fps)	7.6 m/s (25 fps)											
Occupant ridedown Accelerations - g's												
Longitudinal	Lateral											
15	15											
3.h. Vehicle exit angle from the barrier shall not be more than 12 degrees. Within 30.5-m (100-ft) plus the length of the test vehicle from the point of initial impact with the railing, the railing side of the vehicle shall move no more than 6.1-m (20 ft) from the line of the traffic face of the railing.												

4 TEST RESULTS

4.1 Test NEOCR-3 (8165 kg (18,000 lb), 78.1 km/h (48.5 mph), 17.1 deg)

The purpose of Test NEOCR-3 was to evaluate the safety performance of the discontinuous rail section of the Open Concrete Bridge Rail. The location of the impact was 1.5-m (5-ft) upstream from the upstream end of the 11.4-cm (4 ½-in.) gap, as shown in Figure 16. A summary of the test results and the overhead sequential photographs are shown in Figure 17. Additional sequential photographs are shown in Figure 18.

Photographs of the full scale crash test are shown in Figure 19 and 20. After the initial impact with the bridge rail, the right front corner of the vehicle crushed inward. At 0.050 sec, the front corner contacted the 11.4-cm (4 ½-in.) gap, causing the left front tire to blow out. At approximately 0.388 sec, the right rear side of the vehicle contacted the bridge rail causing the right rear tire to blow out. The vehicle became parallel at approximately 0.447 sec and the rear of the truck cleared the gap at approximately 0.539 sec.

The vehicle traveled along the edge of the rail for the total length of bridge rail. Therefore, no exit angle was measured. The blowouts of the front and rear tires on the left side combined with the damage to the front axle caused the vehicle to come to rest 7.62-m (25-ft) downstream of the end of the rail. The vehicle's trajectory is shown in Figure 17. There was no measurable rebound distance as the truck remained in contact with the rail throughout the event. The effective coefficient of friction was determined to be fair (0.35).

Bridge rail damage is shown in Figure 21. Bridge rail damage at the 11.4-cm (4 ½-in.) gap is shown in Figure 22. The majority of the damage was upstream of the 11.4-cm (4 ½-in) gap. Two major diagonal cracks existed on front face and top at Post.

No. 4 as well as extensive concrete spalling at the end of the first section. Tire marks on the face of the rail were visible from the upstream edge of Post No. 4 to Post No. 11, from Post No. 12 to Post No. 14, and from Post No. 16 to Post No. 19. Gouging also occurred on the front face of the rail near Post No. 8 and a diagonal crack was observed on the face and top of the rail at Post No. 3. The maximum permanent set deflection was .95-cm (3/8-in.) at the downstream end of the 11.4-cm (4 ½-in.) gap.

Vehicle damage is shown in Figure 23. Most of the vehicle damage occurred near the left-front corner of the vehicle, consisting primarily of damage to the fender, hood, and bumper. This damage also included major undercarriage damage, disengagement of the front axle, and a severed brake line. Both the left rear wheel and left rear leaf spring were also damaged. There was no deformation to the exterior or interior of the box, as most damage occurred under the height of the box. There was no intrusion nor deformation of the occupant compartment. The vehicle remained upright both during and after the collision. The vehicle damage was assessed by the traffic accident scale (TAD) (8) and the vehicle damage index (VDI) (9), as shown in Figure 17.

The normalized longitudinal occupant impact velocity was determined to be 3.0 m/s (9.7 fps) and the normalized lateral occupant impact velocity was 2.0 m/s (6.6 fps). The highest 0.010-sec average occupant ridedown decelerations were 2.1 g's (longitudinal), and 3.0 g's (lateral). The results of the occupant risk assessment, as determined from the accelerometer data, are summarized in Figure 17. The results are shown graphically in Appendix A.

The performance of the bridge railing system tested was determined to be satisfactory according to the Performance Level 2 criteria given in Tables 1 and 2.

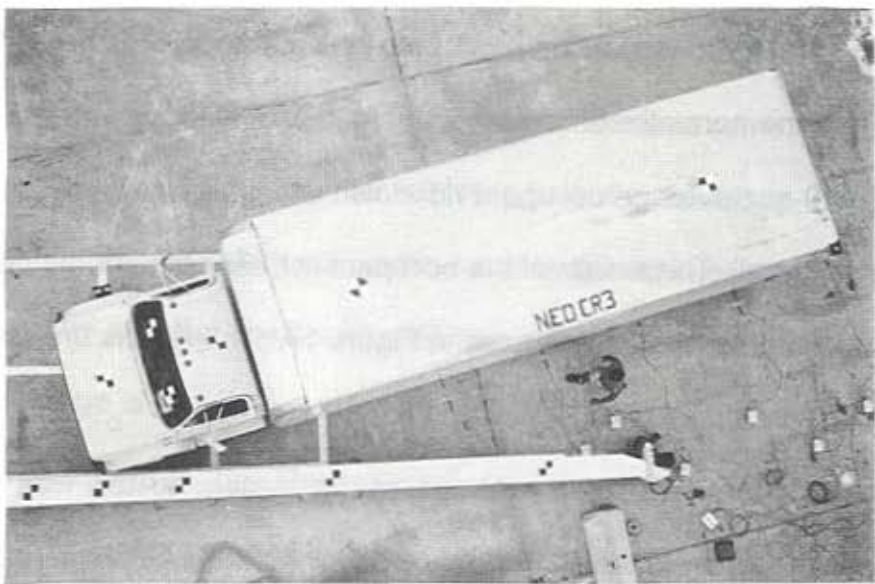
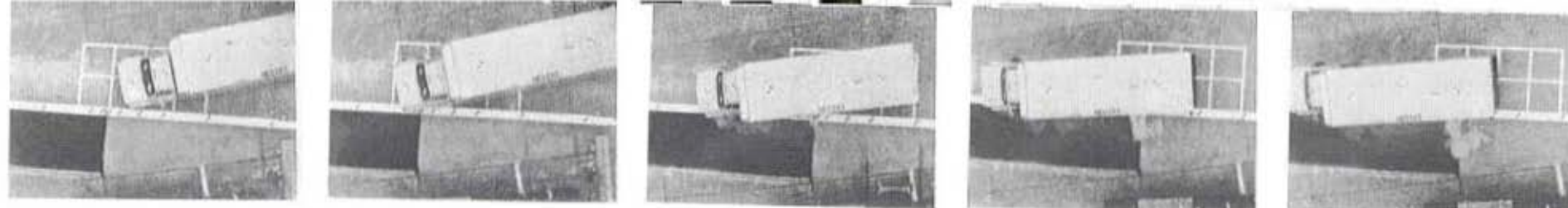


FIGURE 16. Impact Location, Test NEOCR-3



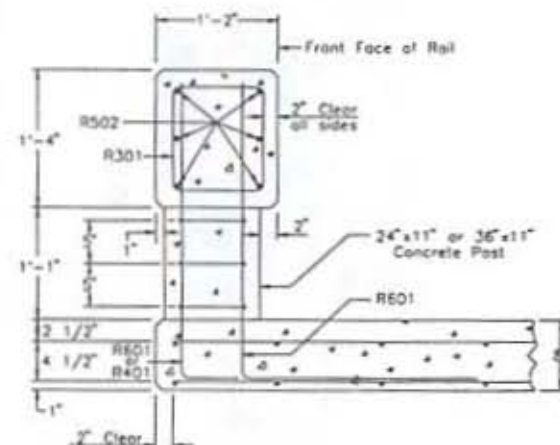
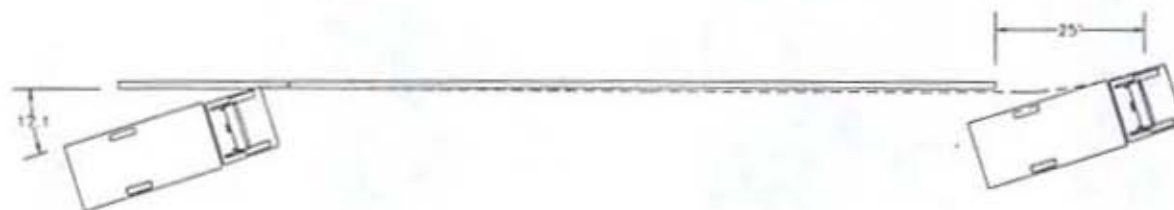
IMPACT

0.080 sec

0.298 sec

0.408 sec

0.447 sec



35

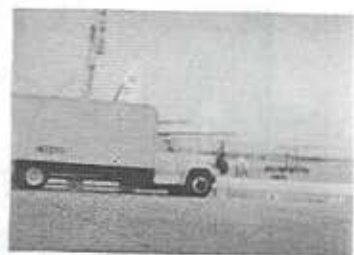
Test Number	NEOCR-3
Date	6/21/94
Installation	Nebraska Open Concrete Rail
Total Length	47.1 m (154 ft - 4 5/8 in.)
Concrete Material	Nebraska 47-BD Mix
Reinforcing Steel Material	Grade 60 Rebar - Epoxy Coated
Concrete Rail	
Length	47.1 m (154 ft - 4 5/8 in.)
Width	35.6 cm (14 in.)
Height	73.7 cm (29 in.)
Depth	40.6 cm (16 in.)
Concrete Posts	
Length	61.0 cm (24 in.)
Width	27.9 cm (11 in.)
Height	33.0 cm (13 in.)
Concrete Posts Adjacent to Gap	
Length	91.4 cm (36 in.)
Width	27.9 cm (11 in.)
Height	33.0 cm (13 in.)
Concrete Bridge Deck	
Length	37.0 m (121 ft - 6 in.)
Width	1.75 m (5 ft - 9 in.)
Depth	20.3 cm (8 in.)

Vehicle	
Model	1986 GMC 7000 Series
Box Length	6.7 m (22 ft)
Test Inertial Weight	8165 kg (18,000 lb)
Vehicle Speed	
Impact	78.1 km/h (48.5 mph)
Exit	NA
Vehicle Angle	
Impact	17.1 deg
Exit	NA
Snagging	None
Vehicle Stability	Satisfactory
Occupant Impact Velocities (Normalized)	
Longitudinal	3.0 m/s (9.7 fps) < 9.1 m/s (30 fps)
Lateral	2.0 m/s (6.6 fps) < 7.6 m/s (25 fps)
Occupant Ridedown Decelerations	
Longitudinal	2.1 G's < 15 G's
Lateral	3.0 G's < 15 G's
Vehicle Damage	
TAD	11-LFQ-3
VDI	11LFW52
Vehicle Rebound Distance	none
Coefficient of Friction (μ)	0.35 (fair)
Bridge Rail Damage	Concrete Cracking and Spalling at Gap

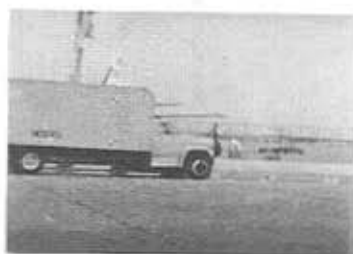
FIGURE 17. Summary and Sequential Photographs, Test NEOCR-3



IMPACT



0.050 sec



0.080 sec



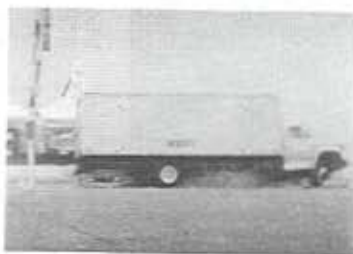
0.179 sec



0.298 sec



0.388 sec



0.408 sec



0.447 sec

FIGURE 18. Additional Sequential Photographs, Test NEOCR-3

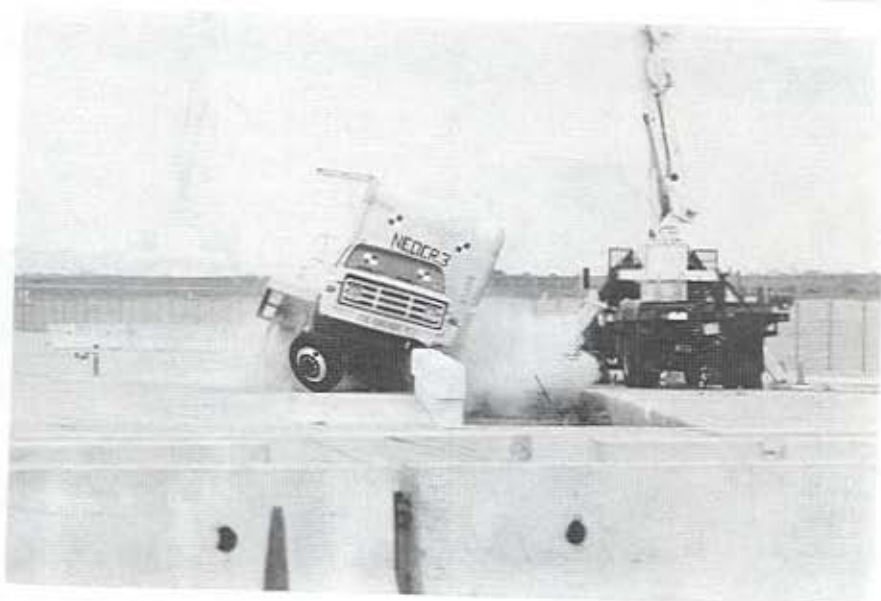


FIGURE 19. Full Scale Test, NEOCR-3



FIGURE 20. Full Scale Test, NEOCR-3

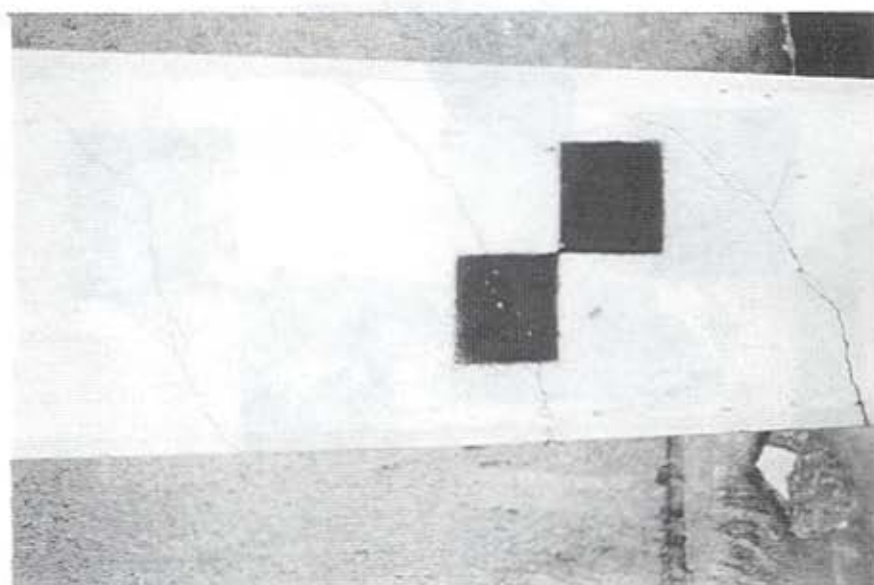
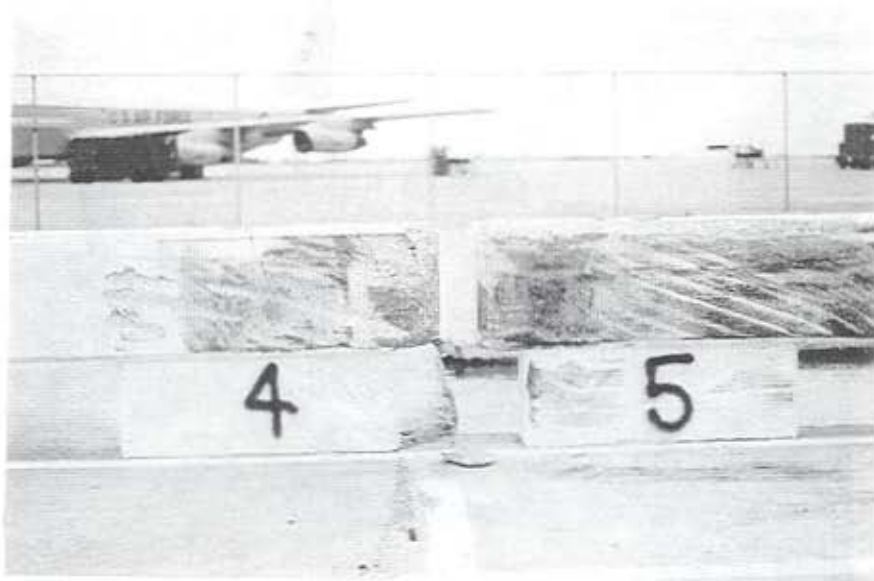


FIGURE 21. Bridge Rail Damage, Test NEOCR-3

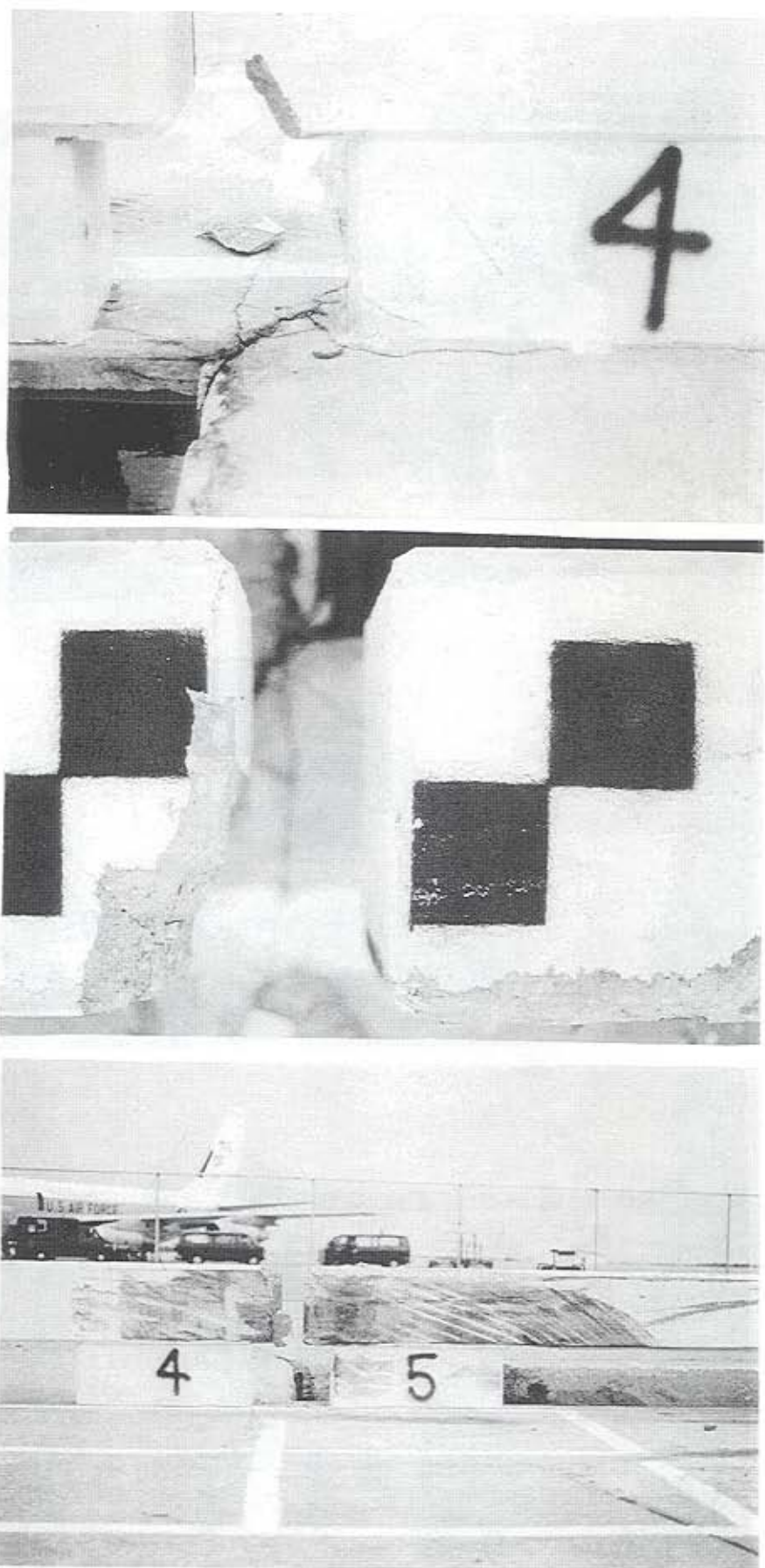


FIGURE 22. Bridge Rail Damage at the 11.4-cm (4 ½-in.) Expansion Gap, Test NEOCR-3

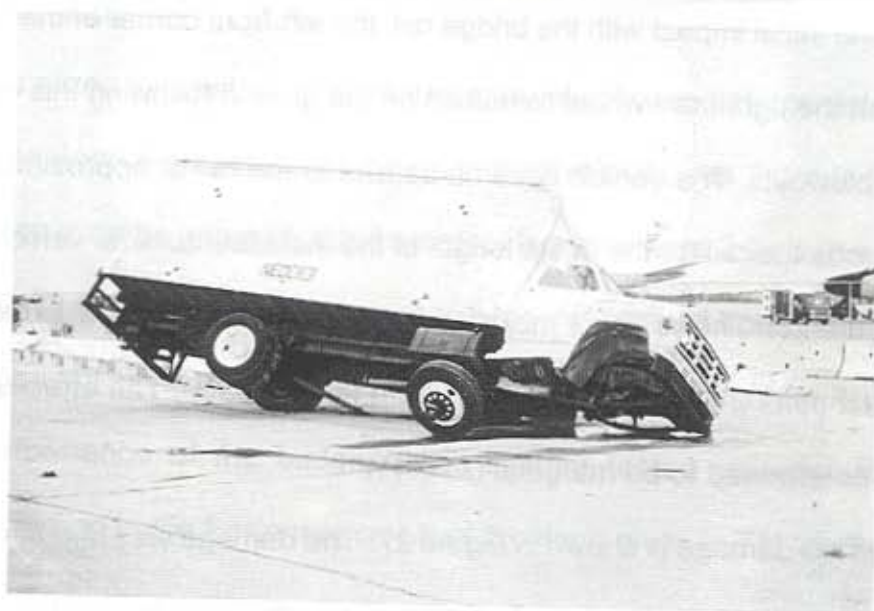


FIGURE 23. Test Vehicle Damage, Test NEOCR-3

4.2 Test NEOCR-4 (8,165 kg (18,000 lb), 83.5 km/h (51.9 mph), 16.8 deg)

The purpose of Test NEOCR-4 was to evaluate the structural adequacy and the redirection capacity of the continuous rail section. The impact location was at the upstream end of Post No. 8, as shown in Figure 24. A summary of the test results and sequential photographs are shown in Figure 25. Additional sequential photographs are shown in Figure 26.

After the initial impact with the bridge rail, the left-front corner of the vehicle crushed inward. All but the right front wheel remained on the ground following this event, and there were no tire blowouts. The vehicle became parallel to the rail at approximately 0.322 sec. The vehicle rode the rail for the entire length of the installation. The vehicle's trajectory is shown in Figure 25. The vehicle's maximum rebound distance was approximately 0.41 m (1-ft 4-in.) at a point 27.4-m (90-ft) downstream from impact. The effective coefficient of friction was determined to be marginal ($\mu=0.41$).

Bridge rail damage is shown in Figure 27. The damage was minor, consisting of tire marks and minor concrete spalling. Tire marks indicated that actual impact was 35.6-cm (14-in.) upstream of the upstream edge of Post No. 9. Concrete spalling occurred at the top of rail at Post No. 8 and gouges were visible from actual impact to downstream end of Post. No. 9. The maximum dynamic deflection obtained from high speed film analysis was 2.9 cm (1.13 in.) at Post No. 9. The maximum permanent set deflection was 1.1 cm (7/16 in.), also at Post. No. 9.

Vehicle damage is shown in Figure 28. All of the vehicle damage occurred on the left-side. This included damage to the front fender, door, and running boards. Damage to the wheels on the left side consisted of the tie rod, control arm, and U-bolt on the left front

being broken, the only damage to the left rear was a bent rim. All tires were still inflated. During impact the box shifted to the left causing bolts connecting the box to be bent on the left side and some broke on the right side. There was also some damage to the left front corner of the box. There was no intrusion nor deformation of the occupant compartment. The vehicle remained upright both during and after the impact. The vehicle damage was assessed by the traffic accident scale (TAD) (7) and the vehicle damage index (VDI) (8), as shown in Figure 25.

The normalized longitudinal occupant impact velocity was determined to be 2.4 m/s (8.0 fps) and the normalized lateral occupant impact velocity was 2.3 m/s (7.7 fps). The highest 0.010-sec average occupant ridedown decelerations were 2.9 g's (longitudinal) and 5.4 g's (lateral). The results of the occupant risk, as determined from the accelerometer data are summarized in Figure 25. The results are shown graphically in Appendix A.

The performance of the bridge railing system tested was determined to be satisfactory according to the Performance Level 2 criteria given in Tables 1 and 2.

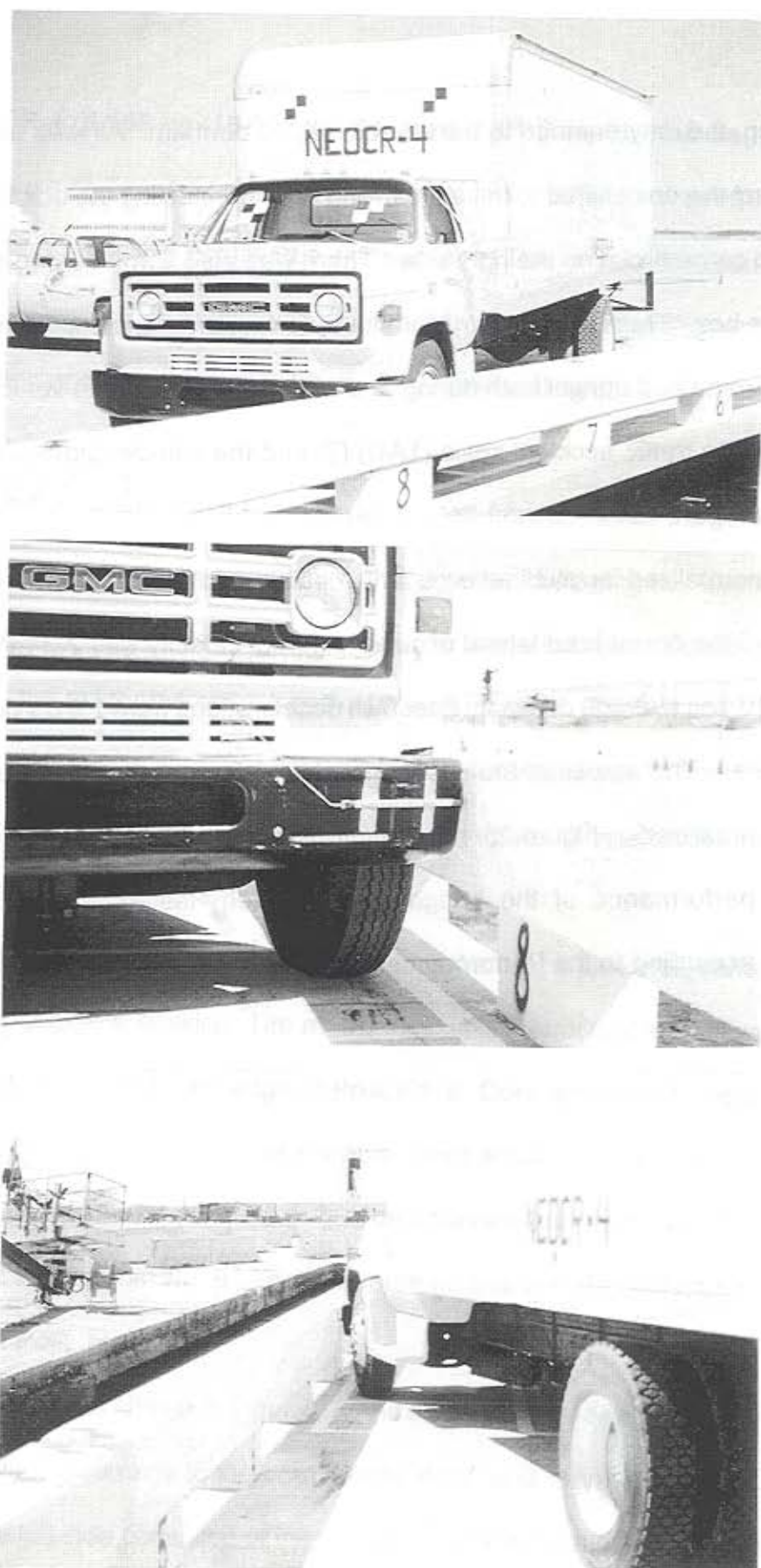
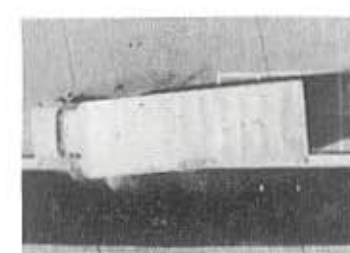
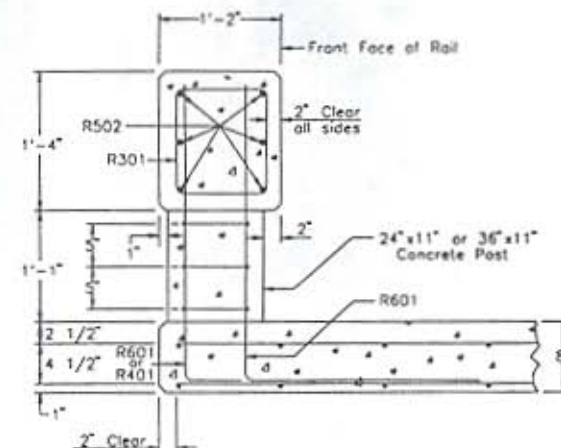
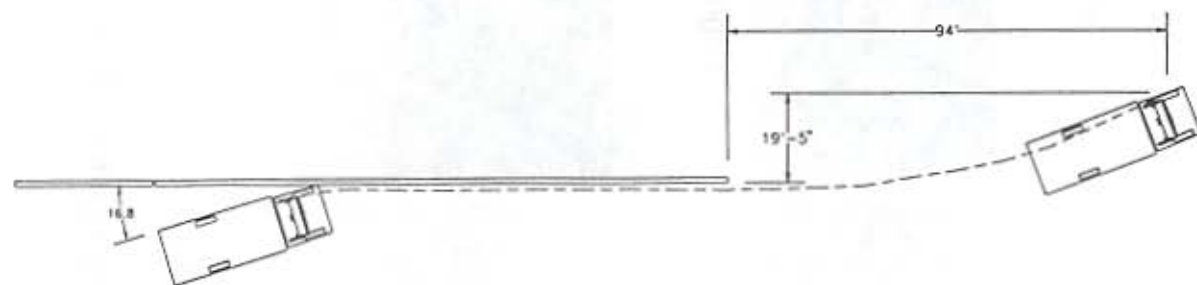


FIGURE 24. Impact Location, Test NEOCR-4



0.322 sec



45

Test Number	NEOCR-4
Date	8/24/94
Installation	Nebraska Open Concrete Rail
Total Length	47.1 m (154 ft - 4 5/8 in.)
Concrete Material	Nebraska 47-BD Mix
Reinforcing Steel Material	Grade 60 Rebar - Epoxy Coated
Concrete Rail	
Length	47.1 m (154 ft - 4 5/8 in.)
Width	35.6 cm (14 in.)
Height	73.7 cm (29 in.)
Depth	40.6 cm (16 in.)
Concrete Posts	
Length	61.0 cm (24 in.)
Width	27.9 cm (11 in.)
Height	33.0 cm (13 in.)
Concrete Posts Adjacent to Gap	
Length	91.4 cm (36 in.)
Width	27.9 cm (11 in.)
Height	33.0 cm (13 in.)
Concrete Bridge Deck	
Length	37.0 m (121 ft - 6 in.)
Width	1.75 m (5 ft - 9 in.)
Depth	20.3 cm (8 in.)

Vehicle	
Model	1987 GMC 7000 Series
Box Length	6.7 m (22 ft)
Test Inertial Weight	8165 kg (18,000 lb)
Vehicle Speed	
Impact	83.5 km/h (51.9 mph)
Exit	NA
Vehicle Angle	
Impact	16.8 deg
Exit	NA
Snagging	None
Vehicle Stability	Satisfactory
Occupant Impact Velocities (Normalized)	
Longitudinal	2.4 m/s (8.0 fps) < 9.1 m/s (30 fps)
Lateral	2.3 m/s (7.7 fps) < 7.6 m/s (25 fps)
Occupant Ridedown Decelerations	
Longitudinal	2.9 G's < 15 G's
Lateral	5.4 G's < 15 G's
Vehicle Damage	
TAD	11-LFQ-2
VDI	11LFWE1
Vehicle Rebound Distance	40.6 cm (16 in.)
Coefficient of Friction (μ)	0.41 (marginal)
Bridge Rail Damage	Minor

FIGURE 25. Summary and Sequential Photographs, Test NEOCR-4



IMPACT



0.202 sec



0.403 sec



0.605 sec



0.807 sec



1.009 sec



1.210 sec



1.412 sec

FIGURE 26. Additional Sequential Photographs, Test NEOCR-4

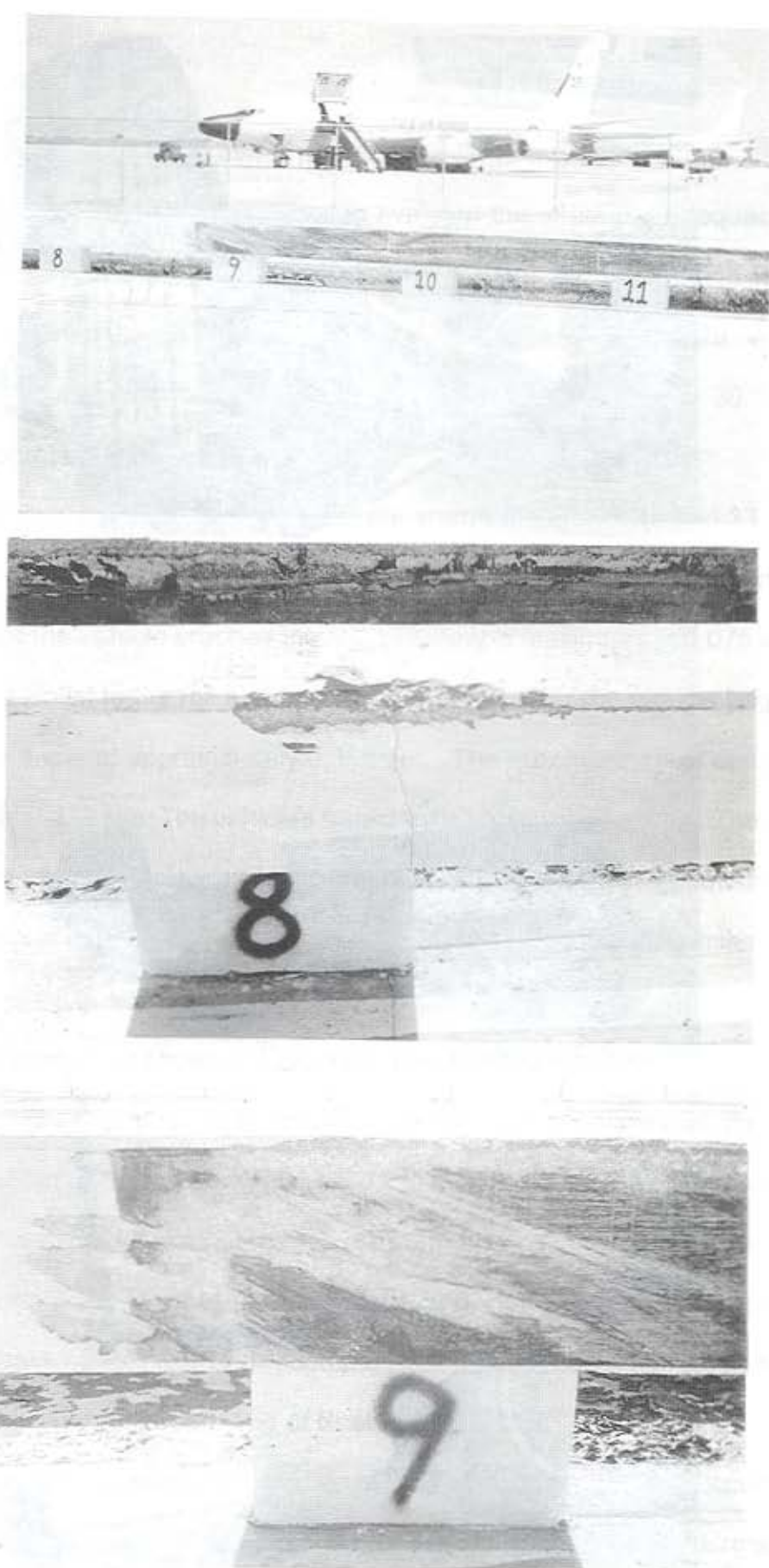


FIGURE 27. Bridge Rail Damage, Test NEOCR-4

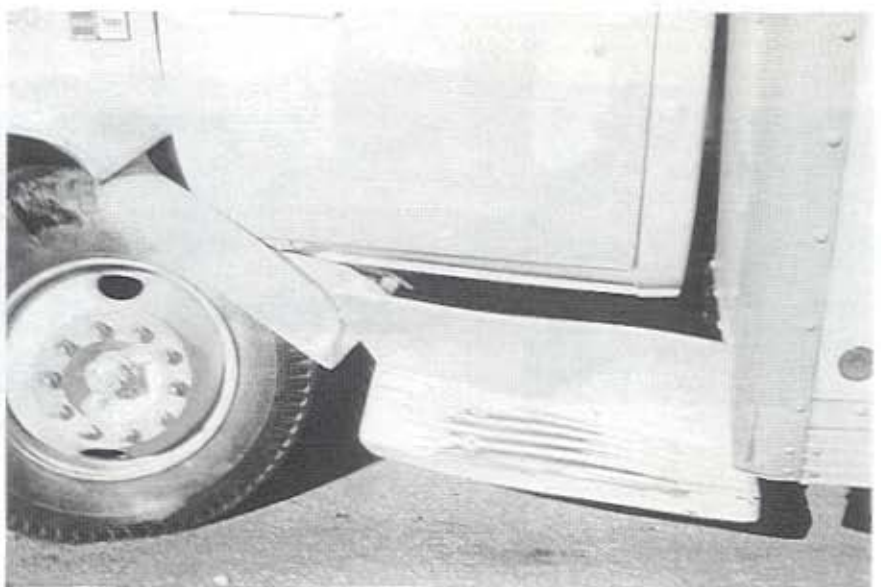
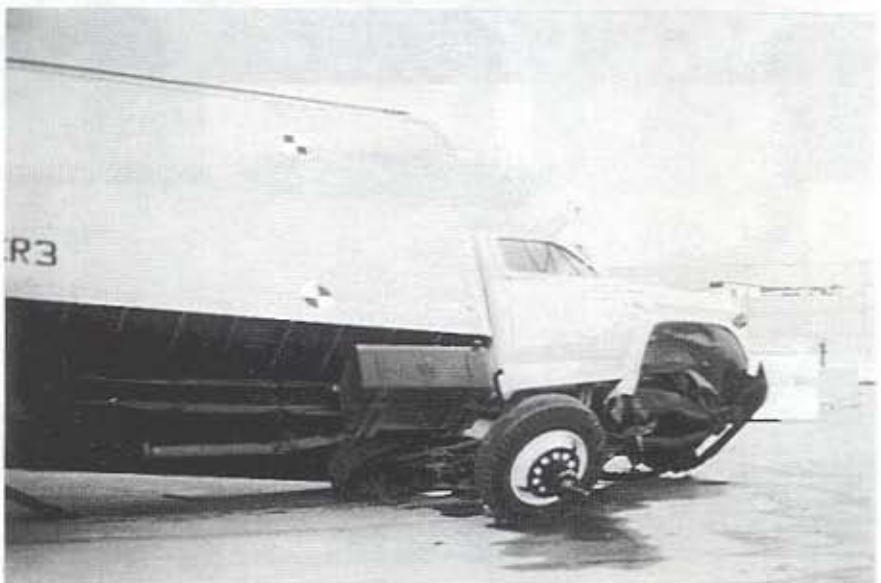
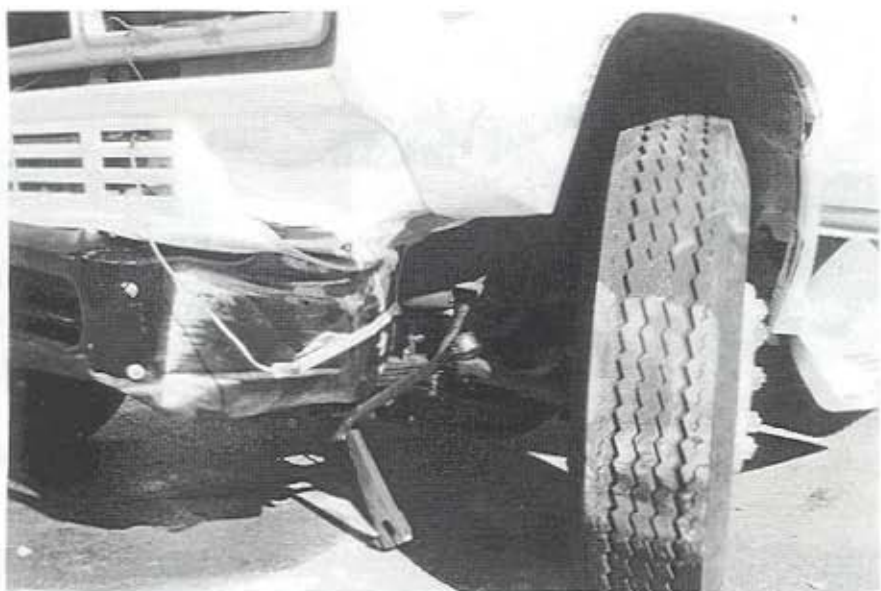


FIGURE 28. Vehicle Damage, Test NEOCR-4

4.3 Test NEOCR-5 (2,447 kg (5,394 lb), 96.2 km/h (59.8 mph), 21.7 deg)

The purpose of Test NEOCR-5 was to evaluate the structural adequacy and the redirection capacity of the continuous rail section. The impact location was at the midspan of the section between Post Nos. 11 and 12, as shown in Figure 29. A summary of the test results and sequential photographs are shown in Figure 30. Additional sequential photographs are shown in Figure 31.

Photographs of the full scale crash test are shown in Figures 32 and 33. After the initial impact with the bridge rail (midspan of the section between Post Nos. 11 and 12), the left-front corner of the vehicle crushed inward, reaching a maximum at 0.075 sec. The vehicle became parallel to the rail at approximately 0.179 sec. The vehicle began to exit at a very shallow angle at approximately 0.359 sec. The maximum roll of approximately 8 deg. occurred at 0.375 sec. The vehicle's trajectory is shown in Figure 30. The maximum rebound distance of the vehicle was approximately 30.5-cm (12-in.) at a location 21.3-m (70-ft) downstream of impact. The effective coefficient of friction was determined to be fair ($\mu=0.31$).

Bridge rail damage is shown in Figure 34. The damage was minor, consisting of tire marks, concrete spalling, and small cracks. Tire marks on the face of the rail were approximately 3.7-m (12-ft) long from Post No. 11 to Post No. 13. Major concrete spalling and scrapes occurred 81.3-cm (32-in) downstream from the downstream end of Post No. 11 for approximately 1.2-m (4-ft) along the bottom of the rail. One diagonal crack formed from the back of Post No. 11 through the deck and another small crack was visible at the back corner of the upstream end of Post No. 11.

Vehicle damage is shown in Figure 35. Most of the vehicle damage occurred on the left-side, consisting primarily of fender, bumper, and undercarriage deformation. The

undercarriage damage consisted of the left front wheel assembly being shoved inward, which caused damage to many key suspension members, including the buckling of the left control arm and the bending of the right control arm, which caused the frame to be twisted. Undercarriage damage is shown in Figure 36. Other damage included deformation inward of the door panel that caused the door to jar out at the top, a cracked windshield on the driver's side, and buckling of the rear bumper. Occupant compartment damage is shown in Figure 37. Damage included an inward crush of the rear of the cab, buckling of the dash, outward buckling of the floor at the driver's side seat location, and downward buckling at driver's side floorboard area. The maximum occupant compartment crush, near the center of the cab compartment floor pan, was approximately 13.3 cm (5 1/4-in.). The center of the dash buckled upward approximately 64 mm (2.5 in.) higher than its original orientation. These occupant compartment deformations were judged to be acceptable, based on the extent and location of the deformations, as discussed in Section 5. The vehicle remained upright both during and after the impact. The vehicle damage was assessed by the traffic accident scale (TAD) (7) and the vehicle damage index (VDI) (8), as shown in Figure 30.

The normalized longitudinal occupant impact velocity was determined to be 5.4 m/s (17.7 fps) and the normalized lateral occupant impact velocity was 6.4 m/s (21.0 fps). The highest 0.010-sec average occupant ridedown decelerations were 9.8 g's (longitudinal) and 9.8 g's (lateral). The results of the occupant risk, as determined from the accelerometer data are summarized in Figure 30. The results are shown graphically in Appendix A.

The performance of the bridge railing system tested was determined to be satisfactory according to the Performance Level 2 criteria given in Tables 1 and 2.

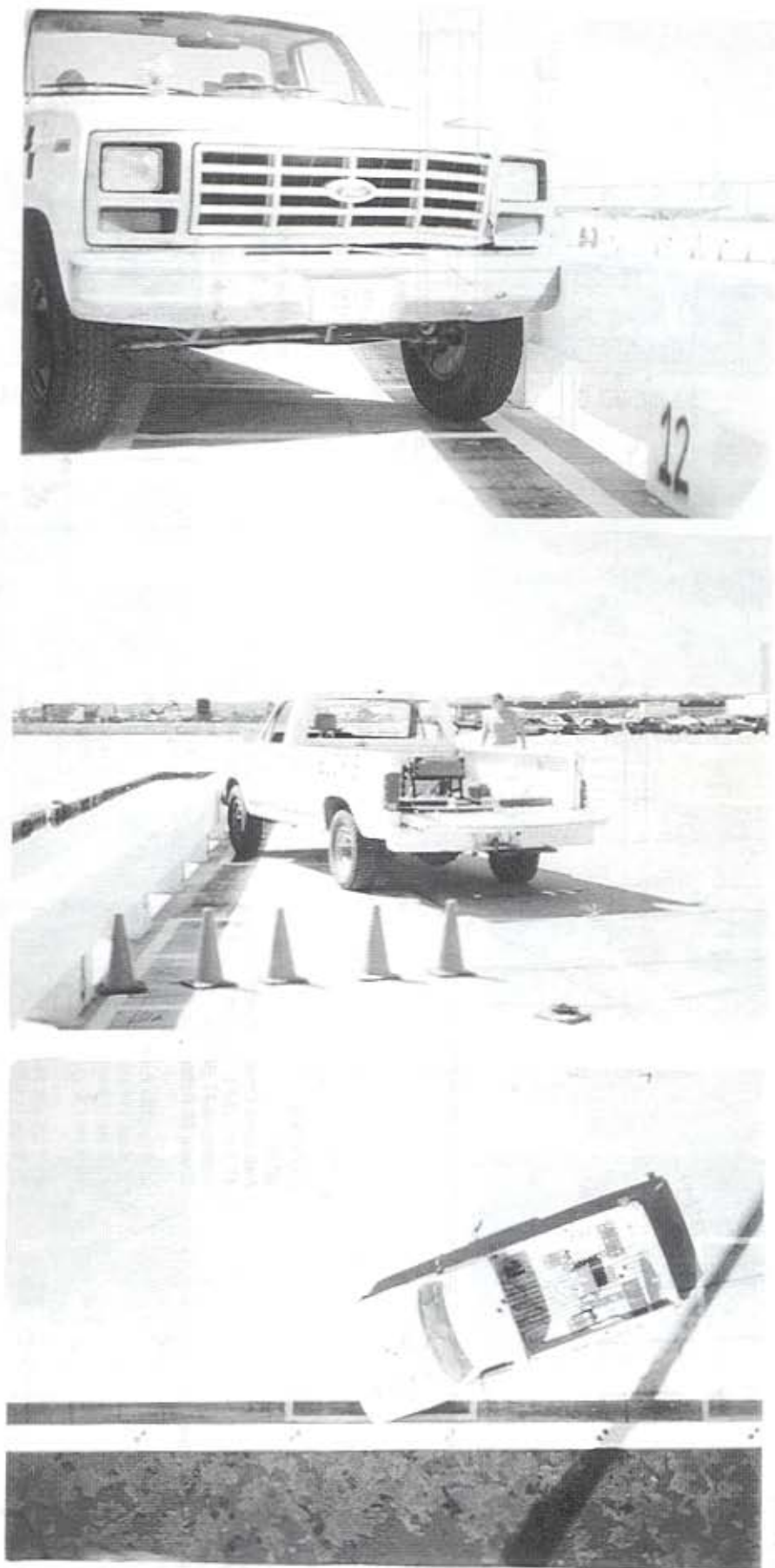
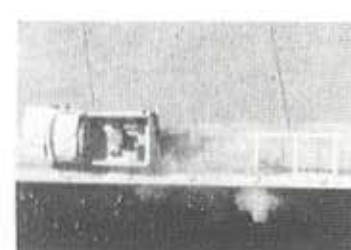
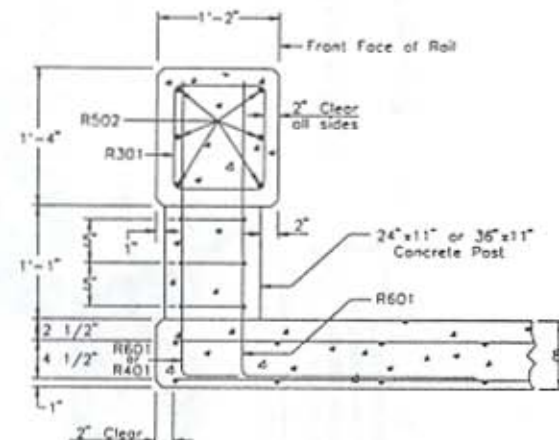
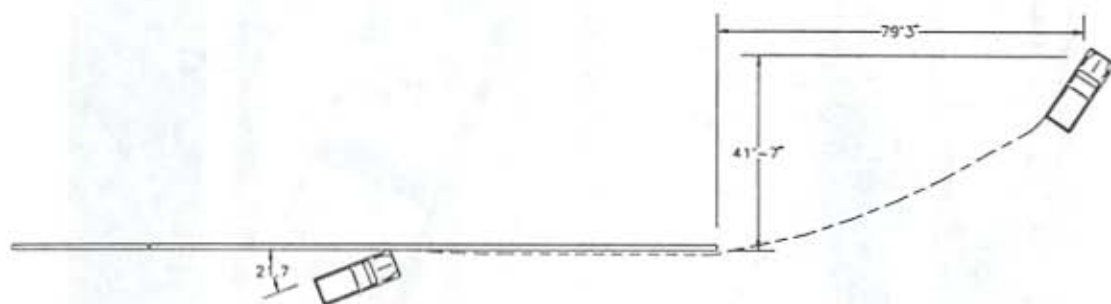


FIGURE 29. Impact Location, Test NEOCR-5



0.478 sec



Test Number	NEOCR-5
Date	9/7/94
Installation	Nebraska Open Concrete Rail
Total Length	47.1 m (154 ft - 4 5/8 in.)
Concrete Material	Nebraska 47-BD Mix
Reinforcing Steel Material	Grade 60 Rebar - Epoxy Coated
Concrete Rail	
Length	47.1 m (154 ft - 4 5/8 in.)
Width	35.6 cm (14 in.)
Height	73.7 cm (29 in.)
Depth	40.6 cm (16 in.)
Concrete Posts	
Length	61.0 cm (24 in.)
Width	27.9 cm (11 in.)
Height	33.0 cm (13 in.)
Concrete Posts Adjacent to Gap	
Length	91.4 cm (36 in.)
Width	27.9 cm (11 in.)
Height	33.0 cm (13 in.)
Concrete Bridge Deck	
Length	37.0 m (121 ft - 6 in.)
Width	1.75 m (5 ft - 9 in.)
Depth	20.3 cm (8 in.)

Vehicle	
Model	1986 Ford F-250
Test Inertial Weight	2447 kg (5,394 lb)
Vehicle Speed	
Impact	96.2 km/h (59.8 mph)
Exit	68.2 km/h (42.4 mph)
Vehicle Angle	
Impact	21.7 deg
Exit	NA
Snagging	None
Vehicle Stability	Satisfactory
Occupant Impact Velocities (Normalized)	
Longitudinal	5.4 m/s (17.7 fps) < 9.1 m/s (30 fps)
Lateral	6.4 m/s (21.0 fps) < 7.6 m/s (25 fps)
Occupant Ridedown Decelerations	
Longitudinal	9.8 G's < 15 G's
Lateral	9.8 G's < 15 G's
Vehicle Damage	
TAD	11-LFQ-4, 11-LP-2
VDI	11LFES2, 11LPES2
Vehicle Rebound Distance	30.5 cm (12 in.)
Coefficient of Friction (μ)	0.31 (fair)
Bridge Rail Damage	Minor

FIGURE 30. Summary and Sequential Photographs, Test NEOCR-5



IMPACT



0.063 sec



0.075 sec



0.125 sec



0.175 sec



0.188 sec



0.375 sec



0.525 sec

FIGURE 31. Additional Sequential Photographs, Test NEOCR-5



FIGURE 32. Full Scale Test, Test NEOCR-5



FIGURE 33. Full Scale Test, Test NEOCR-5

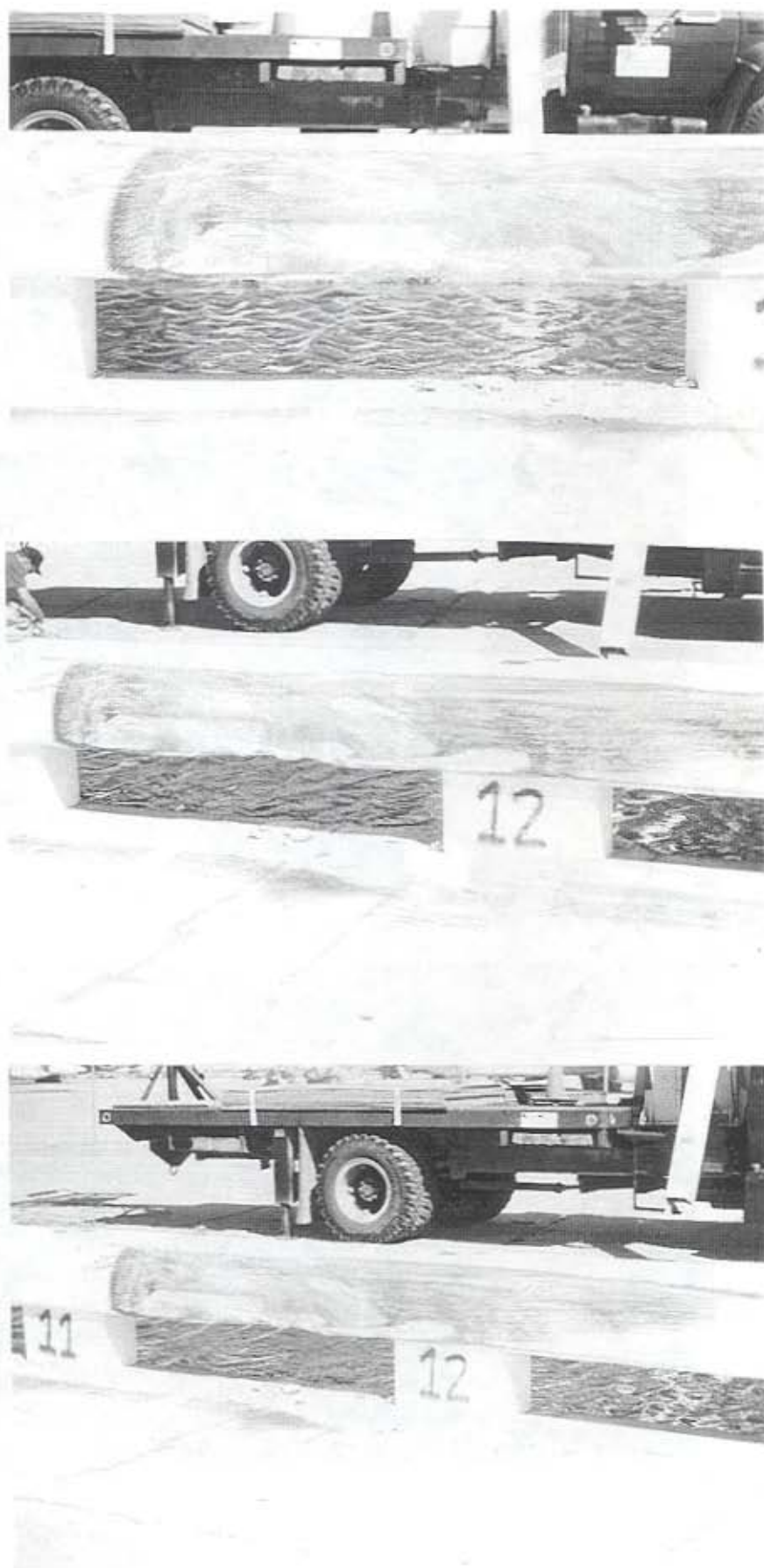


FIGURE 34. Bridge Rail Damage, Test NEOCR-5



FIGURE 35. Vehicle Damage, Test NEOCR-5

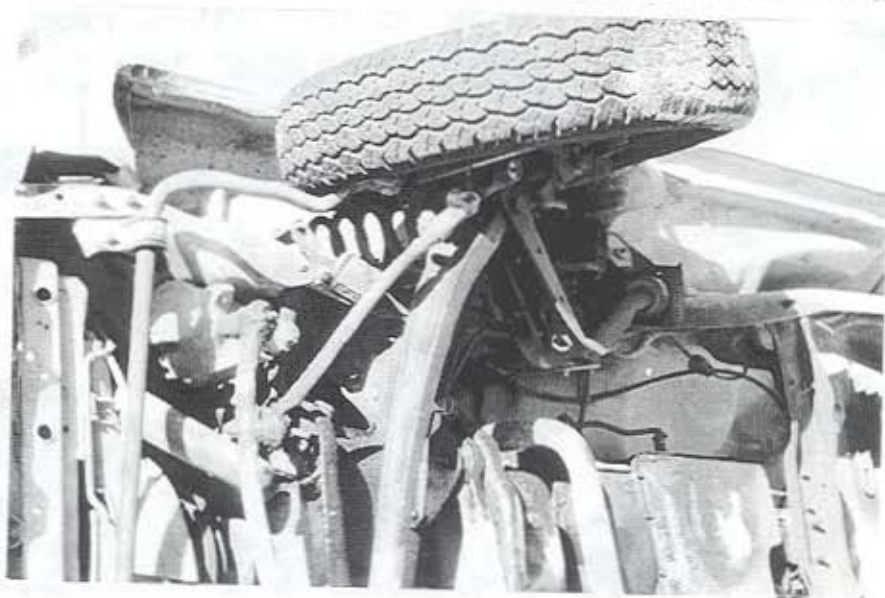
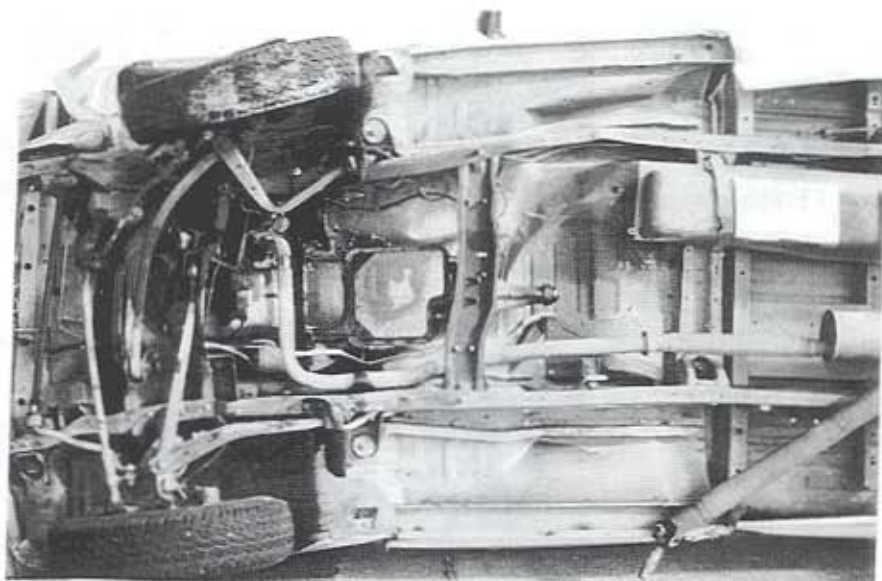


FIGURE 36. Undercarriage Damage, Test NEOCR-5

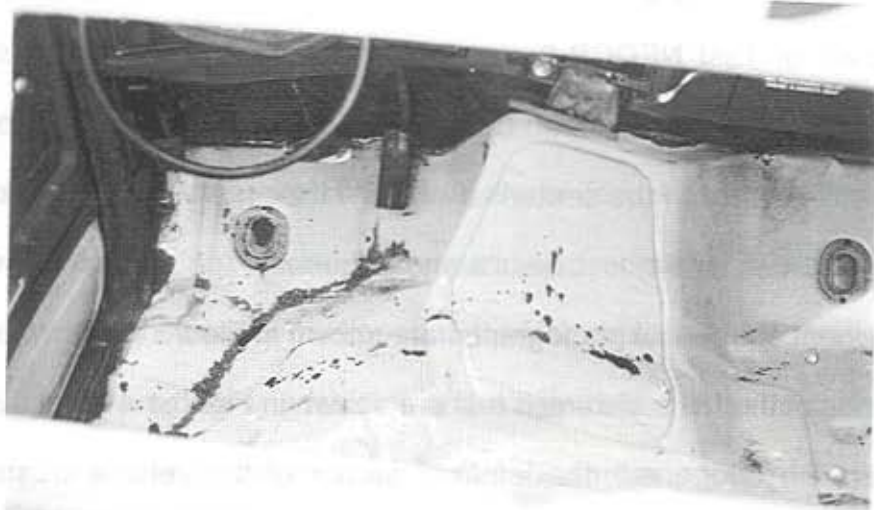


FIGURE 37. Occupant Compartment Damage, Test NEOCR-5

4.4 Test NEOCR-6 (2,449 kg (5,399 lb), 98.2 km/h (61.0 mph), 20 deg)

The purpose of Test NEOCR-6 was to evaluate the safety performance of the discontinuous rail section of the Open Concrete Bridge Rail. The impact location was 1.4-m (4.45-ft) upstream from the centerline of the 11.4-cm (4 ½-in.) gap, as shown in Figure 38. A summary of the test results and sequential photographs are shown in Figure 39. Additional sequential photographs are shown in Figure 40.

Photographs of the full scale crash test are shown in Figures 41 and 42. After the initial impact with the bridge rail, the left-front corner of the vehicle crushed inward, reaching its maximum deformation at 0.119 sec. The vehicle became parallel to the rail at approximately 0.178 sec. The vehicle's trajectory is shown in Figure 39. The right front tire became airborne at approximately 0.138 sec and the right rear tire left the ground at approximately 0.237 sec. These tires returned to the ground at 0.474 sec and 0.553 sec, respectively. The vehicle obtained a maximum roll angle of approximately 8 degrees towards the rail before rolling back and exiting the rail. The vehicle impacted the rail a second time at Post No. 19, at approximately 1.817 sec after impact. The vehicle came to rest after contacting the protective temporary barriers approximately 34-m (112-ft.) downstream from the end of the rail. The vehicle's maximum rebound distance was approximately 1.7-m (67-in.) at a point 21.3-m (70-ft.) downstream from impact. The effective coefficient of friction was determined to be marginal ($\mu=0.40$).

Bridge rail damage is shown in Figure 43. The damage was minor, consisting of tire marks, light concrete spalling from rim contact, and small cracks. Tire marks on the face of the rail ran from approximately 1.8-m (6-ft) upstream of the gap to 16.5-cm (6 ½-in) downstream of the gap and from the centerline of Post No. 19 to the downstream edge of the installation. Minor concrete spalling occurred at Post Nos. 4 and 5. One diagonal

crack formed in the rail near the downstream end of Post No. 3. There was no sign of snag at the 11.4-cm (4 ½-in.) gap.

Vehicle damage is shown in Figure 44. The majority of the vehicle damage occurred on the left-side, consisting primarily of fender, bumper, and undercarriage deformation. The fender was crushed inward approximately two feet. Other damage included deformation inward of the door panel which caused the door to separate from the cab at the top, a cracked windshield, and major deformation to the left front wheel. Occupant compartment damage included crush upward and toward the passenger of the driver's side floorboard and some deformation along the transmission well. The maximum occupant compartment crush, located on the left floor pan area was approximately 89 mm (3 ½-in). These occupant compartment deformations were judged to be acceptable, based on the extent and location of the deformations, as discussed in Section 5. There was no roof, passenger side, or dash board deformation. The vehicle remained upright both during and after the impact. The vehicle damage was assessed by the traffic accident scale (TAD) (7) and the vehicle damage index (VDI) (8), as shown in Figure 39.

The normalized longitudinal occupant impact velocity was determined to be 5.6 m/s (18.5 fps) and the lateral occupant impact velocity was 6.6 m/s (21.6 fps). The highest 0.010-sec average occupant ridedown decelerations were 5.4 g's (longitudinal) and 9.1 g's (lateral). The results of the occupant risk, as determined from the accelerometer data are summarized in Figure 39. The results are shown graphically in Appendix A.

The performance of the bridge railing system tested was determined to be satisfactory according to the Performance Level 2 criteria given in Tables 1 and 2.



FIGURE 38. Impact Location, Test NEOCR-6



IMPACT



0.079 sec



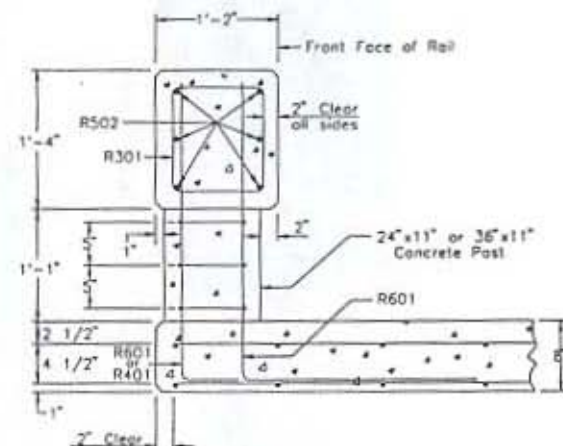
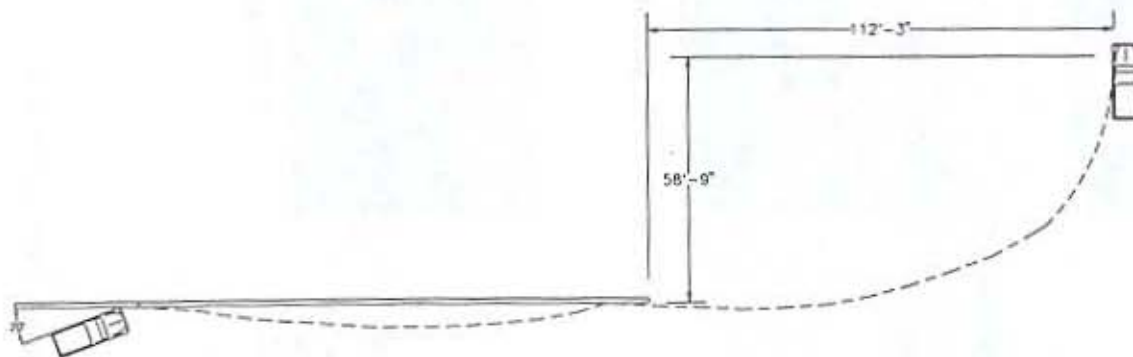
0.138 sec



0.178 sec



0.237 sec



Test Number	NEOCR-6
Date	10/25/94
Installation	Nebraska Open Concrete Rail
Total Length	47.1 m (154 ft - 4 5/8 in.)
Concrete Material	Nebraska 47-BD Mix
Reinforcing Steel Material	Grade 60 Rebar - Epoxy Coated
Concrete Rail	
Length	47.1 m (154 ft - 4 5/8 in.)
Width	35.6 cm (14 in.)
Height	73.7 cm (29 in.)
Depth	40.6 cm (16 in.)
Concrete Posts	
Length	61.0 cm (24 in.)
Width	27.9 cm (11 in.)
Height	33.0 cm (13 in.)
Concrete Posts Adjacent to Gap	
Length	91.4 cm (36 in.)
Width	27.9 cm (11 in.)
Height	33.0 cm (13 in.)
Concrete Bridge Deck	
Length	37.0 m (121 ft - 6 in.)
Width	1.75 m (5 ft - 9 in.)
Depth	20.3 cm (8 in.)

Vehicle	
Model	1985 Dodge Ram 250
Test Inertial Weight	2449 kg (5,399 lb)
Vehicle Speed	
Impact	98.2 km/h (61.0 mph)
Exit	75.2 km/h (46.7 mph)
Vehicle Angle	
Impact	20.0 deg
Exit	NA
Snagging	None
Vehicle Stability	Satisfactory
Occupant Impact Velocities (Normalized)	
Longitudinal	5.6 m/s (18.5 fps) < 9.1 m/s (30 fps)
Lateral	6.6 m/s (21.6 fps) < 7.6 m/s (25 fps)
Occupant Ridedown Decelerations	
Longitudinal	5.4 G's < 15 G's
Lateral	9.1 G's < 15 G's
Vehicle Damage	
TAD	11-LFQ-4, 11-LP-3
VDI	11LFES2, 11LFES2
Vehicle Rebound Distance	1.7 m (67 in.)
Coefficient of Friction (μ)	0.40 (marginal)
Bridge Rail Damage	Minor

FIGURE 39. Summary and Sequential Photographs, Test NEOCR-6



IMPACT



0.079 sec



0.138 sec



0.178 sec



0.237 sec



0.375 sec



0.474 sec



0.553 sec

FIGURE 40. Additional Sequential Photographs, Test NEOCR-6



FIGURE 41. Full Scale Test, Test NEOCR-6

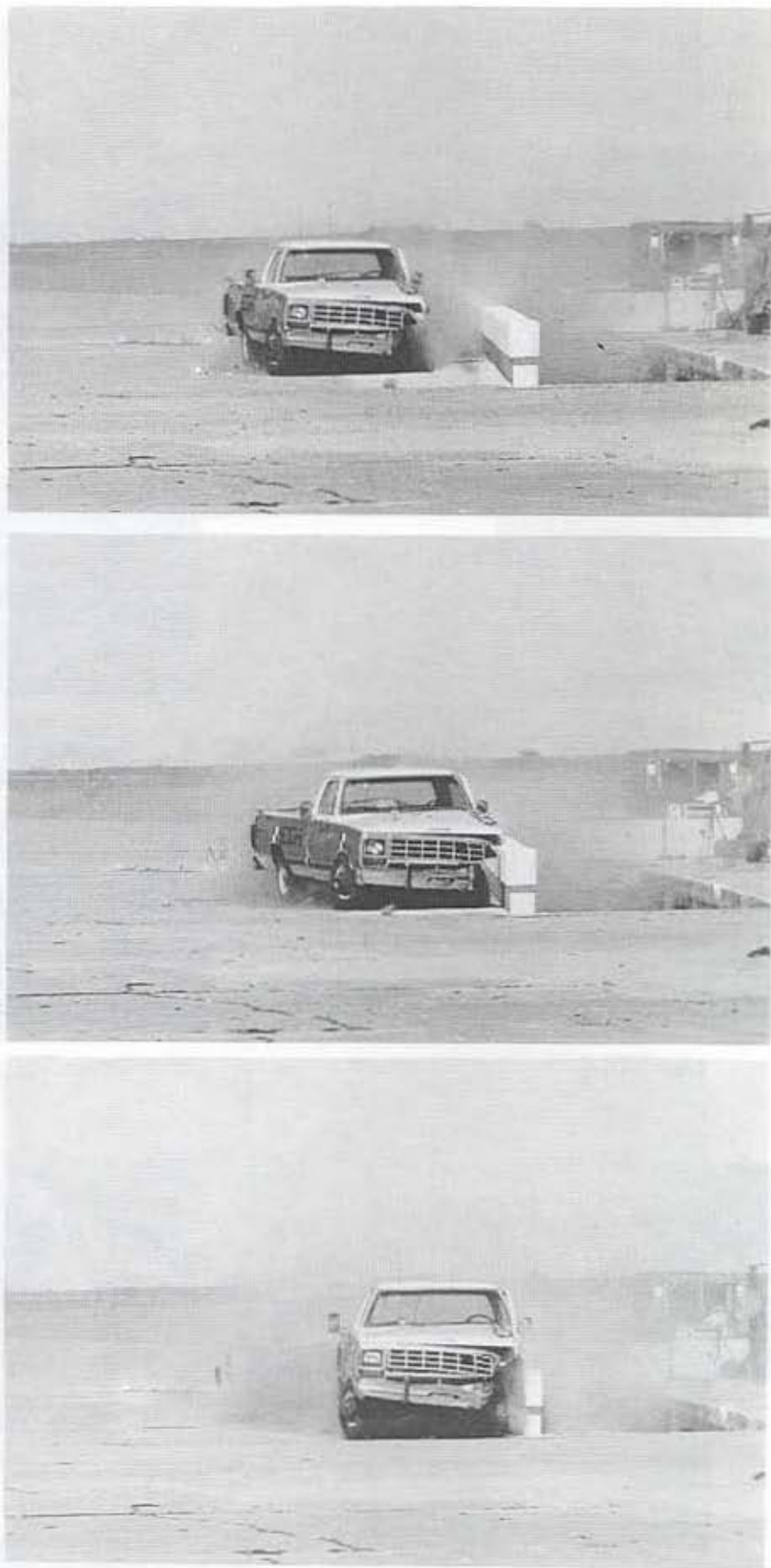


FIGURE 42. Full Scale Test, Test NEOCR-6

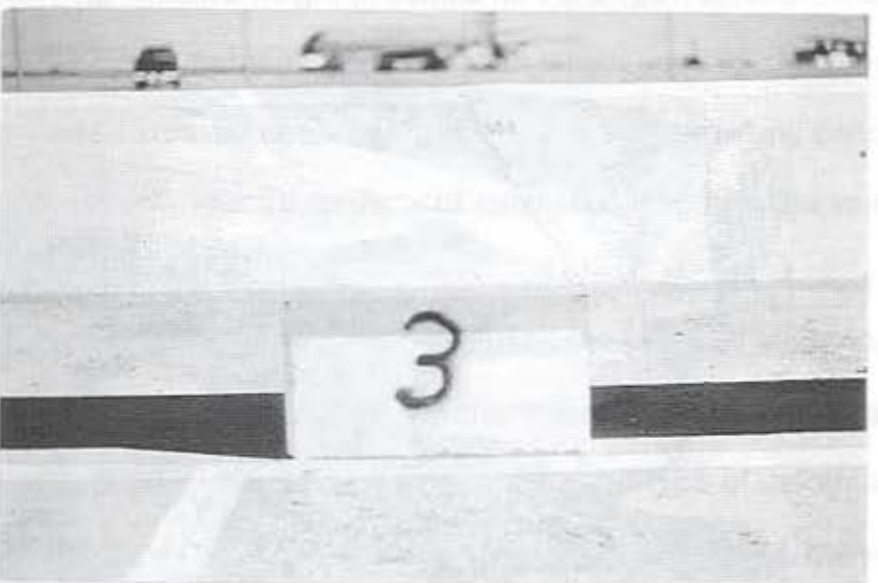
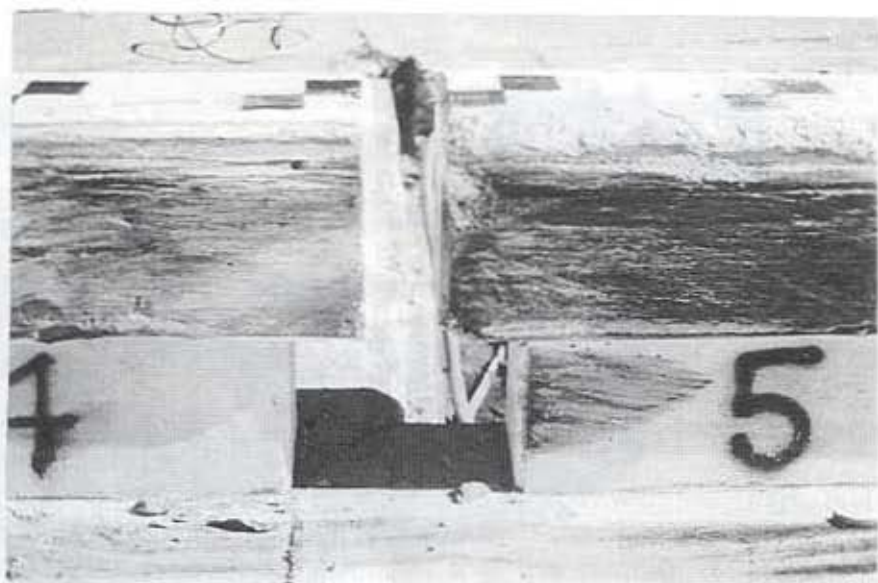


FIGURE 43. Bridge Rail Damage, Test NEOCK-6



FIGURE 44. Vehicle Damage, Test NEOCR-6

5 DISCUSSION

Although Test NEOCR-3 caused significant bridge rail and post damage near the gap location, the structural adequacy was maintained. As mentioned previously, most of this damage occurred when the rear wheel assembly contacted the gap location. Further, both test vehicles were smoothly redirected without exhibiting any tendency to roll over and performed exceptionally well based on redirection capacity with the single-unit truck test.

It was determined for testing purposes that the damage sustained at the gap location following this test was significant enough to repair before conducting the pickup test (Test NEOCR-6) upstream of the gap. The retrofit process involved saw cutting the rail just downstream of Post No. 2 and breaking out the concrete around the dowelled vertical reinforcement in Post Nos. 3 and 4, reforming the rail and posts and casting new concrete with a cold joint near Post No. 2. The retrofit process performed well during the test and offered insight to NDOR on the effects of a cold joint repair near the critical gap location.

These tests were conducted on a bridge railing with a substandard effective height and should establish the effective height threshold for PL-2 open concrete bridge railing systems. It should be noted that the total installation length used to accommodate the single-unit truck test was increased to 47.1 m (154 ft-4 5/8 in.), addressing concerns from the highway safety community about the effects of installation length on the validity of the test results.

Although both of the pickup tests (NEOCR-5 and 6) sustained moderate damage and exhibited occupant compartment deformations, the tests were judged acceptable based on the extent and locations of the deformations. This type of deformation could reasonably be expected to cause injuries to an occupant's feet and ankles, but would most

likely not be considered life threatening. Furthermore, the source of the occupant compartment deformation can be largely contributed to the lateral forces generated by the pickup truck's front wheel assembly contacting the vertical face of the railing and being shoved into the firewall and floor pan area.

This particular problem with occupant compartment deformations in pickup truck tests has been occurring in many research programs throughout the country when using the procedures and criteria provided in the National Cooperative Highway Research Program (NCHRP) Report No. 350, *Recommended Procedures for the Safety Performance Evaluation of Highway Features*(10). The results obtained under NCHRP Report No. 350 testing procedures demonstrate similar damage patterns as those obtained from this research only on a larger scale (more severe), since the impact severity is approximately 36 percent greater than the PL-2 impact severity.

6 CONCLUSIONS

The Performance Level 2 tests on the Nebraska Open Concrete bridge rail proved to be satisfactory according to the safety performance criteria presented in *AASHTO's Guide Specifications for Bridge Railings* (5) and is recommended for field applications. The safety performance evaluation summary is presented in Table 3.

The open concrete bridge rail adequately contained and redirected the vehicles and prevented them from penetrating or going over the bridge rail. Additionally, the vehicles remained upright and stable throughout the entire impact event and came to rest after losing contact with the railing in an upright position. There were no detached elements or debris resulting from the collision with the railing that could have potentially caused undue hazard to the occupants of the vehicles or to adjacent traffic. Even though moderate occupant compartment damage was sustained in the pickup truck tests, the integrity of the occupant compartment was maintained. The vehicle's exiting conditions and rebound distances were judged to be satisfactory. The occupant impact velocities and ridedown accelerations were well within the recommended limits set forth in the AASHTO Guide Specification (5).

The safety performance of the Nebraska Open Concrete Bridge Rail was determined to be satisfactory according to the safety performance evaluation criteria presented in Tables 1 and 2. The summary of the results for the safety performance evaluation is presented in Table 3.

TABLE 3. Summary of Safety Performance Results

Evaluation Criteria		Results															
		NEOCR-3		NEOCR-4		NEOCR-5		NEOCR-6									
3.a.	The test article shall contain the vehicle; neither the vehicle nor its cargo shall penetrate or go over the installation. Controlled lateral deflection of the test article is acceptable.	S		S		S		S									
3.b.	Detached elements, fragments, or other debris from the test article shall not penetrate or show potential for penetrating the passenger compartment or present undue hazard to other traffic.	S		S		S		S									
3.c.	Integrity of the passenger compartment must be maintained with no intrusion and essentially no deformation.	S		S		S		S									
3.d.	The vehicle shall remain upright during and after collision.	S		S		S		S									
3.e.	The test article shall smoothly redirect the vehicle. A redirection is deemed smooth if the rear of the vehicle does no yaw more than 5 degrees away from the railing from time of impact until the vehicle separates from the railing.	S		S		S		S									
3.f.	<p>The smoothness of the vehicle-railing interaction is further assessed by the effective coefficient of friction μ, where $\mu = \frac{(\cos \theta - V_p/V)}{\sin \theta}$.</p> <p><u>Assessment</u></p> <table><tr><td>0.0 - 0.25</td><td>Good</td></tr><tr><td>0.26 - 0.35</td><td>Fair</td></tr><tr><td>> 0.35</td><td>Marginal</td></tr></table>	0.0 - 0.25	Good	0.26 - 0.35	Fair	> 0.35	Marginal	Fair ($\mu = .35$)		Marginal ($\mu = .41$)		Fair ($\mu = .31$)		Marginal ($\mu = .40$)			
0.0 - 0.25	Good																
0.26 - 0.35	Fair																
> 0.35	Marginal																
3.g.	<p>The impact velocity of a hypothetical front-seat passenger against the vehicle interior, calculated from vehicle accelerations and .61-m (2.0-ft) longitudinal and .31-m (1.0-ft) lateral displacements, shall be less than:</p> <p><u>Occupant Impact Velocity</u></p> <table><tr><td><u>Longitudinal</u></td><td><u>Lateral</u></td></tr><tr><td>9.1 m/s (30 fps)</td><td>7.6 m/s (25 fps)</td></tr></table> <p>and for the vehicle highest 10-ms average accelerations subsequent to the instant of hypothetical passenger impact should be less than:</p> <p><u>Occupant Ridedown Accelerations - g's</u></p> <table><tr><td><u>Longitudinal</u></td><td><u>Lateral</u></td></tr><tr><td>15</td><td>15</td></tr></table>	<u>Longitudinal</u>	<u>Lateral</u>	9.1 m/s (30 fps)	7.6 m/s (25 fps)	<u>Longitudinal</u>	<u>Lateral</u>	15	15	Normalized Occupant Impact Velocity - m/s (fps)							
		<u>Longitudinal</u>	<u>Lateral</u>														
		9.1 m/s (30 fps)	7.6 m/s (25 fps)														
		<u>Longitudinal</u>	<u>Lateral</u>														
		15	15														
		Longitudinal	Lateral	Longitudinal	Lateral	Longitudinal	Lateral	Longitudinal	Lateral								
3.0 (9.7)	2.0 (6.6)	2.4 (8.0)	2.3 (7.7)	5.4 (17.7)	6.4 (21.0)	5.6 (18.5)	6.6 (21.6)										
Occupant Ridedown Accelerations (g's)																	
Longitudinal	Lateral	Longitudinal	Lateral	Longitudinal	Lateral	Longitudinal	Lateral										
2.1	3.0	2.4	5.4	9.8	9.8	5.4	9.1										
3.h.	Vehicle exit angle from the barrier shall not be more than 12 degrees. Within 30.5-m (100-ft) plus the length of the test vehicle from the point of initial impact with the railing, the railing side of the vehicle shall move no more than 6.1-m (20-ft) from the line of the traffic face of the railing.	NA		NA		NA		NA									
		none		0.41-m (16 -in.)		30.5-cm (12-in.)		1.7-m (67-in.)									

7 REFERENCES

1. Stout, D., Hinch, J., *Test and Evaluation of Traffic Barriers: Final Report - Technical*, Office of Safety and Traffic Operations R & D, Federal Highway Administration, FHWA-RD-89-119, April 1989.
2. *Recommended Procedures for the Safety Performance Evaluation of Highway Appurtenances*, National Cooperative Highway Research Program Report 230, Transportation Research Board, Washington, D.C., March 1981.
3. Faller, R.K., Pfeifer, B.G., Holloway, J.C., Rosson, B.T., *Performance Level 1 Tests on the Nebraska Open Concrete Bridge Rail*, Report TRP-03-28-91, Midwest Roadside Safety Facility, University of Nebraska-Lincoln, Lincoln, Nebraska, 1991.
4. Powell, G.H., *BARRIER VII : A Computer Program for Evaluation of Automobile Barrier Systems*, Prepared for: Federal Highway Administration, Report No. FHWA-RD-73-51, April 1973.
5. *Guide Specifications for Bridge Railings*, American Association of State Highway and Transportation Officials, Washington, D.C., 1989.
6. Hinch, J., Yang, T-L, and Owings, R., *Guidance Systems for Vehicle Testings*, ENSCO, Inc., Springfield, VA, 1986.
7. *Roadside Design Guide*, American Association of State Highway and Transportation Officials, Washington, D.C., October, 1988.
8. *Vehicle Damage Scale for Traffic Investigators*, Traffic Accident Data Project Technical Bulletin No. 1, National Safety Council, Chicago, IL, 1971.
9. *Collision Deformation Classification, Recommended Practice J224 March 1980*, SAE Handbook Vol. 4, Society of Automotive Engineers, Warrendale, Penn., 1985.
10. *Recommended Procedures for the Safety Performance Evaluation of Highway Features*, National Cooperative Highway Research Program Report 350, Transportation Research Board, Washington, D.C., 1993.

8 APPENDIX

8.1 Appendix A - Accelerometer and Rate Gyro Analysis Plots

NEOCR-3

- Figure A-1 Graph of Longitudinal Deceleration, NEOCR-3
- Figure A-2 Graph of Longitudinal Occupant Impact Velocity, NEOCR-3
- Figure A-3 Graph of Lateral Deceleration, NEOCR-3
- Figure A-4 Graph of Lateral Occupant Impact Velocity, NEOCR-3

NEOCR-4

- Figure A-5 Graph of Longitudinal Deceleration, NEOCR-4
- Figure A-6 Graph of Longitudinal Occupant Impact Velocity, NEOCR-4
- Figure A-7 Graph of Lateral Deceleration, NEOCR-4
- Figure A-8 Graph of Lateral Occupant Impact Velocity, NEOCR-4

NEOCR-5

- Figure A-9 Graph of Longitudinal Deceleration, NEOCR-5
- Figure A-10 Graph of Longitudinal Occupant Impact Velocity, NEOCR-5
- Figure A-11 Graph of Lateral Deceleration, NEOCR-5
- Figure A-12 Graph of Lateral Occupant Impact Velocity, NEOCR-5
- Figure A-13 Graph of Angular Displacements, NEOCR-5

NEOCR-6

- Figure A-14 Graph of Longitudinal Deceleration, NEOCR-6
- Figure A-15 Graph of Longitudinal Occupant Impact Velocity, NEOCR-6
- Figure A-16 Graph of Lateral Deceleration, NEOCR-6
- Figure A-17 Graph of Lateral Occupant Impact Velocity, NEOCR-6
- Figure A-18 Graph of Angular Displacements, NEOCR-6

W4: NEOCR-3 LONGITUDINAL DECELERATION

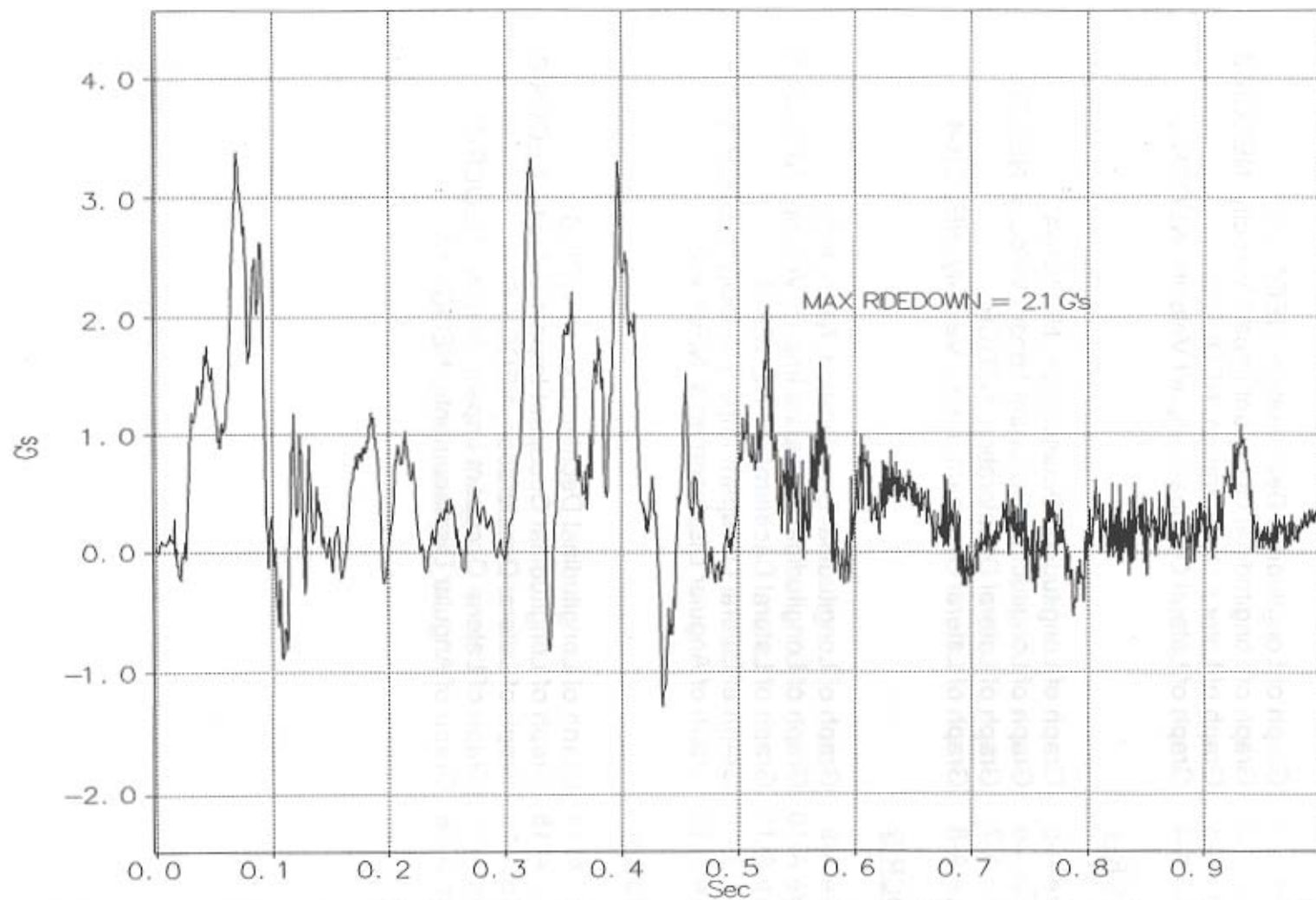


Figure A-1. Graph of Longitudinal Deceleration, NEOCR-3

W5: NEOCR-3 LONGITUDINAL OCCUPANT IMPACT VELOCITY

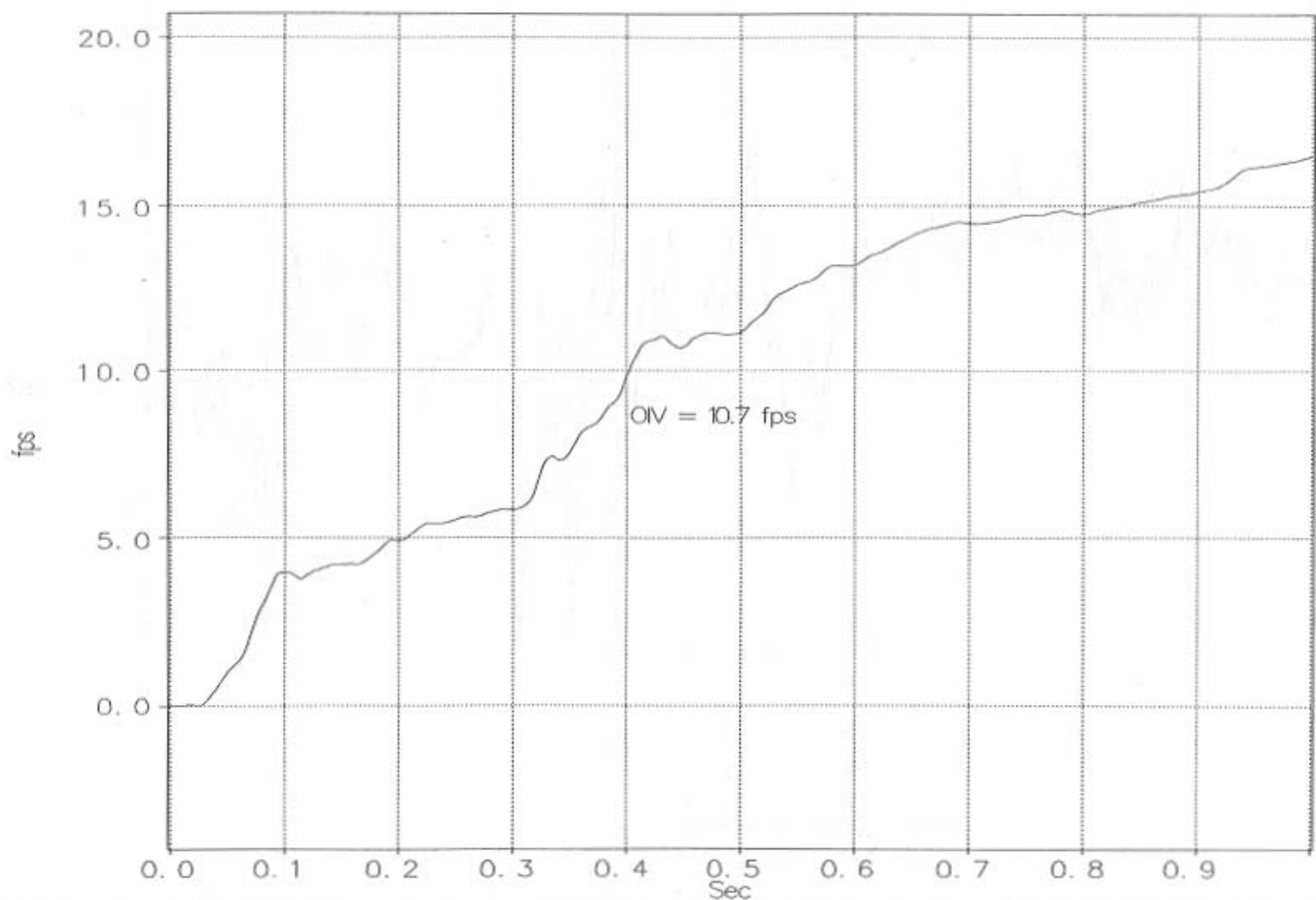


Figure A-2. Graph of Longitudinal Occupant Impact Velocity, NEOCR-3

W5: NEOCR-3 LATERAL DECELERATION

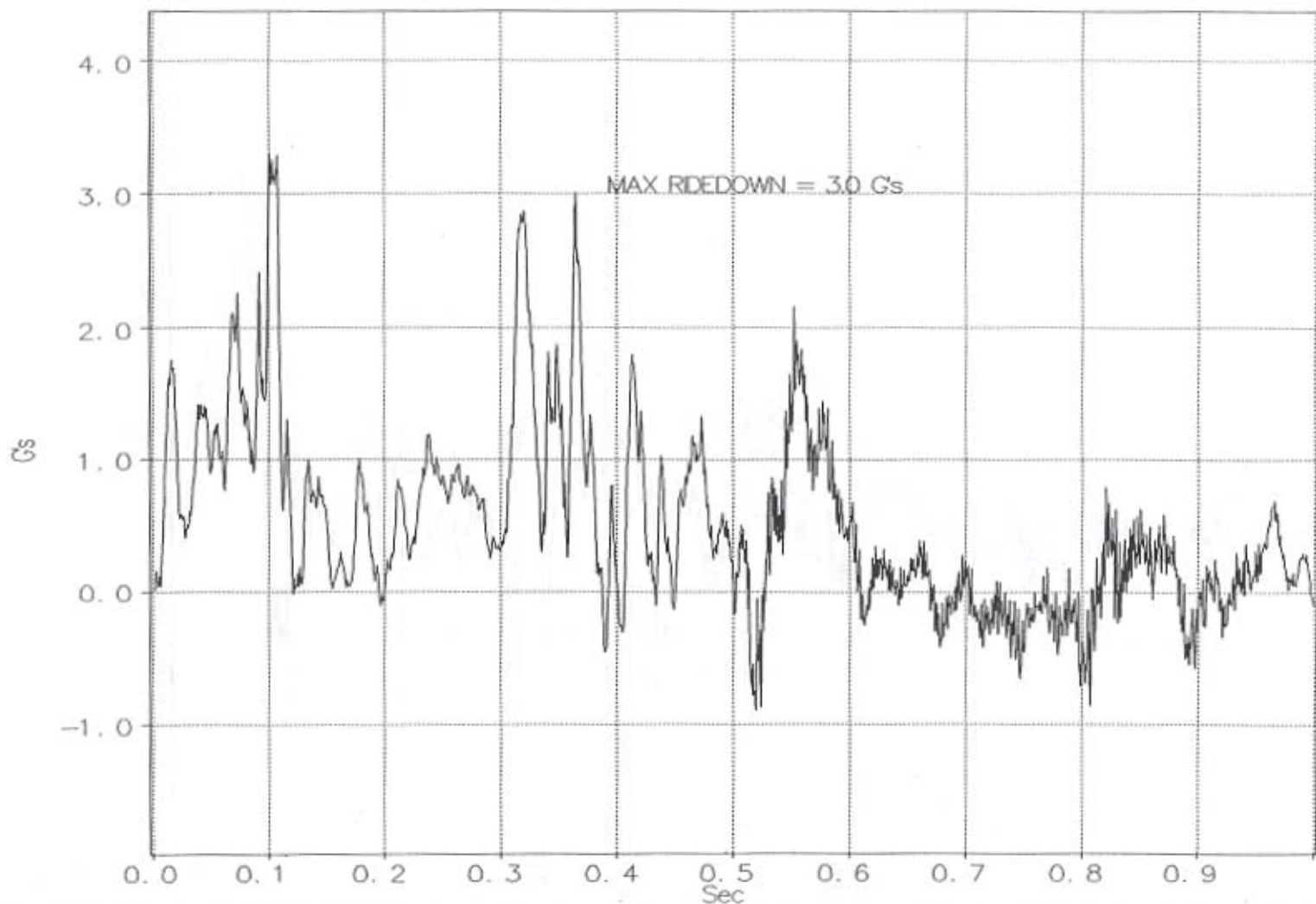


Figure A-3. Graph of Lateral Deceleration, NEOCR-3

W6: NEOCR-3 LATERAL OCCUPANT IMPACT VELOCITY

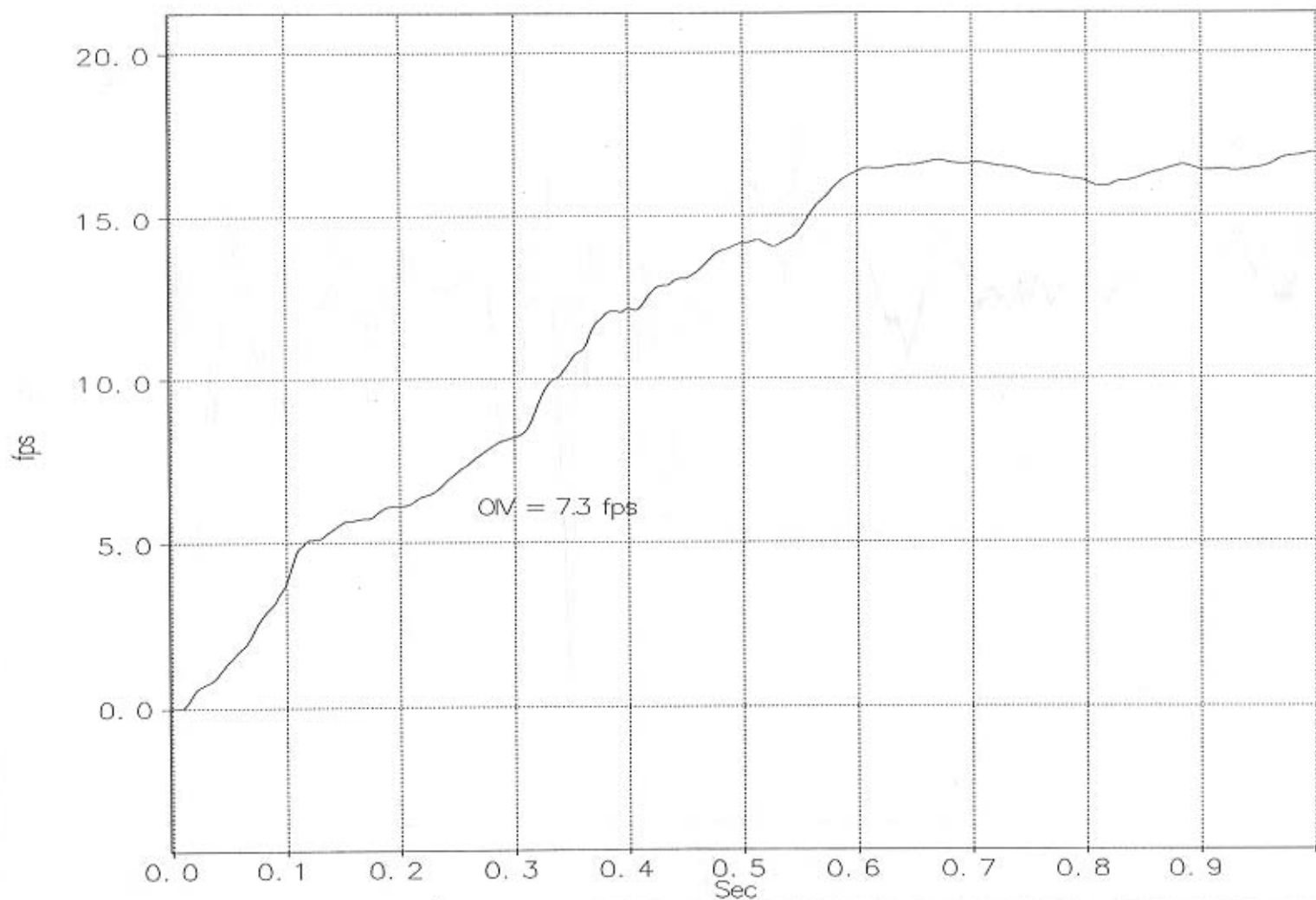


Figure A-4. Graph of Lateral Occupant Impact Velocity, NEOCR-3

W4: NEOCR-4 LONGITUDINAL DECELERATION

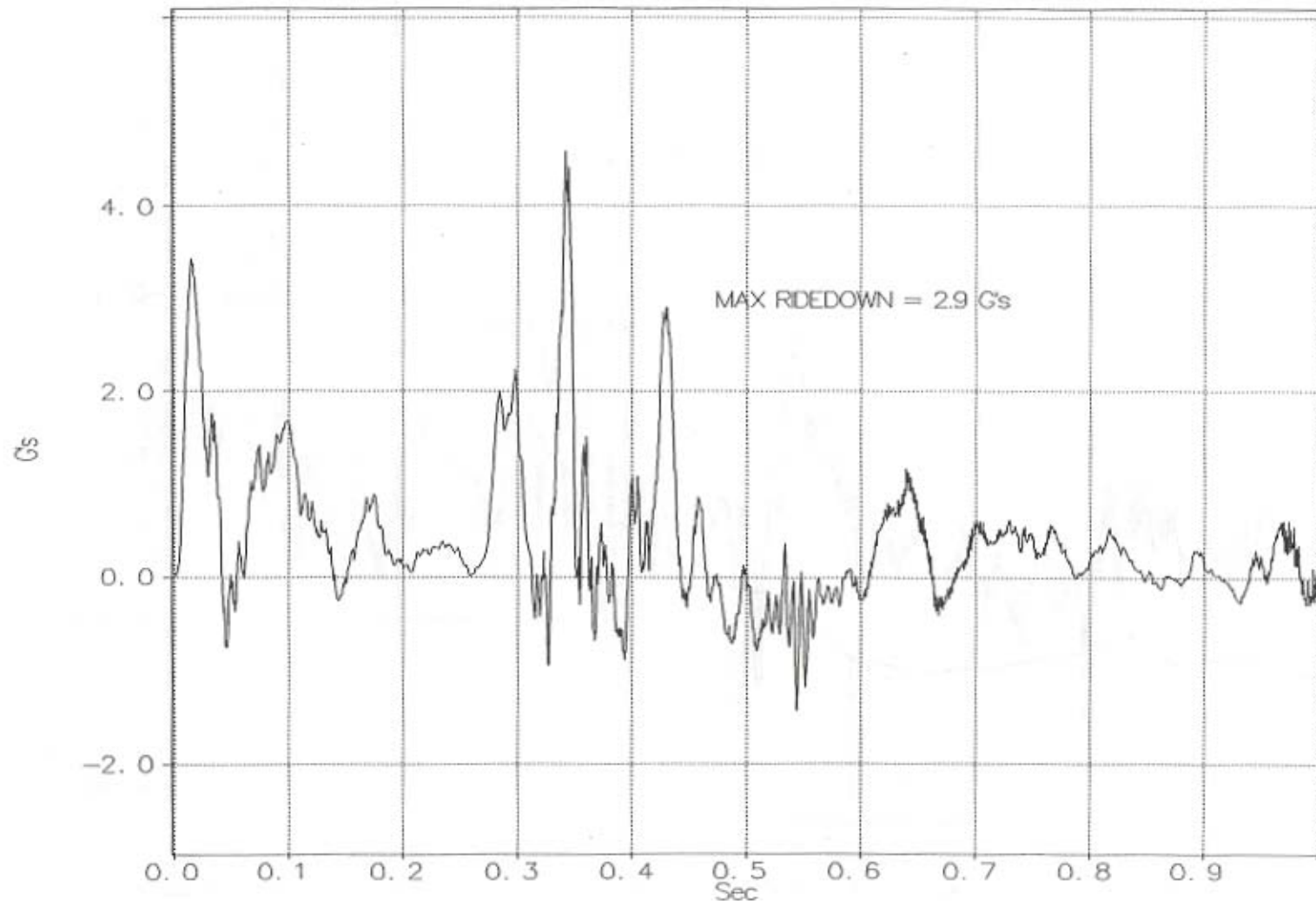


Figure A-5. Graph of Longitudinal Deceleration, NEOCR-4

W5: NEOCR-4 LONGITUDINAL OCCUPANT IMPACT VELOCITY

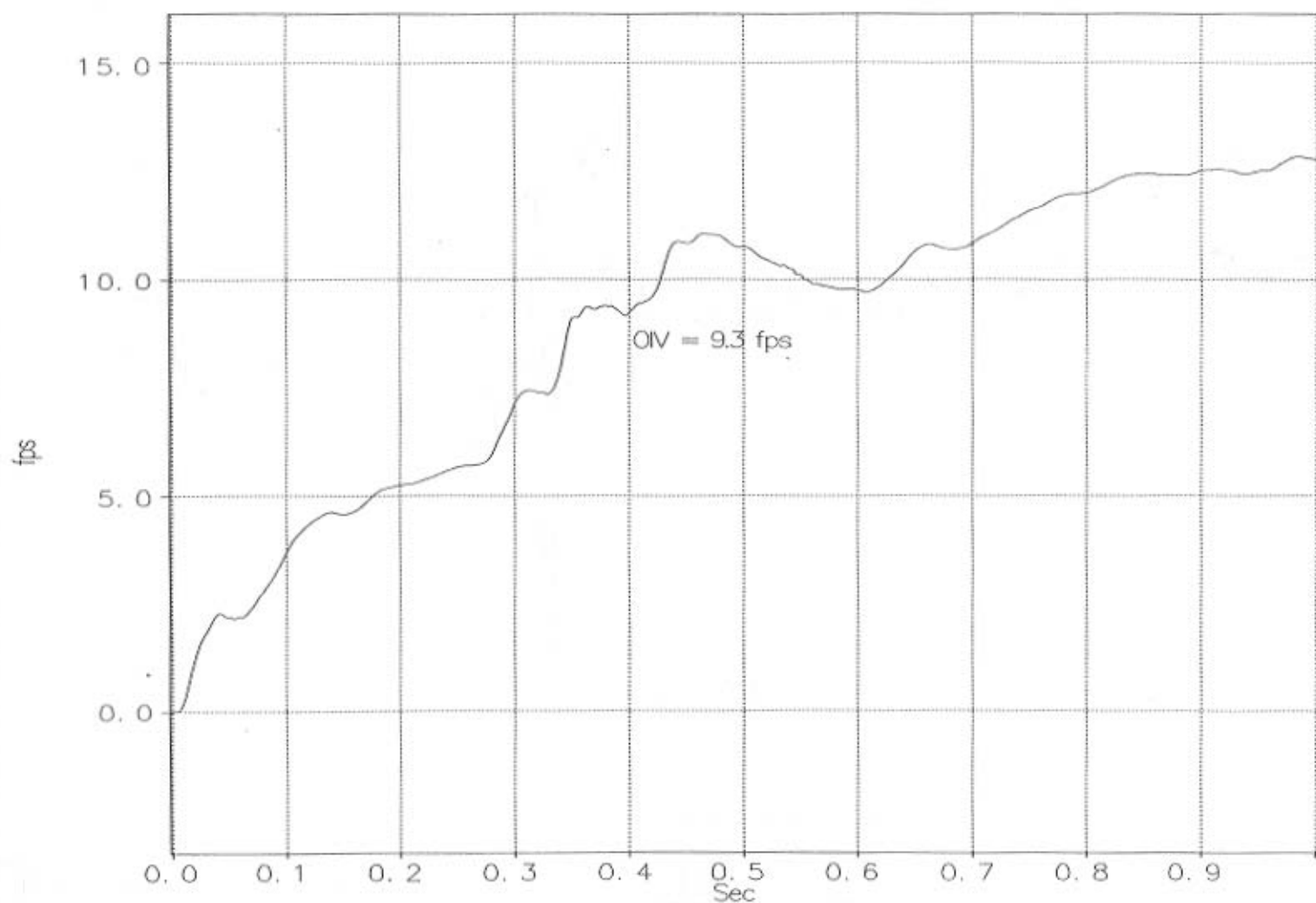


Figure A-6. Graph of Longitudinal Occupant Impact Velocity, NEOCR-4

W5: NEOCR-4 LATERAL DECELERATION

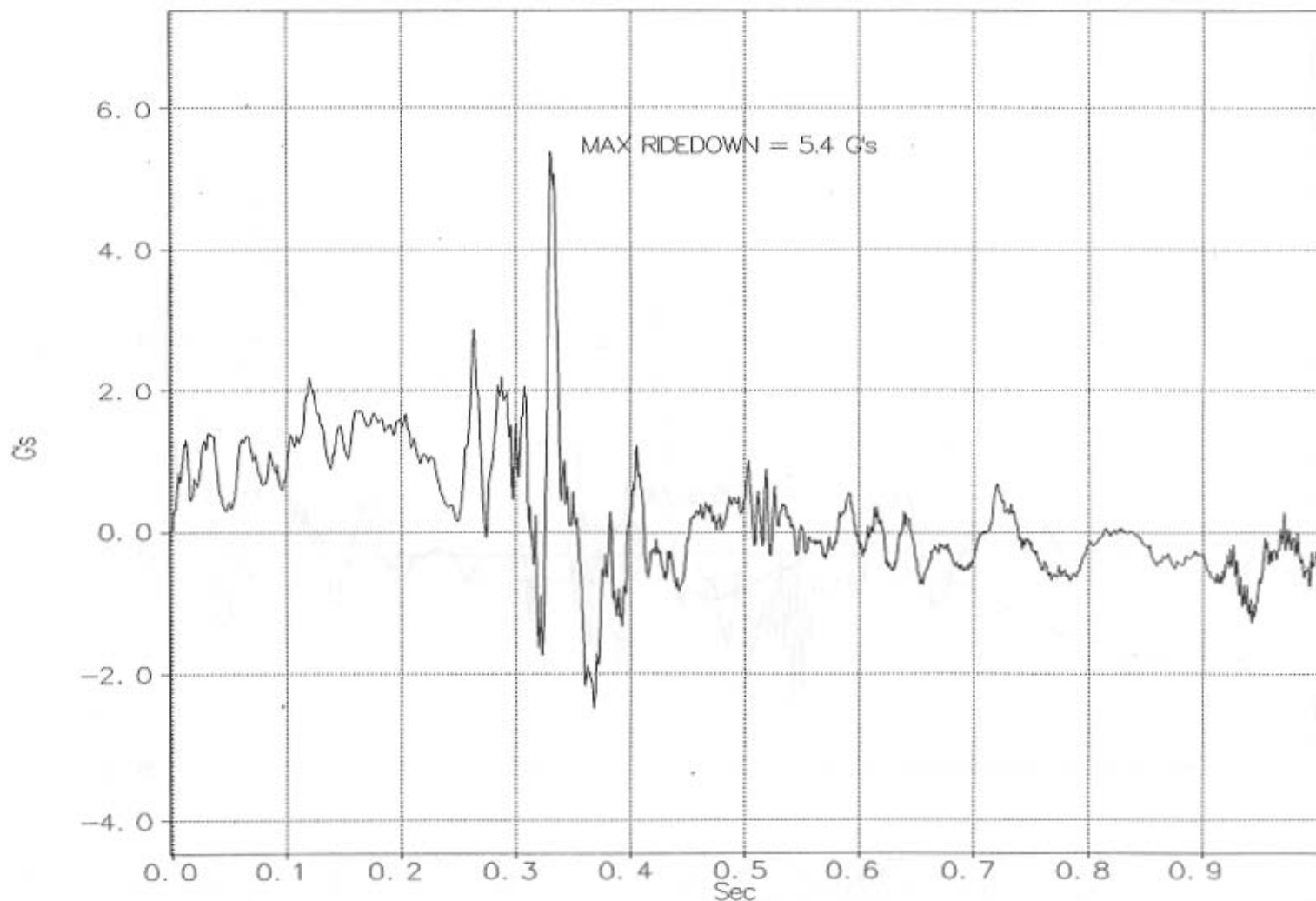


Figure A-7. Graph of Lateral Deceleration, NEOCR-4

W7: NEOCR-4 LATERAL OCCUPANT IMPACT VELOCITY

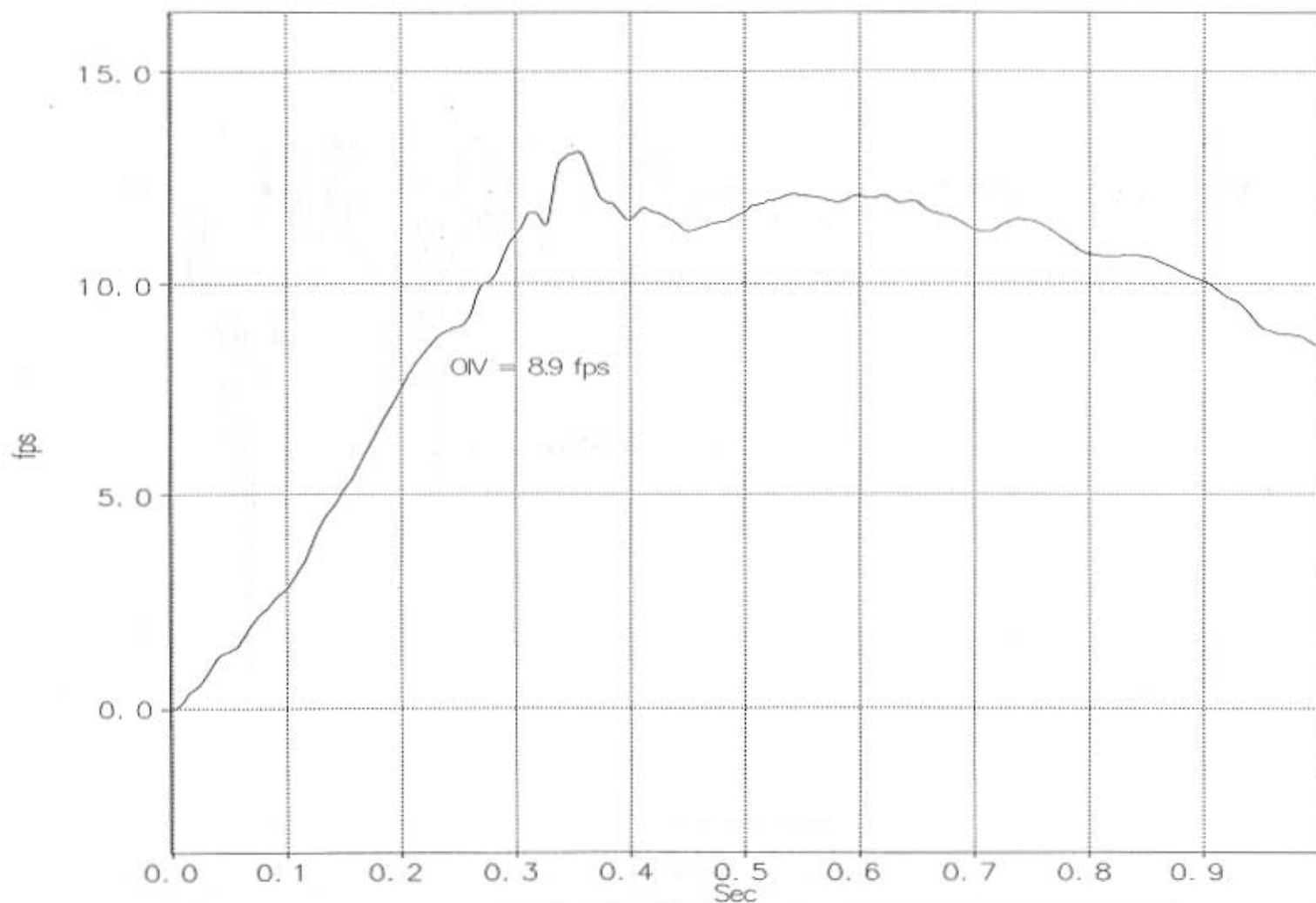


Figure A-8. Graph of Lateral Occupant Impact Velocity, NEOCR-4

W4: NEOCR-5 LONGITUDINAL DECELERATION

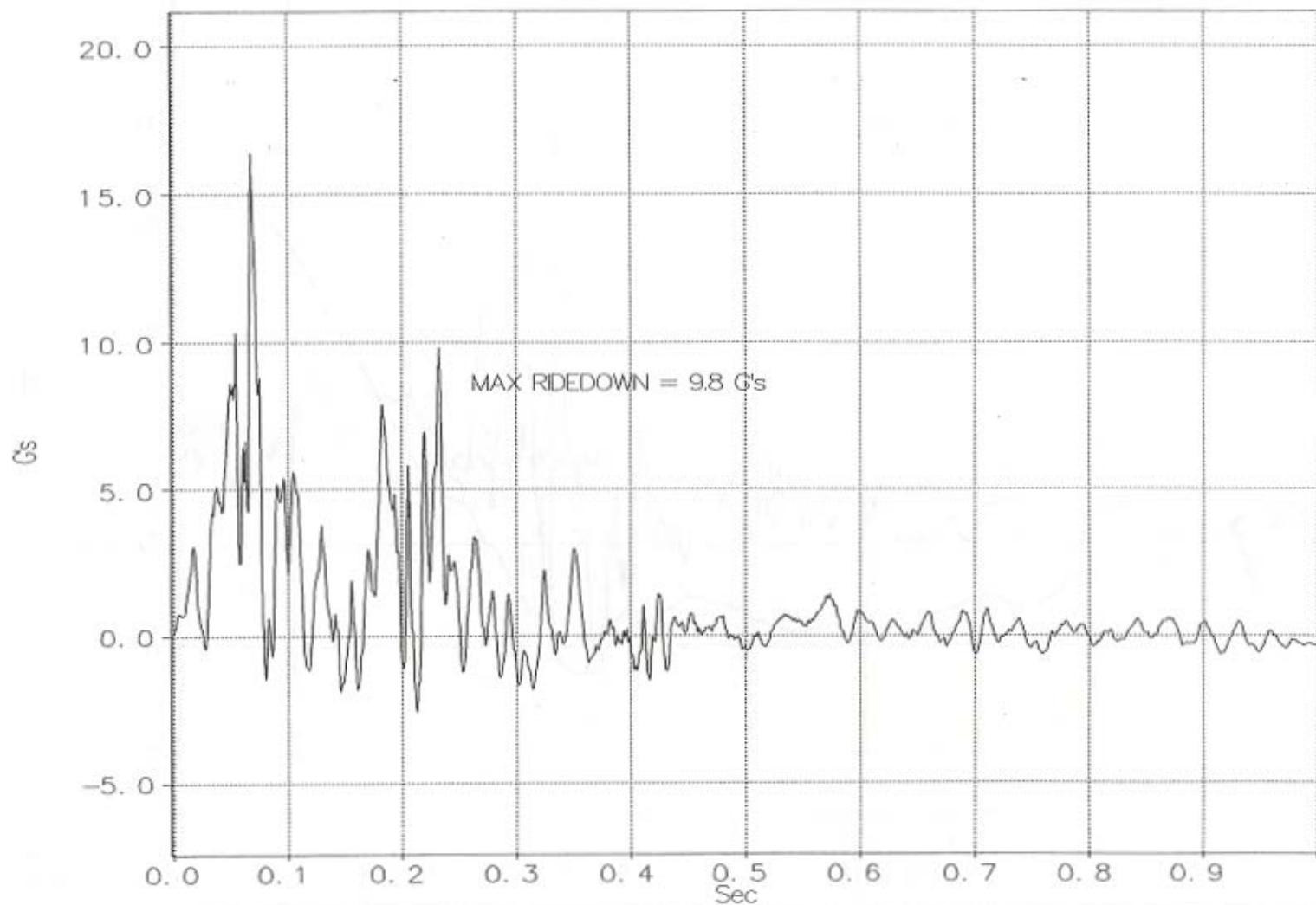


Figure A-9. Graph of Longitudinal Deceleration, NEOCR-5

W5: NEOCR-5 LONGITUDINAL OCCUPANT IMPACT VELOCITY

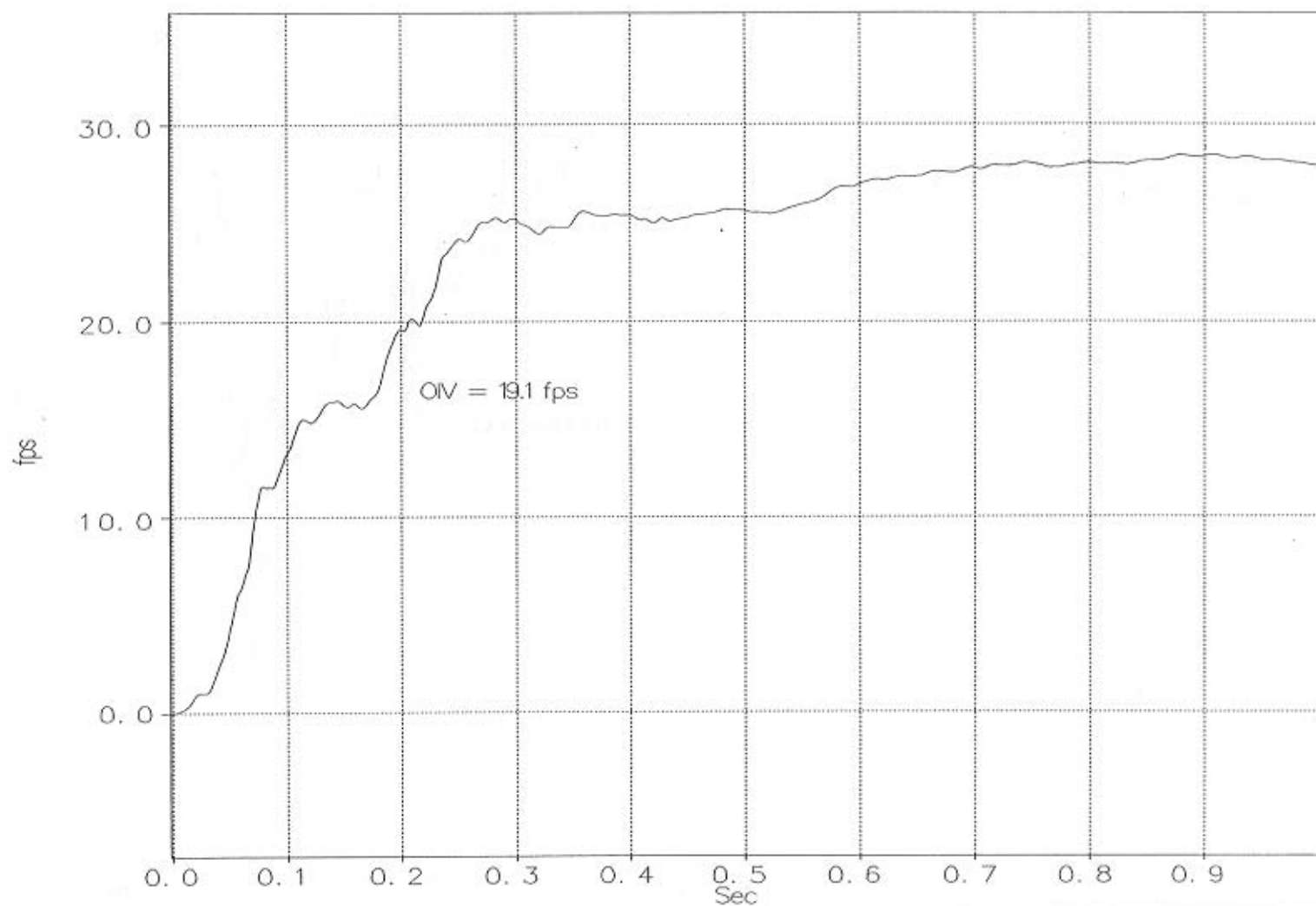


Figure A-10. Graph of Longitudinal Occupant Impact Velocity, NEOCR-5

W5: NEOCR-5 LATERAL DECELERATION

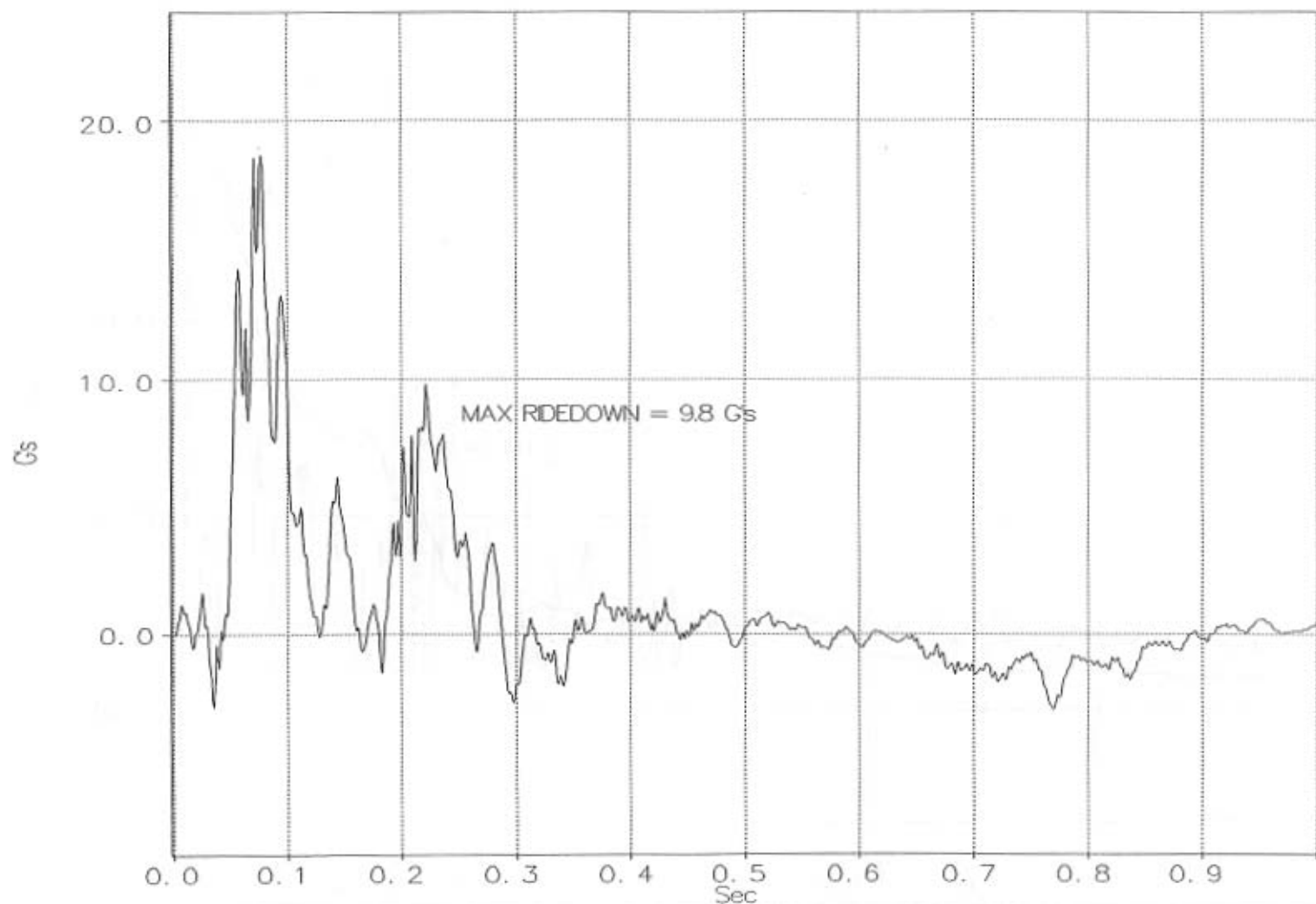


Figure A-11. Graph of Lateral Deceleration, NEOCR-5

W6: NEOCR-5 LATERAL OCCUPANT IMPACT VELOCITY

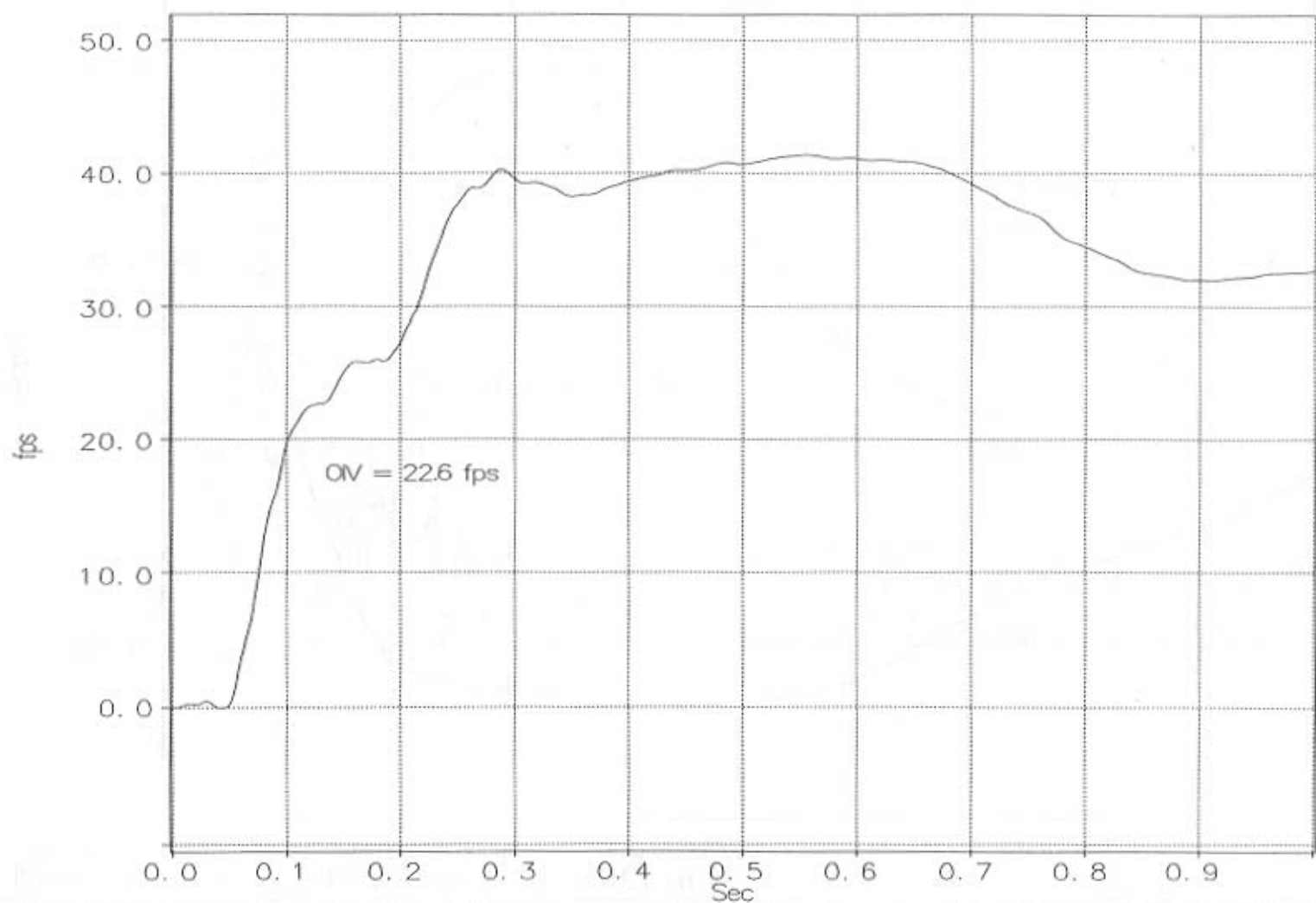


Figure A-12. Graph of Lateral Occupant Impact Velocity, NEOCR-5

W49: NEOCR-5 ANGULAR DISPLACEMENTS

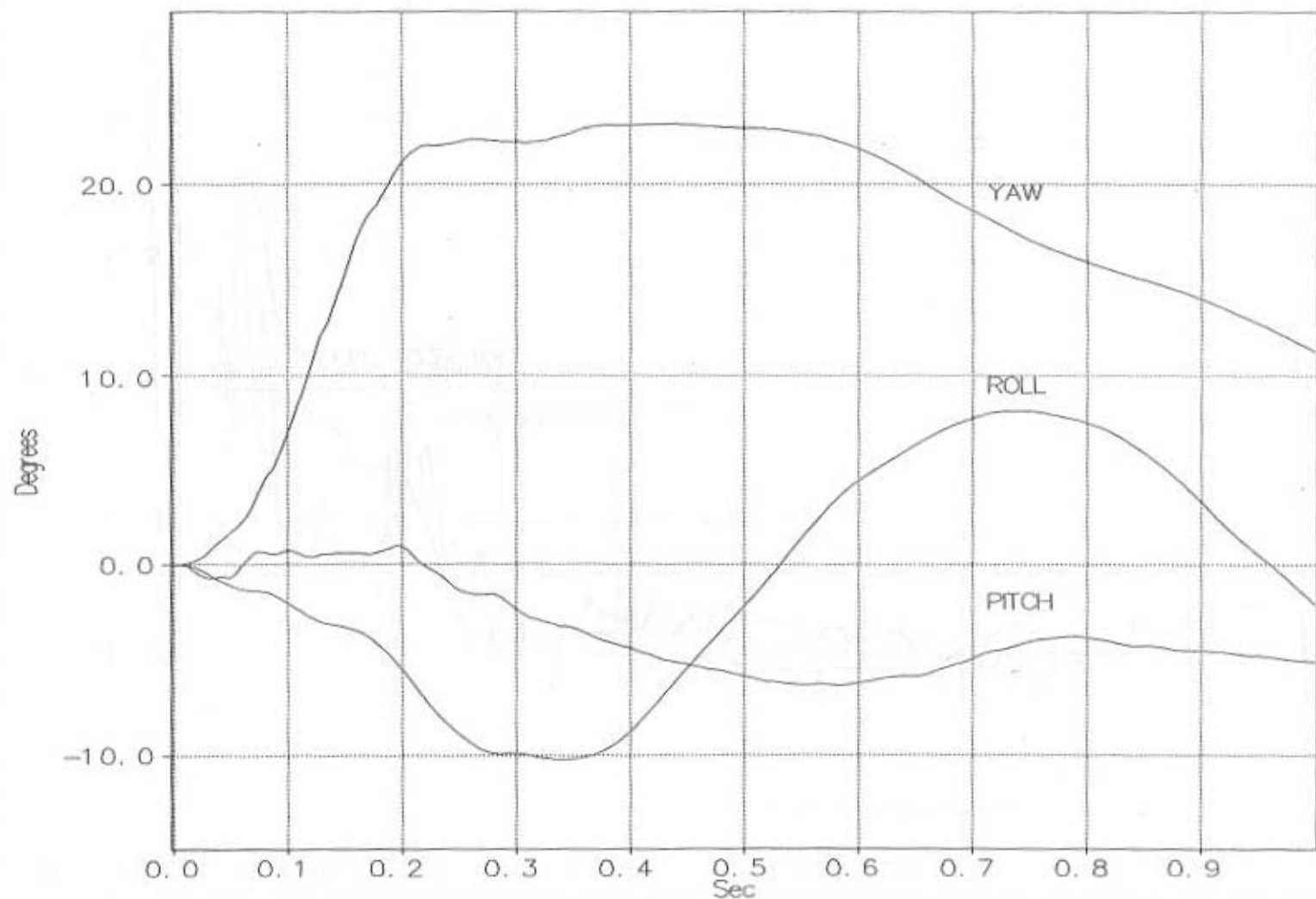


Figure A-13. Graph of Angular Displacements, NEOCR-5

W4: NEOCR-6 LONGITUDINAL DECELERATION

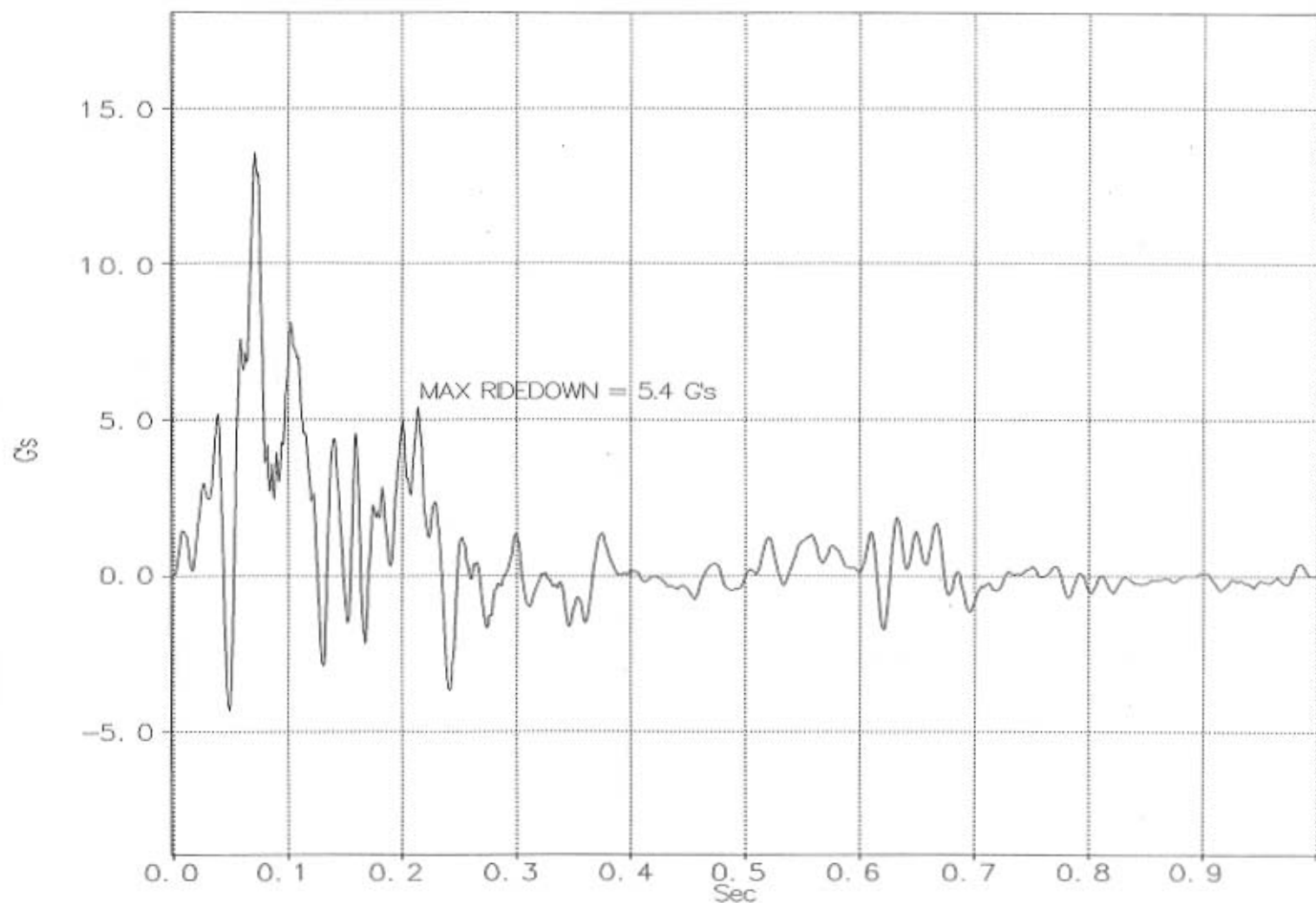


Figure A-14. Graph of Longitudinal Deceleration, NEOCR-6

W5: NEOCR-6 LONGITUDINAL OCCUPANT IMPACT VELOCITY

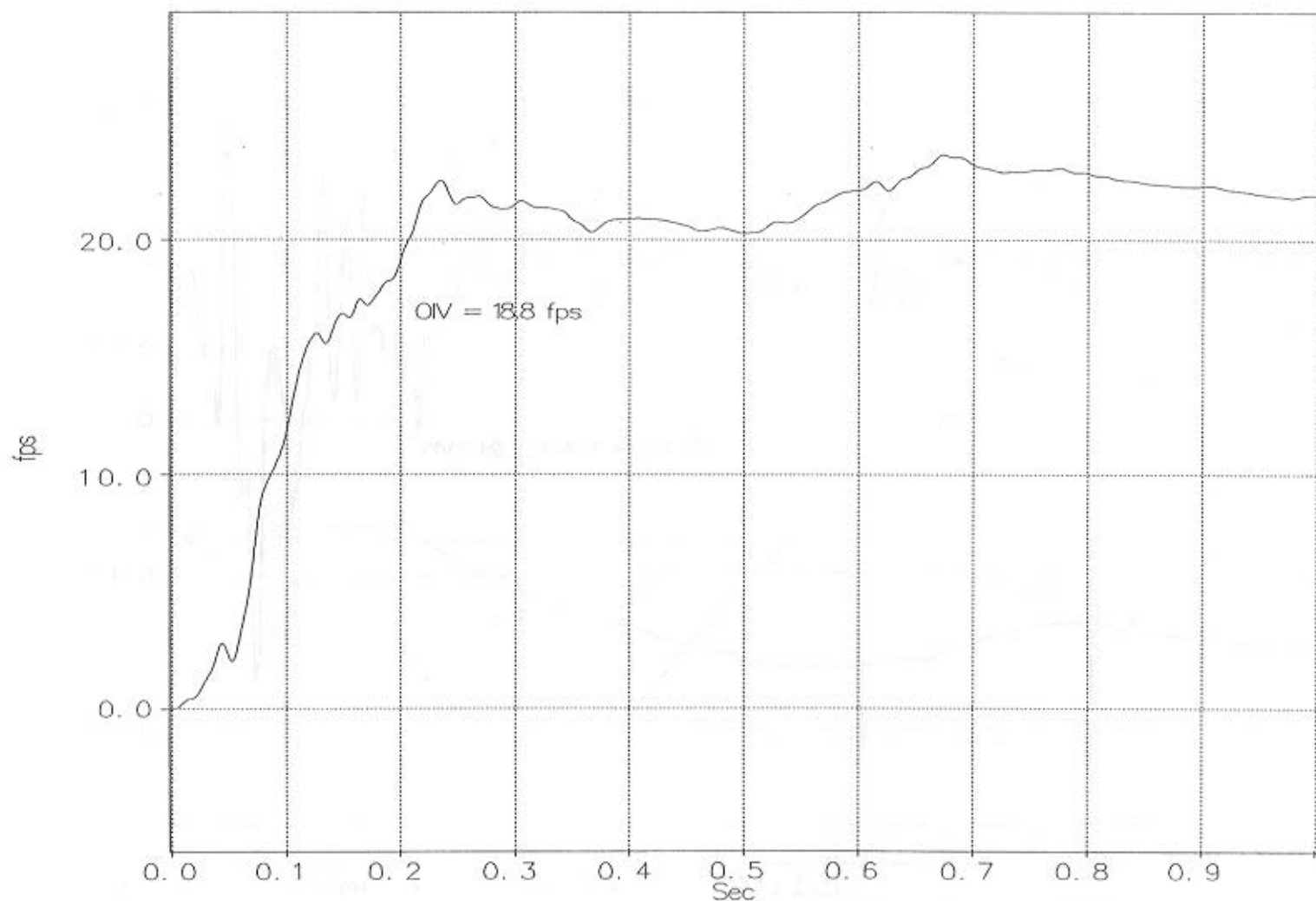


Figure A-15. Graph of Longitudinal Occupant Impact Velocity, NEOCR-6

W5: NEOCR-6 LATERAL DECELERATION

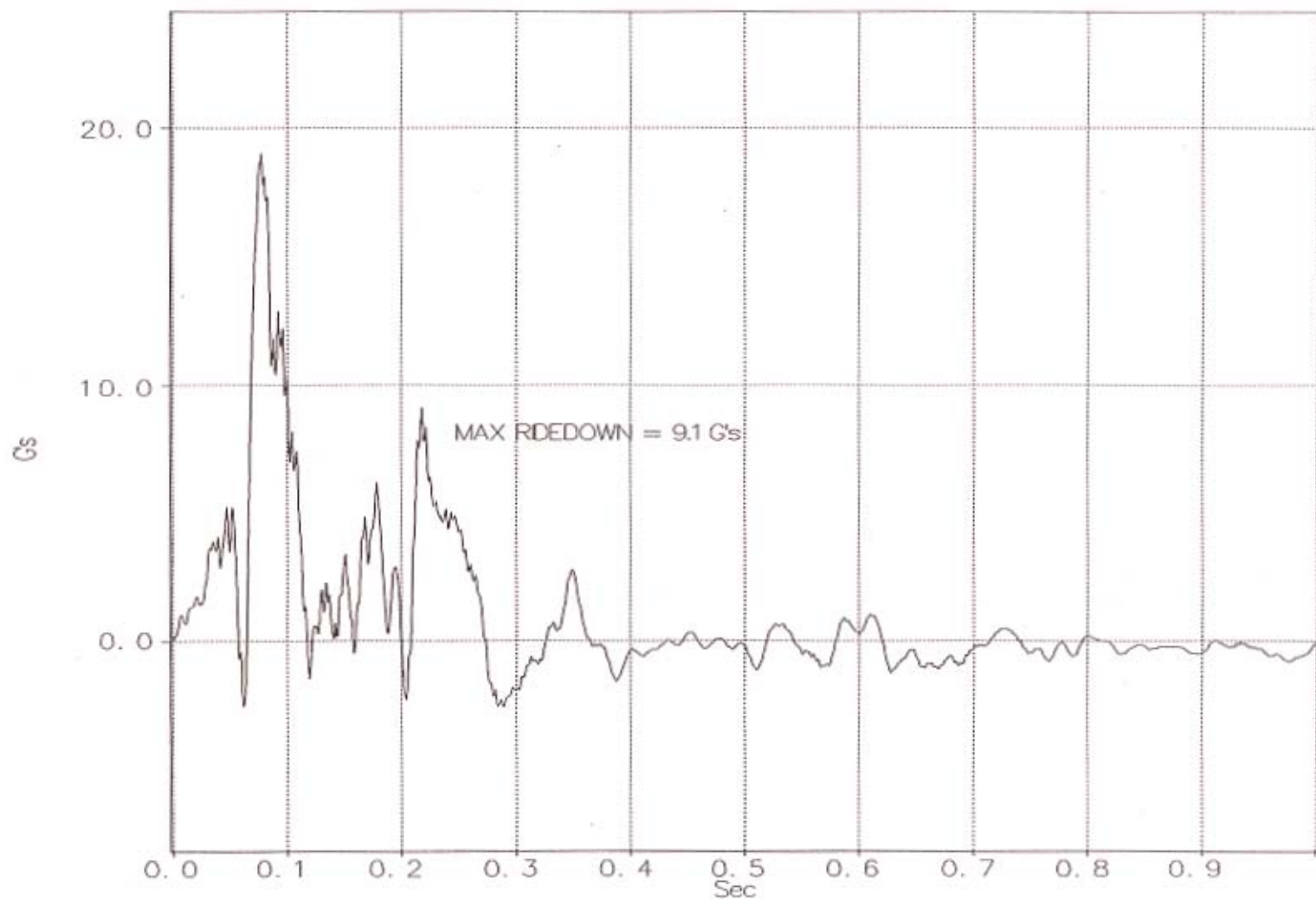


Figure A-16. Graph of Lateral Deceleration, NEOCR-6

W6: NEOCR-6 LATERAL OCCUPANT IMPACT VELOCITY

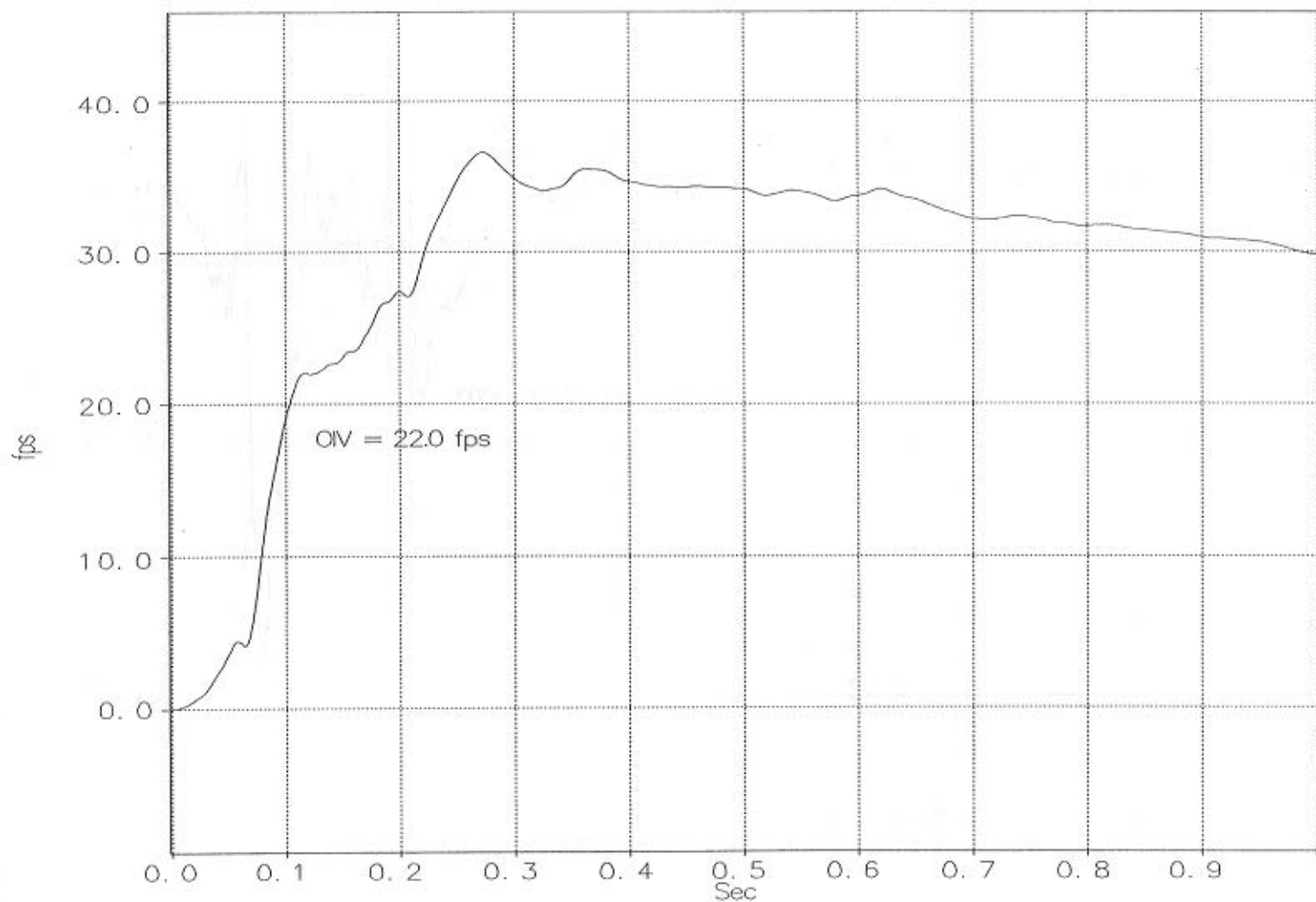


Figure A-17. Graph of Lateral Occupant Impact Velocity, NEOCR-6

W35: NEOCR-6 ANGULAR DISPLACEMENTS

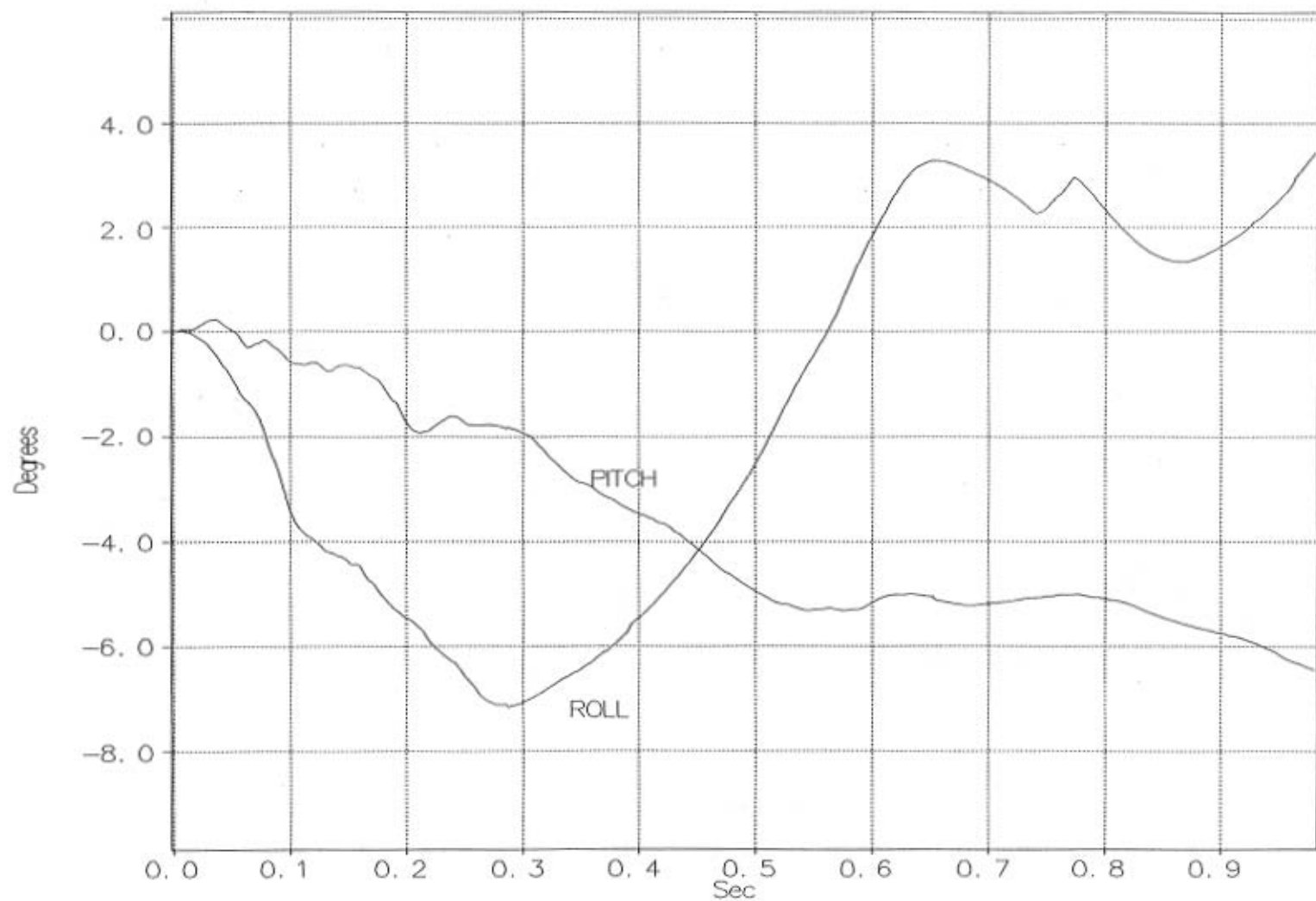


Figure A-18. Graph of Angular Displacements, NEOCR-6